

# Reducing Depolarizing Noise in Grover's Search Algorithm Using Quantum Switches

Thesis submitted in partial fulfillment  
of the requirements for the degree of

**Master of Science**

*in*

*Computational Natural Sciences by Research*

by

Suryansh Srivastava

20171024

suryansh.srivastava@research.iiit.ac.in



INTERNATIONAL INSTITUTE OF  
INFORMATION TECHNOLOGY

HYDERABAD

International Institute of Information Technology

Hyderabad - 500 032, INDIA

June 2024

Copyright © Suryansh Srivastava, 2024  
All Rights Reserved

International Institute of Information Technology  
Hyderabad, India

## CERTIFICATE

It is certified that the work contained in this thesis, titled “*Reducing Depolarizing Noise in Grover’s Search Algorithm Using Quantum Switches*” by Suryansh Srivastava has been carried out under our supervision and has is not submitted elsewhere for a degree.

---

Date

---

Adviser: Dr. Indranil Chakrabarty

---

Date

---

Co-Adviser: Dr. Arun Kumar Pati

To the constants and the variables,  
that lead to qubits' decoherence,  
and fueled my perseverance.

## Acknowledgments

While marking the end of my academic journey at IIIT Hyderabad, this thesis is merely a step forward toward realizing a long-cherished dream of becoming a researcher.

I want to express my foremost gratitude to Prof. Indranil Chakrabarty for his guidance and support since the beginning of my research. Apart from introducing me to the subject itself, he also introduced me to several brilliant minds in the field through the years. That includes my co-advisor, Prof. Arun K. Pati, presently at TCG CREST (CQuERE), whose wisdom and foresight have been priceless throughout this project. I am forever thankful to him for the opportunity to visit HRI Allahabad and for introducing me to the concept of indefinite causal order, the central theme of my research work. I owe a great deal of gratitude to Prof. Samyadeb Bhattacharya, who opened up the world of open quantum systems to me (pun intended). The independent study I pursued under his guidance, along with the course he later taught, provided me with the necessary tools that proved invaluable while working on this project, which he later ended up collaborating on down the line. I am also fortunate to have had an excellent group of professors to look up to, including Prof. Shantanav Chakraborty and Prof. Siddhartha Das, Prof. Subhadip Mitra, Prof. Harjinder Singh (Laltu), Prof. Prabhakar Bhimalapuram, Prof. Kannan Srinathan: who have supported me throughout the journey and kept my love for learning, and scientific curiosity alive by constantly challenging me with stimulating discussions.

I am grateful to Prof. Guruprasad Kar, Prof. Manik Banik, and their colleagues at PAMU for their warm hospitality during my stay at ISI Kolkata's summer school. I also owe my thanks to Prof. Nirman Ganguly from BITS Hyderabad for giving me an interesting set of problems to start with.

I want to give a huge shoutout to my fellow lab dwellers at CQST and CSTAR, who have been an integral part of my journey. Mahathi, Aditya Morolia, Rohan Sharma, Pahul, Srinidhi, Alapan, Rutvij, Zeeshan, Kushagra, Shreyas and others, your presence and support have made this process not only possible but also enjoyable. I want to give a special shoutout to Utkarsh, who has been a friend and mentor. Thank you for patiently reviewing my draft and other annoying long calls.

This thesis is the culmination of a long and challenging journey. As a fan of TV shows, I look back at this journey as a series with numerous episodes spanning multiple seasons (COVID was a weird one), comprising all sorts of tropes and genres added to the mix. The narrative

has been shaped by an ensemble cast of friends: Aashna, Abhinav Vaishya, Anushka, Atirek, Debojit, Devesh, Freya, Keshav, Prafullit, Priyank, Souvik, Shantanu, Shreyas, Shashwat, Sriven, Ujwal, Varun, Vijayraj, Yash, Zubair, and everyone that I have had the privilege to call a friend, but have missed as I write this section at the end of what would hopefully be my last all-nighters at IIIT. Like characters in a show, some have been part of the story since the pilot episode, while some joined or left in later seasons. Regardless of their role or screen time, they all brought their unique knacks, personalities, and perspectives, leaving an indelible mark on the narrative and contributing in their own way to my personal and professional growth. Speaking of shows, I would like to thank my core production team for working tirelessly behind the scenes, far from the action, from even before the show's inception: Ayush, Deepak, and Sukriti.

Lastly, I want to express my deepest gratitude to Ma (Amrita) and Papa (Sanjeeva), the two most significant people in my life to whom I will remain indebted forever. I strive to continue working tirelessly to make them proud. I am also grateful to all my siblings, who have always pushed me to do better. And I want to extend my heartfelt appreciation to all other family members who have always believed in me, no matter what I chose to do. As this chapter of my academic career concludes, I once again extend my deepest gratitude for every laugh shared, every hurdle crossed, and every success celebrated. Here's to the end of an unforgettable chapter and the anticipation of the ones that lie ahead.

## Abstract

Grover’s quantum search algorithm is one of the earliest discoveries in quantum computing. It is a fundamental algorithm that uses quantum superposition to provide a quadratic speedup for unstructured search tasks over the best possible classical method (linear search). However, this advantage is substantially affected due to the presence of quantum noise. Quantum noise arises due to the interaction between quantum systems and their environments. The resultant errors manifest between the execution of two quantum gates can be effectively modeled using quantum channels. In this study, we look at the effect of total partial depolarizing channel error, affecting the entire quantum register coherently with a certain probability. This modeling approach simulates continuous noise exposure in quantum computers and the stochastic nature of error introduction. In this scenario, implementing an error correction method is non-trivial and costly.

Quantum theory allows for a scenario in which quantum channels, representing the flow of quantum information, are organized in a coherent superposition of alternative orders. This phenomenon, known as indefinite causal order, has sparked significant interest in recent years as researchers seek to understand its implications. A quantum switch is a device that operationalizes the concept of indefinite causal order. In a quantum switch, the advantages appear significantly due to the coherent superposition of alternative configurations of the quantum components, which are controlled by an additional control system.

In this work, we propose a new approach to mitigate the impact of quantum noise on Grover’s search algorithm using quantum switches. For this, we assume the resultant noise at every iteration to be originating in discrete steps within the iteration such that it can be modeled as a composition of two depolarising channels. In particular, we propose two theoretical frameworks for incorporating these quantum switches in a noisy Grover’s algorithm and take the success probability of finding  $g$ , the desired element at any given iteration, as the sole quantifier of the switch’s action in diminishing the effect of noise in search space. In the first framework, we apply the superposition of channels’ orders using a quantum switch and make a measurement followed by post-selection at every iteration or application of Grover operator  $\mathcal{G}$ . In the second framework, we delay the measurement until the very end. In other words, if we want to look at the quantum switch’s action at the  $k^{th}$  step, we already have  $k - 1^{th}$  measurements followed by post-selections for the first framework. In contrast, we will only

have a single measurement at the end of  $k^{th}$  iteration in the second case. The measurements we make on the quantum switch intermittently between the iterations followed by post-selection destroy the quantum correlations between the target input system and the control qubit. Since these correlations are believed to capture the additional information in the combined system, the second framework is expected to retain more information than the first framework during the run of Grover's Algorithm under the influence of noise.

We observe in plots that the second framework gives a significant advantage in the success probability of Grover's algorithm running on a search space of  $2^4$  elements or 4 qubits. Thus, we explore the quantum switch's potential role as a tool for maintaining quantum computing's promise against the challenges posed by quantum noise, marking a significant step forward in the field of quantum computing and information theory.

# Contents

Chapter	Page
1 Introduction . . . . .	1
1.1 Motivation . . . . .	1
1.2 Prior Work . . . . .	3
1.3 Research Focus and Contributions . . . . .	4
1.4 Outline . . . . .	5
2 Foundations and Preliminaries . . . . .	6
2.1 Historical Overview . . . . .	6
2.1.1 Stern-Gerlach experiment . . . . .	7
2.2 Mathematical Preliminaries . . . . .	10
2.2.1 Vector Spaces . . . . .	11
2.2.2 Inner Product Spaces . . . . .	12
2.2.3 Linear Operators and Matrix Transformations . . . . .	13
2.2.3.1 Matrix Representation of Linear Operators . . . . .	14
2.2.3.2 Eigenvalues and Eigenvectors . . . . .	14
2.2.3.3 Commutator of two operators . . . . .	14
2.2.3.4 Linear Transpose of a matrix and Adjoint of an operator . . . . .	15
2.2.3.5 Tensor Products and Composition of vector spaces . . . . .	15
2.2.3.6 Trace of an Operator . . . . .	16
2.2.3.7 Partial Trace . . . . .	17
2.2.3.8 Spectral Decomposition . . . . .	17
2.2.4 Hilbert Spaces . . . . .	18
2.2.5 Post Selection . . . . .	18
2.3 Postulates of Quantum mechanics . . . . .	18
2.3.1 Postulate 1: State Space, Describing the state of a system . . . . .	19
2.3.2 Measurement on the system . . . . .	19
2.3.2.1 Postulate 2: Observables, Describing physical quantities . . . . .	19
2.3.2.2 Postulate 3: Projective Measurement . . . . .	20
2.3.3 Postulate 4: Time Evolution of system . . . . .	22
2.3.4 Postulate 5: Composite Systems . . . . .	22
2.4 Density Operator Formalism . . . . .	24
2.4.1 General Properties of the Density Operator . . . . .	24
2.4.2 Density Operator Representations . . . . .	25
2.4.3 The Reduced Density Operator . . . . .	25

2.5	Introduction to Quantum Computation	26
2.5.1	Quantum Bits (Qubits)	26
2.5.2	Multiple Qubits	27
2.5.3	Bloch Sphere Representation of Qubit States	27
2.5.4	Quantum Gates	28
2.5.5	Single-Qubit Gates	28
2.5.5.1	Pauli Gates ( <b>X</b> , <b>Y</b> , <b>Z</b> )	28
2.5.6	Multi-Qubit Gates	29
2.5.6.1	Hadamard Gate (H)	29
2.5.6.2	Controlled NOT Gate (CNOT)	30
2.5.7	Universal Quantum Gates	30
2.5.8	Quantum Algorithms	30
3	Noise in Quantum Systems and Search Algorithm	33
3.1	Quantum Operations	34
3.1.1	System coupled to environment	34
3.1.2	Operator-Sum representation	35
3.1.3	Axiomatic Formulas	36
3.1.4	Revisiting the Postulates	37
3.1.4.1	Schmidt Decomposition	40
3.1.4.2	Purification	40
3.2	Quantum Noise	41
3.2.1	Modeling Noise as a Quantum Depolarizing Channel	42
3.2.1.1	Generalised Depolarizing Channel	42
3.2.1.2	Depolarizing Channel Noise Model	42
3.2.1.3	Error probability $e$ and its relation with the channel parameter $t$	43
3.2.1.4	Total vs Local Depolarizing Channel	45
3.2.1.5	Complete vs. Partial Depolarizing Channel	45
3.3	Ideal Grover's Quantum Search Algorithm	45
3.4	Influence of Noise on Grover's Quantum Search Algorithm	49
3.4.1	State Evolution with Error	50
3.4.2	Success Probability	50
4	Investigating Noisy Grover's Search using Quantum Switches	52
4.1	Quantum Switch	53
4.1.1	Introduction to Indefinite Causal Order	53
4.1.2	Mathematical Formulation of Quantum Switch	53
4.2	Application of Quantum Switch to Grover Search Algorithm	56
4.2.1	Framework 1, $F_{\xi}$ : Measurement after every iteration	58
4.2.1.1	State Evolution with Error	58
4.2.1.2	Success Probability	60
4.2.2	Framework 2, $F_{\omega}$ : Measurement at the end	61
4.2.2.1	Analysing the output state obtained after the first iteration	61
4.2.2.2	Block Matrix Notation	63
4.2.2.3	State Evolution with Error	66
4.2.2.4	Success Probability	69

5	Summary and Future Prospects . . . . .	72
	<i>Appendix A: Detailed Calculations</i> . . . . .	75
A.1	Calculations for the first iteration ( $k = 1$ ) in noisy Grover's Search with Algorithm with quantum switch . . . . .	75
A.2	Measurement of the system . . . . .	81
A.3	Calculations for next iterations ( $k > 1$ ) in Grover's Search Algorithm with the second framework . . . . .	83
A.4	Find the state after $k$ Grover iterations where the system is correlated with $k$ switches = $\rho_{\omega,k}(k)$ . . . . .	89

## List of Figures

Figure		Page
2.1	<i>Experimental Setup for Stern-Gerlach Experiment</i> By Tatoute - Own work, CC BY-SA 4.0 . . . . .	7
2.2	<i>Sequential Stern-Gerlach experiments: measurements alter states</i> Own work drawn using asymptote by Francesco Versaci . . . . .	9
2.3	Wave collapse on observing the particle at point C . . . . .	11
2.4	Bloch Sphere Representation . . . . .	28
2.5	main quantum algorithms and their relationships . . . . .	31
3.1	The Grover search algorithm with k Grover iterations . . . . .	46
3.2	Quantum circuit representation of Grover’s algorithm (The Grover oracle $U_\omega$ flips the sign of $ s\rangle$ if it is the marked element.) By Fawly - Own work, CC BY-SA 4.0	47
3.3	<b>Geometric Picture for the working of Grover’s Search algorithm:</b> Grover’s search algorithm employs a geometric approach to find a marked item within an unsorted database efficiently. Initially, the quantum state $ \psi\rangle$ is positioned at an angle $\theta/2$ relative to the state $ \alpha\rangle$ , which is orthogonal to $ \beta\rangle$ , the superposition of all potential solutions. The process begins with an oracle operation $O$ , which reflects $ \psi\rangle$ about $ \alpha\rangle$ , producing a new state $O \psi\rangle$ . Following this, the Grover diffusion operator, $2 \psi\rangle\langle\psi  - I$ , reflects $O \psi\rangle$ about $ \psi\rangle$ , yielding the state $G \psi\rangle$ . Each Grover iteration $G$ effectively rotates the state vector $ \psi\rangle$ by an angle $\theta$ towards $ \beta\rangle$ . Repeated iterations amplify the probability amplitude of the correct solution states. After roughly $\mathcal{O}(\sqrt{N/M})$ iterations, where $N$ is the total number of states and $M$ is the number of solutions, the state vector approaches $ \beta\rangle$ . At this point, measuring the quantum state on a computational basis yields a solution with high probability. The algorithm’s efficiency is notable because the angle $\theta$ is proportional to $\sqrt{M/N}$ , resulting in significantly fewer iterations compared to classical search methods. . . . .	48
3.4	This figure illustrates the effect of noise on the Grover operator $\mathcal{G}$ , shown by the shaded bar. Measurement at the end evaluates the impact of noise on the operator’s success probability. . . . .	49

4.1 *Fixed order vs superposition of orders. (a) A quantum particle, prepared in the state  $\rho$ , goes first through channel  $\mathcal{N}_1$  and then through channel  $\mathcal{N}_2$ . This configuration is associated with the state  $\rho_c = |1\rangle\langle 1|$  of a control qubit, in which the choice of order is encoded. (b) The quantum particle goes first through  $\mathcal{N}_2$  and then through  $\mathcal{N}_1$ . This alternative configuration is associated with the qubit state  $\rho_c = |0\rangle\langle 0|$ . (c) The quantum switch creates a superposition of the two configurations (a) and (b). It takes a control qubit in a superposition state, such as  $\rho_c = |+\rangle\langle +|$ , and correlates the order of the two channels with the state of the qubit.* . . . . . 54

4.2 Framework 1 ( $F_\xi$ ): The figure depicts the application of switch to Grover’s search algorithm (modeled by the Grover operator  $\mathcal{G}$ ) to mitigate the noise that arises because of the total depolarizing channel. The channel is the ash-colored bar, while the yellow region represents the switch. The dotted line indicates that the post-selection happens at every step, which is specific to this framework. . . . . 59

4.3 These plots show the effect of noise strength  $(1 - t)$  on the success probability of finding the target element in the search space in Noisy Grover’s search algorithm. We are taking the search space to be  $d = 2^4$ , and thus the algorithm should stop at  $k_{Gr} = \frac{\pi}{4}\sqrt{16} = \pi \approx 3$  iterations. The Plots from left to right show these variations for different iterations:  $k = 1$  (top-left),  $k = 2$  (top-right), and 3 (bottom-left). Here, the green curve represents the Success probability without using any switches, and the magenta curve represents the success probability on applying switches as described in fig.4.2 . . . . . 62

4.4 The figure depicts the application of the switch to Grover’s search algorithm (modeled by the Grover operator  $\mathcal{G}$ ). The channel is the ash-colored bar, while the yellow region represents the switch. The dotted line at the end indicates that the post-selection happens at the very end, which is specific to this particular framework. Here, we take a register of  $k$  switches, thus allowing us to preserve the system and switch correlation until the end. . . . . 65

4.5 These plots show the effect of noise strength  $(1 - t)$  on the success probability of finding the target element in the search space in Noisy Grover’s search algorithm. We are taking the search space to be  $d = 2^4$ , and thus the algorithm should stop at  $k_{Gr} = \frac{\pi}{4}\sqrt{16} = \pi \approx 3$  iterations. The Plots from left to right show these variations for different iterations:  $k = 1$  (top-left),  $k = 2$  (top-right), and 3 (bottom-left). Here, the green curve represents the Success probability without using any switches, and the magenta curve represents the success probability on applying switches as described in fig.4.4 . . . . . 71

## List of Tables

Table	Page
3.1 Summarising Closed Quantum Systems v/s Open Quantum Systems . . . . .	40
5.1 Coefficient of $\rho$ of Grover's search algorithm across up to 3 iterations for. Success probability can be calculated using . . . . .	73

## Chapter 1

### Introduction

“God still has a few tricks up his sleeve”

Stephen Hawking, [Does God Play Dice](#)

“If I have seen further, it is by standing on the shoulders of Giants.”

– Isaac Newton, [in a letter to Robert Hooke](#)

#### 1.1 Motivation

In the early inception of quantum computing, pivotal contributions were made by Paul Benioff and Richard Feynman, whose work laid the foundational stones for this revolutionary field. In the 1980s, Benioff was the first to propose a quantum mechanical model of a Turing machine [1], conceptualizing the idea of quantum computation in a formal, mathematical framework. This idea opened avenues for considering computation in the quantum realm, fundamentally differing from the conventional classical computational paradigms. Concurrently, Feynman articulated the intrinsic limitations of classical computers in simulating quantum phenomena in his 1981 talk [2]. He proposed the idea of a quantum computer, a machine that could simulate quantum systems efficiently and tackle problems beyond the reach of the classical model of computation. Since then, quantum computing has evolved dramatically from theoretical musings to a tangible research domain. Moreover, it was anticipated that around the early 2020s, Moore’s Law would start to intersect with quantum principles. This is primarily due to the onset of quantum effects as the scale of integration in conventional semiconductor chips is pushed to its limits. Quantum computing stands as a promising candidate for future technological advancement, offering the potential for significant speedup in various tasks over classical computing.

The present quantum era is dominantly characterized by noisy intermediate-scale quantum (NISQ) devices [3], a term coined and popularised by John Preskill [4], a class of quantum computers that operate on a modest number of qubits, ranging from a few tens to a few hundred and are constrained by operational noise and errors. Unlike fault-tolerant quantum computing paradigms, which demand many logical and ancillary qubits to implement error corrections, these devices operate in a regime where error correction is either minimal or absent, which makes them susceptible to various types of noise, such as phase-flip, bit-flip, and depolarizing noise. Owing to technological limitations, they exhibit short coherence times, often on the order of microseconds, further constraining the computational depth of quantum circuits that can be implemented effectively. NISQ technology serves as an intermediate milestone in the evolutionary roadmap of quantum computing as they have promising practical applications even with their imperfections, as they offer enough computational power to harness quantum phenomena, explore specific quantum algorithms, and provide insights into the challenges and potentials of scaling quantum systems. Noise can diminish the quantum advantage of quantum algorithms over classical computers. Especially for algorithms that rely on iterative processes, like Grover’s algorithm, noise can be particularly detrimental.

In classical computing, searching through an unsorted database of  $N$  items requires queries in the order of  $\Omega(N)$ <sup>1</sup>. Ideally, Grover’s search algorithm can offer a quadratic speedup over its classical counterpart for unstructured search problems. Grover’s search algorithm uses quantum superposition to achieve this task in order of  $O(\sqrt{N})$ <sup>2</sup> queries, demonstrating a quadratic speedup over the upper bound for linear search. It relies on iteratively refining states to arrive at a solution. However, its repetitive nature also magnifies errors’ disadvantages, as every iteration in Grover’s search algorithm presents opportunities for errors to be introduced or compounded, leading to a higher chance of getting incorrect outputs.

Researchers in the field of quantum computing are always on the lookout for different approaches to overcome these challenges posed by quantum noise. Recently, the potential of indefinite causal order (ICO) has captured significant attention as a resource for enhancing computational [5] and communication [6] capabilities under noisy scenarios. This novel concept leverages the peculiarities of quantum theory by putting quantum processes in superposition. A quantum switch is a quantum device that operationalizes the concept of ICO. Recent advancements have highlighted the prospect of using quantum switches to provide quantum advantages across a diverse array of tasks. Thus, our primary objective in this thesis is to investigate the application of quantum switches as a means of noise mitigation in noisy Grover’s search algorithm.

---

<sup>1</sup>Describes a lower bound on the time complexity (best possible worst-case scenario), showing the minimum amount of time an algorithm must take to complete as a function of the input size  $n$ .

<sup>2</sup>Describes an upper bound on the time complexity (worst-case scenario), showing the maximum amount of time an algorithm can take to complete as a function of the input size  $n$ .

## 1.2 Prior Work

A focus has been placed on the implications of noise on diverse quantum properties, ranging from entanglement [7][8] to broader correlation aspects [9], both in closed and open quantum systems [10]. Specifically, there have been significant insights into the influence of depolarizing channels, representing noise, on Grover’s search algorithm [11, 12]. The algorithm’s performance is greatly affected in cases involving imperfect oracles [13, 14] or when it encounters environmental quantum noise [15]. This reduction in efficiency highlights the algorithm’s sensitivity to external factors. While NISQ devices are inherently noisy, research is ongoing to mitigate the effects of noise. In particular, studies were reported on the effects of the depolarizing channel noise as a manifestation of noise on the Grover Search algorithm [11, 12]. Despite the challenges posed by noise in quantum search algorithms, several strategies have been proposed to maintain their quantum superiority [16, 17, 18].

Current research in quantum information theory is increasingly focusing on the concept of indefinite causal order (ICO) in quantum systems and its potential as a resource for various information processing tasks. Initially proposed by Hardy [19, 20] and applied in information theory by Chiribella, D’Ariano, Perinotti, and Valiron [21], this concept led to the development of a quantum switch. This switch uses an auxiliary system to control the order of two operations,  $E_1$  and  $E_2$ , on a quantum state  $\rho$ , rendering the order indefinite. Oreshkov [22] expanded this idea using process matrix formalism, creating a more comprehensive framework for causal indefiniteness. This approach has applications in areas such as quantum channel probing [23], nonlocal games [22], quantum metrology [24], quantum communication [25, 26, 27, 28, 29], reducing quantum communication complexity [6], and enhancing quantum computing [30, 31] and thermodynamics [32]. A notable recent application has been in transforming absolutely separable states into resourceful states [33]. Experimental validation of the practicality and benefits of indefinite causal order has also been recently achieved [34, 35, 36]. Apart from potential applications, it is also noteworthy that quantum switches have been studied in several configurations. Sazim, Sedlak, Singh, and Pati [37] studied the effects on quantum communication capacity with  $n$  channels in ICO. The quantum switch has also been applied on channels put in series and in [5], although the calculations were simplified by only considering the reverse and the forward order as in the case of Frey [38]. There has been recent work by Das and Bandyopadhyay [39] using the quantum switches in a hierarchical configuration implementing a switch of switches.

### 1.3 Research Focus and Contributions

The thesis aims to investigate how the concept of indefinite causal order can be effectively harnessed to mitigate the effects of noise that accumulates in Grover’s search algorithm across iterations and reduces its success probability at any given iteration. A systematic and comprehensive methodology is implemented in this thesis to address the problem of noise in Grover’s search algorithm and explore the potential effectiveness of applying quantum switches to mitigate that noise. We also briefly try to reason and uncover the fundamental mechanisms underlying noise reduction through this novel approach. Theoretical frameworks and principles related to quantum switches and the quantum search algorithm will be studied and analyzed. A noise model using a depolarising channel will be developed to describe the evolution of the noisy quantum search algorithm. Computational calculations will be run to calculate the success probability numerically and assess the performance of Grover’s search algorithms under different noise conditions, thus investigating the effectiveness of noise mitigation using quantum switches.

The study on the use of quantum switches to reduce noise in the quantum search algorithm has profound implications for the field of quantum computing. If successful, it could lead to the development of more resilient and error-tolerant quantum algorithms, particularly those that are affected by noise accumulation during iterations. This could unlock the potential for complex computational tasks that were previously impeded by noise and errors. The results of this research can also contribute to the development of strategies to enhance the performance and reliability of quantum computing systems for practical applications.

In this study, we explore a novel approach involving the use of a quantum switch to potentially lessen the adverse effects of noise, modeled by a depolarizing channel, on the success probability of the Grover search algorithm. We utilize success probability as a measure to gauge the switch’s ability to tolerate errors before the algorithm loses its speedup over its classical counterparts. We investigate two specific frameworks: one involves measuring at the end of each iteration to trace out the switch, and the other employs a register of switches, allowing the input state to pass through each iteration with different switches applied until the end without intermediate measurements. Our findings indicate that the second approach more effectively preserves the algorithm’s advantage in noisy conditions. The results demonstrate that the quantum switch can significantly counteract the noise accumulation in the algorithm, thus maintaining its effectiveness for a longer duration.

## 1.4 Outline

The rest of the thesis is structured as follows. Chapter 2, titled "Foundations and Preliminaries," lays the foundations of closed and open quantum theory, quantum information and computation, and mathematical prerequisites that are indispensable for comprehending the studies conducted. Chapter 3, titled "Noise in Quantum Search Algorithm," dives deeper into two themes: Noise and Grover's Search Algorithm. It starts by extending the theory of open quantum systems introduced in the previous chapter. It arrives at quantum channels and how they can be used to model noise, explicitly focusing on depolarising channels. We talk briefly about quantum algorithms before focusing our attention specifically on Grover's search algorithm and the effect of noise on it.

Chapter 4, aptly named "Applying Quantum Switches to Noisy Grover's Search Algorithm," contains the thesis's core original results and analyses, where we develop and study two frameworks that involving quantum switches applied to noise in Grover search iterations. We describe these frameworks and their respective effect on minimizing the impact of noise on the probability of finding the desired element in an unstructured database successfully. Chapter 5, titled "Conclusion and Future Works," concludes the thesis by summarising our findings and mentioning the openings of different possibilities for further research endeavors based on our findings.

## Chapter 2

### Foundations and Preliminaries

“It is impossible to communicate honestly the beauty of the laws of nature so that people can really feel it if people do not have a thorough knowledge of mathematics. I’m sorry, but it seems to be so”

“I am going to tell you what nature behaves like. If you will simply admit that maybe she does behave like this, you will find her a delightful, entrancing thing.”

– Richard P. Feynman, [The Character of Physical Law](#)<sup>1</sup>

This chapter aims to provide an exhaustive but brief introduction to the foundational concepts essential for understanding the rest of the thesis. It starts by talking about some historical contexts that led to the development of the quantum mechanical framework. We specifically talk about a pivotal experiment, the Stern-Gerlach experiment, to highlight the inadequacies and some salient features of quantum mechanics. The following section delves into the core mathematical structures and principles that are fundamental to the mechanics of quantum systems, presenting an organized and comprehensive overview of these critical concepts. Before diving into quantum theory and its postulates, we revisit concepts in linear algebra. Continuing, the chapter delves into the core hypotheses that form the foundation of quantum mechanics.

#### 2.1 Historical Overview

The first quarter of the 20th century marked a revolutionary era in natural sciences, characterized by a radical shift from classical to quantum physics. While classical physics had been the established framework for understanding the macroscopic aspects of our world, experiments like the Compton effect, the Franck-Hertz experiment, and the Davisson-Germer-Thomson experiment began to reveal its limitations. Moreover, some key theoretical developments, such as Planck’s radiation law, Einstein’s explanation of the photoelectric effect, and Bohr’s model of

---

<sup>1</sup>The lectures were delivered as part of the Messenger Lectures series. The quotes are from [The Relation of Mathematics and Physics](#) and [Probability and Uncertainty: the quantum mechanical view of nature](#) respectively.

the atom, suggested that classical theories were insufficient at the atomic scale. This led to a gradual but inevitable retreat from classical concepts. With its deterministic and continuous nature, classical physics failed to explain phenomena at the atomic and subatomic levels. It led to the emergence of quantum mechanics, a theory vastly more encompassing and applicable than its predecessor, that fundamentally altered our understanding of the microscopic world.

The transition from classical to quantum mechanics was neither immediate nor straightforward. It was a journey marked by trial and error, with great physicists like Heisenberg, Schrödinger, and Dirac contributing to the formulation of quantum mechanics. Unlike classical physics, quantum mechanics introduced concepts such as quantization, probability amplitude, and duality - initially met with skepticism but eventually became the cornerstone of modern physics.

In our quest to grasp the "quantum-mechanical way of thinking," we begin with the Stern-Gerlach experiment - an experiment that starkly illustrates the inadequacy of classical concepts.

### 2.1.1 Stern-Gerlach experiment

In 1921, Otto Stern envisioned a pioneering concept for an experiment that would later be actualized in collaboration with Walther Gerlach in Frankfurt. The Stern-Gerlach experiment [40] is a fundamental example of the deviation from classical physics and the necessity for an alternative theoretical framework. The experiment and its implications, which were instrumental in the advent of quantum theory, are elaborated below.

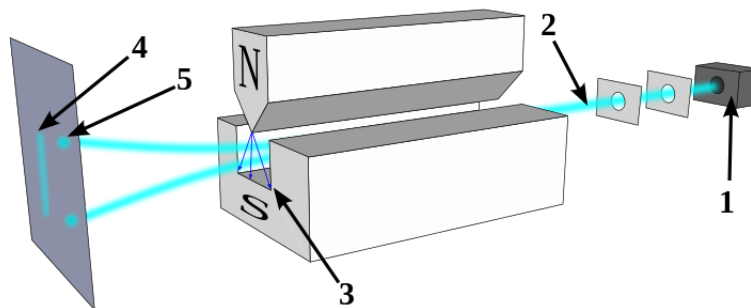


Figure 2.1: *Experimental Setup for Stern-Gerlach Experiment*  
By Tatoute - Own work, CC BY-SA 4.0

The experimental arrangement is depicted in fig.2.1. An oven (1) heats silver (Ag) atoms, which escape through an aperture. These atoms traverse a collimator (2), followed by exposure to a non-uniform magnetic field characterized by a gradient along the  $\hat{z}$ -axis (3) in the diagram. The impact of this magnetic field on the atoms will be discussed subsequently. Upon traversing the magnetic field, the atoms encounter a detection screen, recording their impact locations, which indicate the deflection they experienced due to the magnetic field.

Utilizing classical physics as a framework, one might hypothesize the following. In Ag atoms, out of 47 electrons, 46 form a symmetric cloud with no net angular momentum, but the 47th electron's unpaired spin results in a non-zero magnetic moment  $\mu$ , related to the spin  $S$  of the 47<sup>th</sup> electron as  $\mu \propto -S$ . The magnetic moment's interaction energy with the magnetic field is given by  $-\mu \cdot B$ , leading to a force in the  $\hat{z}$ -direction described by:

$$F_z = \frac{\partial}{\partial z}(\mu \cdot B) \approx \mu_z \frac{\partial B_z}{\partial z}$$

The magnetic moment's  $\hat{z}$ -component,  $\mu_z$ , determines the force magnitude experienced by the atom in the field. With the magnetic field intensifying upwards and its direction being negative  $\hat{z}$ , the atoms are subjected to forces based on the orientation and magnitude of  $\mu_z$ .

Classical physics would predict a continuous distribution of atom impacts along the z-axis on the detection screen (4). Contrary to this, the experimental results showed discrete impact points (5), indicating the quantization of magnetic moments in the  $\hat{z}$ -direction. The observed deflection pattern of the atomic beam, as shown in fig.2.1, remains consistent across different magnetic field orientations. The beam bifurcates into two distinct spots aligned with the magnet's poles, demonstrating the atoms' quantum properties. Specifically, atoms deflected upward, towards the north pole, are labeled as  $Z+$ , and those deflected downward, towards the south pole, as  $Z-$ . This labeling signifies the atoms' alignment with the magnetic field's orientation and discrete landing positions.

In subsequent experiments, as shown in fig.2.2, various configurations of sequential Stern-Gerlach apparatus were used to investigate this phenomenon further. These experiments led to two critical insights:

1. Using two  $\hat{z}$ -oriented Stern-Gerlach devices in sequence, with only the  $Z+$  beam from the first directed into the second, confirmed the persistence of the  $Z+$  state.
2. An arrangement of a  $\hat{z}$ -oriented followed by an  $\hat{x}$ -oriented Stern-Gerlach device revealed that atoms initially in the  $Z+$  state could exhibit both  $X+$  and  $X-$  states.
3. The most intriguing setup involved three devices in  $\hat{z}$ - $\hat{x}$ - $\hat{z}$  orientation. Atoms initially filtered as  $Z+$  and then as  $X+$  showed both  $Z+$  and  $Z-$  outcomes in the final stage, suggesting the collapse of quantum states upon measurement.

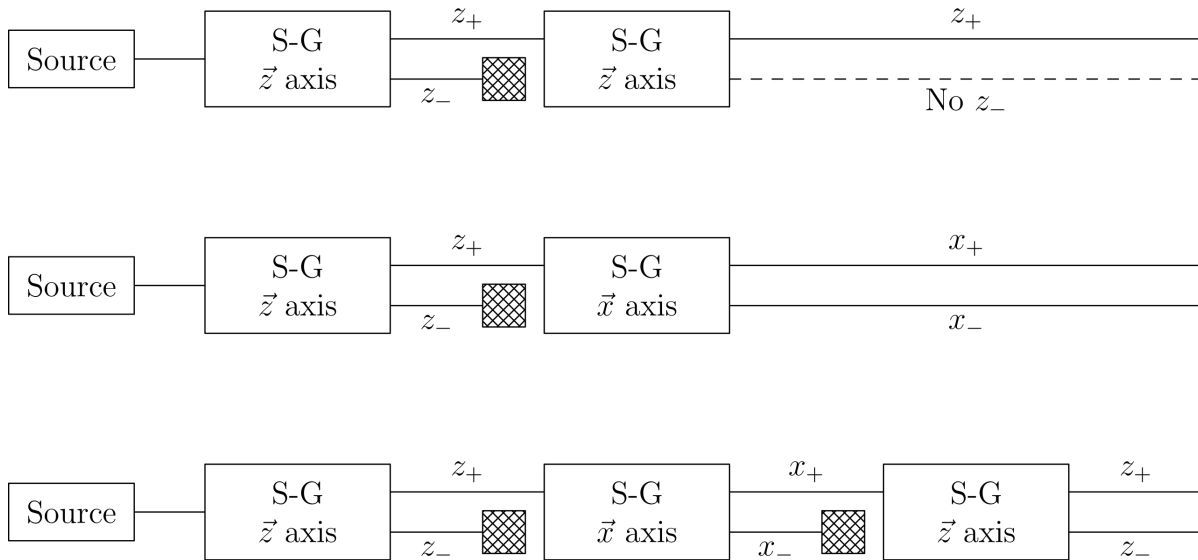


Figure 2.2: *Sequential Stern-Gerlach experiments: measurements alter states*  
 Own work drawn using asymptote by Francesco Versaci

### Insights from the Stern-Gerlach Experiment

The Stern-Gerlach experiment offers several key insights into the nature of quantum mechanics.

**Quantization of Spin Angular Momentum** Firstly, it demonstrates that the spin angular momentum of particles is quantized. Had the spin angular momentum been continuous, a varied range of deflections would have resulted in a continuous distribution on the detector instead of discrete spots. Instead, we observe that atoms, upon passing through the experiment's apparatus, impacted only two specific regions on the detector.

**Quantum Superposition of Spin States** Consider the modified Stern-Gerlach setup as depicted in fig.2.2(b). The splitting of the atom stream into  $+\hat{x}$  and  $-\hat{x}$  directions when subjected to the second Stern-Gerlach apparatus oriented along the  $\hat{x}$  axis, substantiates the existence of spin in a superposition state, revealing the probabilistic nature of quantum measurement outcomes.

**Impact of Measurement on Quantum State** The third vital conclusion pertains to the influence of measurement on quantum states. Considering the experiment with three sequential measurements as shown in fig.2.2(c), it becomes evident that each measurement along a particular axis (first  $\hat{z}$ , then  $\hat{x}$ , and finally  $\hat{z}$  again) alters the quantum state. Interestingly, the final measurement results in a split along both  $+\hat{z}$  and  $-\hat{z}$  directions, indicating that the prior measurement along the  $\hat{x}$  axis has perturbed the initially homogeneous quantum state. This phenomenon also illustrates the uncertainty principle, highlighting the non-commutativity of spin measurements along different axes.

The Stern-Gerlach experiment is a paradigmatic example of how empirical evidence can compel us to revise our fundamental postulates, leading to the development of physical laws that embrace the peculiarities of the quantum realm.

Quantum mechanics has an element of unpredictability, where knowing a particle's wave function does not guarantee predicting its exact behavior. Consider the act of measuring a particle's position and finding it at a specific location, say point C. This scenario raises an intriguing question: Was the particle actually at point C before we measured it?<sup>2</sup> Historically, this question has opened up three main lines of thought. The realist approach suggests that the particle was indeed at point C all along, hinting that quantum mechanics might not tell the whole story by failing to predict the particle's exact location. Advocates of this view believe in the concept of hidden variables that could fill in the gaps in our understanding. On the other hand, the Copenhagen interpretation, a cornerstone of orthodox quantum mechanics, argues that the particle did not have a definite position until it was measured. This perspective has become the go-to explanation for many physicists, suggesting that the act of measurement itself brings the particle's position into reality, confined within the probabilistic bounds set by its wave function. Then there is the agnostic viewpoint, which sidesteps making any concrete claims about the particle's state before measurement, considering such discussions to be more philosophical than scientific.

However, Bell's groundbreaking work in 1964 has strongly backed the Copenhagen interpretation, leading to a consensus that particles do not possess definite attributes until they are observed. This exploration of quantum uncertainty and the discussions surrounding the nature of quantum states highlight why the Copenhagen interpretation has risen to prominence. It elegantly bridges the gap between the quantum world's inherent mysteries and the concrete outcomes we observe in experiments, viewing the collapse of the wave function as an integral part of measuring a particle. Pioneered by giants like Bohr and Heisenberg, this interpretation has profoundly influenced how we understand and engage with quantum mechanics. In this thesis, we are not looking to question the Copenhagen interpretation but rather to build on the solid foundation it provides as we venture further into the quantum domain.

## 2.2 Mathematical Preliminaries

Quantum Computing and Quantum Information Theory are deeply rooted in the principles of linear algebra and functional analysis. The mathematical formalism introduced in this section,

---

<sup>2</sup>When introducing quantum mechanics to an audience with basic knowledge of units and measurement, one can start with this famous example from the textbook of Griffiths and Schroeter, which is also quoted in a lovely article by Mermin titled "Is the moon there when nobody looks?" in Physics Today. This example is a thought experiment that encourages one to break from the classical approach of measurement and state. It also invites us to ponder the philosophical and quantum-mechanical aspects of reality. This was also, incidentally, my first introduction to the quantum mechanical way of thinking

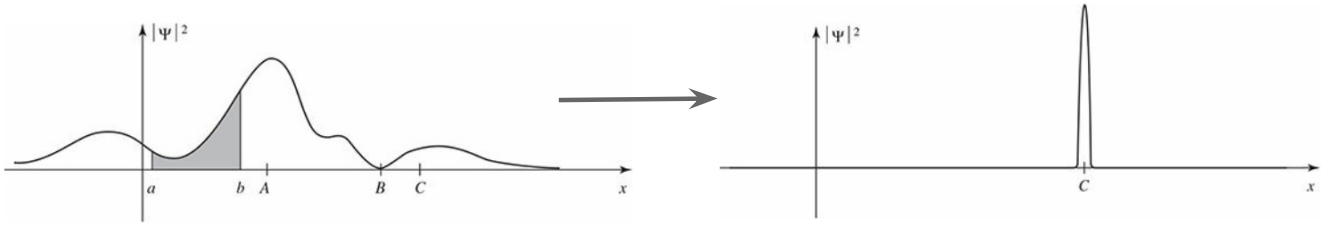


Figure 2.3: Wave collapse on observing the particle at point C

especially the concept of Hilbert spaces, is integral to the mathematical apparatus in quantum theory, providing a rigorous foundation for describing quantum systems.[44, 45]

### 2.2.1 Vector Spaces

A **field** is a set  $\mathcal{F}$  equipped with two operations, addition and multiplication, that satisfies the properties of closure, associativity, commutativity, the existence of identity elements (0 for addition, 1 for multiplication, where  $0 \neq 1$ ), the existence of additive inverses, the existence of multiplicative inverses for all non-zero elements, and the distributive property of multiplication over addition. A **vector space**  $\mathcal{V}$  is a set of objects  $\vec{v}$  called vectors, defined over a field  $\mathcal{F}$  of scalars, and is equipped with two operations, satisfying the following rules:

- **Vector Addition:** For all  $\vec{u}, \vec{v} \in \mathcal{V}$ ,  $\vec{u} + \vec{v} \in \mathcal{V}$ .
  1. **Associativity:** For all  $\vec{u}, \vec{v}, \vec{w} \in \mathcal{V}$ ,  $(\vec{u} + \vec{v}) + \vec{w} = \vec{u} + (\vec{v} + \vec{w})$ .
  2. **Commutativity:** For all  $\vec{u}, \vec{v} \in \mathcal{V}$ ,  $\vec{u} + \vec{v} = \vec{v} + \vec{u}$ .
  3. **Additive Identity:** There exists a vector  $\vec{0} \in \mathcal{V}$  such that  $\vec{v} + \vec{0} = \vec{v}$  for every  $\vec{v} \in \mathcal{V}$ .
  4. **Additive Inverse:** For every  $\vec{v} \in \mathcal{V}$ , there exists a vector  $-\vec{v} \in \mathcal{V}$  such that  $\vec{v} + (-\vec{v}) = \vec{0}$ .
- **Scalar Multiplication** For every scalar  $c \in \mathcal{F}$  and vector  $\vec{v} \in \mathcal{V}$ ,  $c\vec{v} \in \mathcal{V}$ .
  1. **Distributivity over Vector Addition:** For all  $c \in \mathcal{F}$  and  $\vec{u}, \vec{v} \in \mathcal{V}$ ,  $c(\vec{u} + \vec{v}) = c\vec{u} + c\vec{v}$ .
  2. **Distributivity over Field Addition:** For all  $c, d \in \mathcal{F}$  and  $\vec{v} \in \mathcal{V}$ ,  $(c+d)\vec{v} = c\vec{v} + d\vec{v}$ .
  3. **Associativity:** For all  $c, d \in \mathcal{F}$  and  $\vec{v} \in \mathcal{V}$ ,  $c(d\vec{v}) = (cd)\vec{v}$ .
  4. **Multiplicative Identity:** For every  $\vec{v} \in \mathcal{V}$ ,  $1\vec{v} = \vec{v}$ , where 1 is the multiplicative identity in  $\mathcal{F}$ .

Vector spaces over  $\mathbb{C}$  are called complex vector spaces, and those over  $\mathbb{R}$  are real vector spaces. A subset  $\mathcal{W}$  of  $\mathcal{V}$  ( $\mathcal{W} \subseteq \mathcal{V}$ ) is referred to as a (linear) subspace if it, too, forms a vector space under these operations.

### Bases and linear independence

A collection of vectors  $\{\vec{v}_1, \vec{v}_2, \dots, \vec{v}_m\} \in \mathcal{V}$  is termed **linearly independent**, if  $\sum_{i=1}^m a_i \vec{v}_i = 0$  implies that each scalar  $a_i$  is zero.

The **span** of a set of vectors  $\{\vec{v}_1, \vec{v}_2, \dots, \vec{v}_m\} \subseteq \mathcal{V}$  in the field  $\mathcal{F}$  is the collection of all vectors that can be represented as a linear combination of these vectors, i.e.,  $\sum_{i=1}^m a_i \vec{v}_i$  with  $a_i \in \mathcal{F}$ .

A **basis** of  $\mathcal{V}$  is a linearly independent set  $\mathcal{B}$  whose span is the entire space  $\mathcal{V}$ . The **dimension**  $d$  of  $\mathcal{V}$  is defined as the number of elements in any basis of  $\mathcal{V}$ . Given an ordered basis  $\mathcal{B} = \{\vec{v}_1, \vec{v}_2, \dots, \vec{v}_d\}$ , any vector  $\vec{w} \in \mathcal{V}$  can be uniquely expressed as a linear combination  $\sum_{i=1}^d w_i \vec{v}_i$  and represented as  $(w_1, w_2, \dots, w_d)$ .

### 2.2.2 Inner Product Spaces

An **inner product** on a vector space  $\mathcal{V}$  is a **sesquilinear** (linear in one argument, and the linearity of the other argument is modified by complex conjugation) function  $\langle \cdot, \cdot \rangle$  from  $\mathcal{V} \times \mathcal{V}$  to field  $\mathcal{F}$  of  $\mathbb{C}$  or  $\mathbb{R}$ , that maps every ordered pair of vectors  $\vec{v}, \vec{w} \in \mathcal{V}$ , to a scalar  $\langle \vec{v}, \vec{w} \rangle \in \mathcal{F}$  satisfying:

1. **Positive Definiteness:** For all  $\vec{v} \in \mathcal{V}$ ,  $\langle \vec{v}, \vec{v} \rangle \geq 0$ . And  $\langle \vec{v}, \vec{v} \rangle = 0$  if and only if  $\vec{v} = \vec{0}$ .
2. **Linearity in second element:**  $\forall \vec{u}, \vec{v}, \vec{w} \in \mathcal{V}$ ,  $\langle \vec{v}, \vec{u} + \vec{w} \rangle = \langle \vec{v}, \vec{u} \rangle + \langle \vec{v}, \vec{w} \rangle$ . And  $\forall c \in \mathcal{F}$ ,  $\langle \vec{u}, c\vec{v} \rangle = c\langle \vec{u}, \vec{v} \rangle$ .
3. **Conjugate Symmetry:** For all  $\vec{u}, \vec{v} \in \mathcal{V}$ ,  $\langle \vec{u}, \vec{v} \rangle = (\langle \vec{v}, \vec{u} \rangle)^*$ , where  $*$  denotes complex conjugate.

We denote positive square root of  $\langle \vec{v}, \vec{v} \rangle$  by  $\|\vec{v}\|$ , called the **norm** of  $\vec{v}$  with respect to the inner product. This norm corresponds to the Euclidean norm and is often referred to as the "magnitude" of the vector. A **unit vector** is obtained by dividing a non-zero vector by its norm. A collection of vectors  $\{\vec{v}_i\}$  is termed orthogonal if  $\langle \vec{v}_i, \vec{v}_j \rangle = 0$  for  $i \neq j$ . If these vectors also have a norm of 1, the set is classified as **orthonormal**.

An **inner product space** is a vector space  $\mathcal{V}$  equipped with an inner product.

### Dirac Notation and Dual Spaces

Since quantum mechanics is the primary focus of this thesis, we will introduce Dirac notation, also known as bra-ket notation, introduced by physicist Paul Dirac in his 1939 work [46]. It is a

standard notation for linear algebraic objects in complex vector spaces. In quantum mechanics, vectors  $\vec{v}$  within a vector space are conventionally denoted as  $|v\rangle$ , often referred to as a *ket* vector. We can also denote the inner product as  $\langle v|, |w\rangle$ , though the standard quantum mechanical notation for the inner product is written as  $\langle v|w\rangle$ , which justifies the terminology of the notation.<sup>3</sup> Here,  $|v\rangle$  and  $|w\rangle$  are vectors belonging to an inner product space, and  $\langle v|$  is what we call a **dual vector**, often referred to as a *bra* vector. This concept of dual vectors is commonly referred to as **linear functionals** because,  $\langle v|$  is a linear function  $\langle v| : \mathcal{V} \rightarrow \mathcal{F}$ , mapping a vector  $|w\rangle$  from inner product space  $\mathcal{V}$  to a scalar  $\langle v|w\rangle \in \mathcal{F}$ , field of  $\mathbb{C}$  or  $\mathbb{R}$ .

$$\langle v|(|w\rangle) \equiv \langle v|, |w\rangle \equiv \langle v|w\rangle \quad (2.1)$$

## Matrix Representation of Vectors

Given a vector  $|v\rangle \in \mathcal{V}$  of dimension  $d$ , and an orthonormal basis,  $\{|v_i\rangle\}$  where  $i = 1 \dots d$ ,  $|v\rangle$  can be expressed in terms of the basis vectors as:

$$|v\rangle = \sum_i c_i |v_i\rangle, \quad \text{where } c_i = \langle v_i|v\rangle. \quad (2.2)$$

Once we establish such an orthonormal basis, we observe that every vector within this vector space is a tuple of scalars  $c_i \in \mathcal{F}$  (often  $\mathbb{C}$  or  $\mathbb{R}$ ) of size  $d$ . We conventionally write these as  $d \times 1$  column matrices. E.g., consider the vector space  $\mathbb{C}^2$  over  $\mathbb{C}$ . An orthonormal basis for this space is given by the vectors  $|v_1\rangle$  and  $|v_2\rangle$  and any vector  $|v\rangle = (a_1, a_2)$  in  $\mathbb{C}^2$  can be expressed as a linear combination of  $|v_1\rangle$  and  $|v_2\rangle$  as:

$$|v\rangle = a_1|v_1\rangle + a_2|v_2\rangle = \begin{pmatrix} a_1 \\ a_2 \end{pmatrix} \quad \text{where, } |v_1\rangle = \begin{pmatrix} 1 \\ 0 \end{pmatrix} |v_2\rangle = \begin{pmatrix} 0 \\ 1 \end{pmatrix} \quad (2.3)$$

We can think of dual vectors as row matrices.

### 2.2.3 Linear Operators and Matrix Transformations

Linear operators are functions  $\mathbf{A} : \mathcal{V} \rightarrow \mathcal{W}$  that map vectors from one space to another while preserving linearity.

$$\mathbf{A} \left( \sum_i c_i |v_i\rangle \right) = \sum_i c_i \mathbf{A}|v_i\rangle \quad (2.4)$$

$\mathbf{A}(|v\rangle)$  is often shortened as  $\mathbf{A}|v\rangle$  and a mapping from  $\mathcal{V}$  to itself is simply said to be a linear operator  $\mathbf{A}$  on  $\mathcal{V}$ . For linear operators,  $\mathbf{A} : \mathcal{V} \rightarrow \mathcal{W}$  and  $\mathbf{B} : \mathcal{W} \rightarrow \mathcal{X}$ , their composition  $\mathbf{BA}$  is defined as:  $(\mathbf{BA})(|v\rangle) \equiv \mathbf{B}(\mathbf{A}(|v\rangle))$ .  $\mathbf{BA}|v\rangle$  is used as shorthand for  $(\mathbf{BA})(|v\rangle)$ .

---

<sup>3</sup>The term "bra-ket" is derived from the word "bracket," where a "bra"  $\langle\phi|$  and a "ket"  $|\psi\rangle$  form a complete bracket  $\langle\phi|\psi\rangle$

### 2.2.3.1 Matrix Representation of Linear Operators

Given a linear operator  $\mathbf{A} : \mathcal{V} = \mathcal{F}^n \rightarrow \mathcal{W} = \mathcal{F}^m$  both defined over  $\mathcal{F}$ , with bases  $|v_1\rangle, \dots, |v_m\rangle$  and  $|w_1\rangle, \dots, |w_n\rangle$  respectively, the operator can be represented as an  $m \times n$  matrix  $\mathbf{A}$  with entries  $A_{ij}$  and its action on a vector follows matrix multiplication rules:

$$\mathbf{A}|v_j\rangle = \sum_i A_{ij}|w_i\rangle \quad (2.5)$$

Given the action of a linear operator  $\mathbf{X}$  on  $\mathbb{C}^2$ , with basis vectors  $|0\rangle = \begin{pmatrix} 1 \\ 0 \end{pmatrix}$  and  $|1\rangle = \begin{pmatrix} 0 \\ 1 \end{pmatrix}$ .

$$\mathbf{X}|0\rangle = X_{11}|0\rangle + X_{21}|1\rangle = |1\rangle \Rightarrow X_{11} = 0, X_{21} = 1$$

$$\mathbf{X}|1\rangle = X_{12}|0\rangle + X_{22}|1\rangle = |0\rangle \Rightarrow X_{12} = 1, X_{22} = 0$$

Therefore, the matrix representation of  $\mathbf{X}$  is  $\begin{pmatrix} 0 & 1 \\ 1 & 0 \end{pmatrix}$ , which is also called a Pauli-X matrix, named after Wolfgang Pauli, and belongs to a family of matrices that represent linear operators of significance, as discussed in later section 2.5.5.1. This matrix-operator equivalence allows for a seamless interchange between concepts from matrix theory and operator theory, enriching the understanding of linear transformations in vector spaces.

### 2.2.3.2 Eigenvalues and Eigenvectors

For a linear operator  $\mathbf{A}$  on  $\mathcal{V}$ , an eigenvector  $|v\rangle \in \mathcal{V}$  of  $\mathbf{A}$  is defined as a vector which, when acted upon by  $\mathbf{A}$ , results in a scalar multiple of itself. This relationship is expressed as:

$$\mathbf{A}|v\rangle = \lambda|v\rangle, \quad (2.6)$$

where  $\lambda$  is the eigenvalue corresponding to the eigenvector  $|v\rangle$ . Geometrically, eigenvectors of  $\mathbf{A}$  are vectors that undergo linear transformation exclusively in the form of elongation or contraction, with the scaling factor being the corresponding eigenvalue. <sup>4</sup>

### 2.2.3.3 Commutator of two operators

The commutator for a pair of linear operators  $A$  and  $B$  is defined as  $C = [A, B] = AB - BA$ . Operators  $A$  and  $B$  are considered to commute if and only if their commutator  $[A, B] = 0$ . Conversely, a non-zero commutator indicates non-commutativity and serves as a quantifier for it. The properties of commutators include:

1. The distributive property over product operations holds, such that  $[A, BC] = [A, B]C + B[A, C]$  and similarly,  $[AB, C] = A[B, C] + [A, C]B$ .

---

<sup>4</sup>explained beautifully with simulations in this playlist by 3b1b: [Essence of Linear Algebra](#)

2. Self-commutation is always zero,  $[A, A] = 0$ , and this extends to powers of the operator, implying  $[A, A^n] = 0$  for any positive integer  $n$ .

#### 2.2.3.4 Linear Transpose of a matrix and Adjoint of an operator

For a matrix  $\mathbf{A}$ , its transpose  $\mathbf{A}^T$  is obtained by flipping  $\mathbf{A}$  over its diagonal. Key properties include:  $(\mathbf{A}^T)^T = \mathbf{A}$ ,  $(\mathbf{A} + \mathbf{B})^T = \mathbf{A}^T + \mathbf{B}^T$ ,  $(c\mathbf{A})^T = c\mathbf{A}^T$  and,  $(\mathbf{AB})^T = \mathbf{B}^T \cdot \mathbf{A}^T$  for matrices  $\mathbf{A}$ ,  $\mathbf{B}$  and scalar  $c$ . We can extend this to the concept of an adjoint, which is crucial in operator theory. The adjoint is obtained by taking the **element-wise conjugate** and **transpose** of the operator matrix, also called Hermitian conjugate. For any operator  $\mathbf{A}$  on an inner product space  $\mathcal{V}$ , its adjoint denoted by  $\mathbf{A}^\dagger$  is defined as:

$$\forall |u\rangle, |v\rangle \in \mathcal{V}, \quad \langle u | \mathbf{A} | v \rangle = \langle \mathbf{A}^\dagger u | v \rangle. \quad (2.7)$$

**Hermitian operators:** An operator  $\mathbf{H}$  is Hermitian if it equals its adjoint:  $\mathbf{H} = \mathbf{H}^\dagger$ .

$$(\mathbf{H} |v\rangle)^\dagger = (\lambda |v\rangle)^\dagger \implies |v\rangle^\dagger \mathbf{H}^\dagger = \lambda^\dagger |v\rangle^\dagger \implies |v\rangle^\dagger \mathbf{H} |v\rangle = \lambda^\dagger |v\rangle^\dagger |v\rangle \implies \lambda |v\rangle^\dagger |v\rangle = \lambda^\dagger |v\rangle^\dagger |v\rangle$$

Thus,  $\lambda = \lambda^\dagger$  implies that the eigenvalues of Hermitian operators are real.

**Unitary operators:** An operator  $\mathbf{U}$  is unitary if  $\mathbf{U}\mathbf{U}^\dagger = \mathbf{U}^\dagger\mathbf{U} = \mathbb{I}$ , where  $\mathbb{I}$  is the identity operator, signifying no change or transformation.

#### 2.2.3.5 Tensor Products and Composition of vector spaces

For a matrix  $\mathbf{A} = A_{ij}$  of dimensions  $m \times n$  and another matrix  $\mathbf{B}$  of dimensions  $m' \times n'$ . The tensor product (also known as the Kronecker product) of  $\mathbf{A}$  and  $\mathbf{B}$  is the  $mm' \times nn'$  matrix given by:

$$A \otimes B = \begin{pmatrix} A_{11}B & \cdots & A_{1n}B \\ A_{21}B & \cdots & A_{2n}B \\ \vdots & \ddots & \vdots \\ A_{m1}B & \cdots & A_{mn}B \end{pmatrix}. \quad (2.8)$$

The concept of tensor products in matrix notation is exemplified through block matrix multiplication. The following examples illustrate the utility of block matrix representation in the computation of tensor products of two vectors and operators, which will be used extensively for some parts of the thesis.

$$\begin{pmatrix} a_1 \\ a_2 \end{pmatrix} \otimes \begin{pmatrix} b_1 \\ b_2 \end{pmatrix} = \begin{pmatrix} a_1 \begin{pmatrix} b_1 \\ b_2 \end{pmatrix} \\ a_2 \begin{pmatrix} b_1 \\ b_2 \end{pmatrix} \end{pmatrix} = \begin{pmatrix} a_1 b_1 \\ a_1 b_2 \\ a_2 b_1 \\ a_2 b_2 \end{pmatrix}. \quad (2.9)$$

$$\begin{pmatrix} a_{11} & a_{12} \\ a_{21} & a_{22} \end{pmatrix} \otimes \begin{pmatrix} b_{11} & b_{12} \\ b_{21} & b_{22} \end{pmatrix} = \begin{pmatrix} a_{11} \begin{pmatrix} b_{11} & b_{12} \\ b_{21} & b_{22} \end{pmatrix} & a_{12} \begin{pmatrix} b_{11} & b_{12} \\ b_{21} & b_{22} \end{pmatrix} \\ a_{21} \begin{pmatrix} b_{11} & b_{12} \\ b_{21} & b_{22} \end{pmatrix} & a_{22} \begin{pmatrix} b_{11} & b_{12} \\ b_{21} & b_{22} \end{pmatrix} \end{pmatrix} = \begin{pmatrix} a_{11}b_{11} & a_{11}b_{12} & a_{12}b_{11} & a_{12}b_{12} \\ a_{11}b_{21} & a_{11}b_{22} & a_{12}b_{21} & a_{12}b_{22} \\ a_{21}b_{11} & a_{21}b_{12} & a_{22}b_{11} & a_{22}b_{12} \\ a_{21}b_{21} & a_{21}b_{22} & a_{22}b_{21} & a_{22}b_{22} \end{pmatrix} \quad (2.10)$$

Tensor products can combine different vector spaces. Given two vector spaces  $\mathcal{V}$  and  $\mathcal{V}'$ , with dimensions  $d$  and  $d'$ , and bases  $\{v_0, \dots, v_{d-1}\}$  and  $\{v'_0, \dots, v'_{d'-1}\}$  respectively, their formed tensor product space  $\mathcal{T} = \mathcal{V} \otimes \mathcal{V}'$  is a  $d \cdot d'$ -dimensional space spanned by  $\{v_i \otimes v'_j | 0 \leq i \leq d-1, 0 \leq j \leq d'-1\}$ . Applying a linear operation  $\mathbf{A}$  to  $\mathcal{V}$  and  $\mathbf{B}$  to  $\mathcal{V}'$  corresponds to applying the tensor product  $\mathbf{A} \otimes \mathbf{B}$  to  $\mathcal{T}$ . It is important to note that the tensor product of two scalar values ( $1 \times 1$  matrices) is simply a scalar, and the tensor product of two column vectors is a column vector. Some properties of tensor products include:

- Scalar multiplication:  $c(\mathbf{A} \otimes \mathbf{B}) = (c\mathbf{A}) \otimes \mathbf{B} = \mathbf{A} \otimes (c\mathbf{B})$  for any scalar  $c$ .
- Distributive property:  $\mathbf{A} \otimes (\mathbf{B} + \mathbf{C}) = (\mathbf{A} \otimes \mathbf{B}) + (\mathbf{A} \otimes \mathbf{C})$ .
- Associative property:  $\mathbf{A} \otimes (\mathbf{B} \otimes \mathbf{C}) = (\mathbf{A} \otimes \mathbf{B}) \otimes \mathbf{C}$ .
- Multiplicative property:  $(\mathbf{A} \otimes \mathbf{B})(\mathbf{C} \otimes \mathbf{D}) = (\mathbf{AC}) \otimes (\mathbf{BD})$ .
- Conjugate transpose:  $(\mathbf{A} \otimes \mathbf{B})^\dagger = \mathbf{A}^\dagger \otimes \mathbf{B}^\dagger$ , with the order of tensor factors remaining unchanged.
- The tensor product obeys bilinearity:  $(\alpha|v_1\rangle + \beta|v'_1\rangle) \otimes |v_2\rangle = \alpha|v_1\rangle \otimes |v_2\rangle + \beta|v'_1\rangle \otimes |v_2\rangle$ .
- The inner product in the composite space is  $\langle v_1|v'_1\rangle \langle v_2|v'_2\rangle$ .

### 2.2.3.6 Trace of an Operator

For an operator  $\mathbf{A}$  acting on  $\mathcal{V}$ , its trace is defined as:

$$\text{Tr}[A] = \sum_i \langle i|A|i\rangle, \quad \text{where } \{|i\rangle\}, i = 1 \dots d \text{ represents an orthonormal basis of } \mathcal{V}. \quad (2.11)$$

When  $\mathbf{A}$  is represented as a matrix, the trace corresponds to the sum of its diagonal elements which follows:

- Additive property:  $\text{Tr}[\mathbf{A} + \mathbf{B}] = \text{Tr}[\mathbf{A}] + \text{Tr}[\mathbf{B}]$ .
- Cyclic property:  $\text{Tr}[\mathbf{ABC}] = \text{Tr}[\mathbf{BCA}] = \text{Tr}[\mathbf{CAB}]$ .  $\text{Tr}[\mathbf{AB}] = \text{Tr}[\mathbf{BA}]$  follows from here.
- Relation to eigenvalues:  $\text{Tr}[\mathbf{A}]$  equals the sum of the eigenvalues of  $\mathbf{A}$ .
- Trace of Tensor product:  $\text{Tr}[\mathbf{A} \otimes \mathbf{B}] = \text{Tr}[\mathbf{A}]\text{Tr}[\mathbf{B}]$ .

## Outer Product representation of Linear operators

Given vectors from two inner product spaces,  $|v\rangle, |v'\rangle \in \mathcal{V}$ , and  $|w\rangle \in \mathcal{W}$ , we define  $|w\rangle\langle v|$  as the linear operator that maps from  $|v'\rangle$  from  $\mathcal{V}$  to  $\mathcal{W}$  as:

$$(|w\rangle\langle v|)(|v'\rangle) \equiv |w\rangle\langle v|v'\rangle = \langle v|v'\rangle|w\rangle \quad (2.12)$$

It can be interpreted as: representing the action of  $|w\rangle\langle v|$  on  $|v'\rangle$  and also as:  $|w\rangle$  times the scalar  $\langle v|v'\rangle$ . Linear combinations of such outer product operators will also be linear operators, and hence the operator  $\sum_i a_i |w_i\rangle\langle v_i|$  acts on  $|v'\rangle$  to produce  $(\sum_i a_i |w_i\rangle\langle v_i|)|v'\rangle = \sum_i a_i |w_i\rangle\langle v_i|v'\rangle$ . Thus eq.(2.2), can be written as:

$$|v\rangle = \left( \sum_i |v_i\rangle\langle v_i| \right) |v\rangle \text{ implying } \sum_i |v_i\rangle\langle v_i| = \mathbb{I}, \quad (2.13)$$

where,  $\{|v_i\rangle\}$  is an orthonormal basis for  $\mathcal{V}$  and  $\mathbb{I}$  is the identity operator in  $\mathcal{V}$ . This illustrates the **completeness relation**, and we call the set  $\{|v_i\rangle\}$  is complete.

For a linear operator  $\mathbf{A} : \mathcal{V} \rightarrow \mathcal{W}$ , with orthonormal bases  $\{|v_i\rangle\}$  in  $\mathcal{V}$  and  $\{|w_j\rangle\}$  in  $\mathcal{W}$ , we can use the completeness relation to express  $\mathbf{A}$  as:

$$\mathbf{A} = \mathbb{I}_{\mathcal{W}} \mathbf{A} \mathbb{I}_{\mathcal{V}} = \sum_{ij} |w_j\rangle\langle w_j| \mathbf{A} |v_i\rangle\langle v_i| = \sum_{ij} \langle w_j| \mathbf{A} |v_i\rangle |w_j\rangle\langle v_i| \text{ where } A_{ji} = \langle w_j| \mathbf{A} |v_i\rangle \quad (2.14)$$

### 2.2.3.7 Partial Trace

The partial trace, for an operator  $|a_1\rangle\langle a_2| \otimes |b_1\rangle\langle b_2|$ , over system B is a map of operators defined as:

$$\text{Tr}_B[|a_1\rangle\langle a_2| \otimes |b_1\rangle\langle b_2|] \equiv |a_1\rangle\langle a_2| \text{Tr}_B[|b_1\rangle\langle b_2|], \quad (2.15)$$

with  $|a_1\rangle$  and  $|a_2\rangle$  in  $\mathbf{A}$ 's state space, and  $|b_1\rangle$  and  $|b_2\rangle$  in  $\mathbf{B}$ 's. The trace on the right-hand side is the usual trace for system B, so  $\text{Tr}_B[|b_1\rangle\langle b_2|] = \langle b_2|b_1\rangle$ . This operation is linear in its input by definition.

### 2.2.3.8 Spectral Decomposition

A self-adjoint operator  $\mathbf{A}$  can be represented through its spectral decomposition. The eigenstates of  $\mathbf{A}$  form a complete orthonormal set in  $\mathcal{H}$ , allowing  $\mathbf{A}$  to be expressed as:

$$\mathbf{A} = \sum_i a_i E_i, \quad (2.16)$$

where  $a_i$  denotes the eigenvalues of  $\mathbf{A}$ , and  $E_i$  is the orthogonal projection onto the eigenspace associated with  $a_i$ . These projections  $E_i$  satisfy the orthogonality and self-adjoint conditions:

$$E_n E_m = \delta_{n,m} E_n, \quad E_n^\dagger = E_n, \quad \delta_{n,m} = 1, \text{ for } m = n, \text{ otherwise, } \delta_{n,m} = 0$$

$\delta_{n,m}$  is called the Kronecker delta. The orthogonal projection onto a one-dimensional space spanned by a vector  $|\psi\rangle$  is denoted as  $|\psi\rangle\langle\psi|$ , where  $\langle\psi|$  is the corresponding bra vector. Therefore, the spectral decomposition of  $A$  can alternatively be written as

$$A = \sum_n |n\rangle a_n \langle n|, \quad (2.17)$$

with  $\{|n\rangle\}$  being the orthonormal basis of eigenstates for  $A$ , and fulfilling  $A|n\rangle = a_n|n\rangle$ .

### 2.2.4 Hilbert Spaces

A Hilbert space, denoted as  $\mathcal{H}$ , is an **inner product space** over the field of complex numbers  $\mathbb{C}$ , **complete** with respect to the norm induced by the inner product. Here, completeness can be intuitively thought of in terms of a space having no "points missing" either from within it or at its boundary. e.g., the set of rational numbers is not complete. Hilbert spaces are central to the study of quantum mechanics, forming the mathematical backbone of the theory. In the context of quantum computation and information, these spaces are finite-dimensional, where completeness always holds, and thus, they become equivalent to complex inner product spaces.

### 2.2.5 Post Selection

In the realm of probability theory, the concept of post-selection involves conditioning the probability distribution based on the occurrence of a specific event. When we apply post-selection to an event  $E$ , the probability of another event  $F$  is modified from the initial probability  $\Pr[F]$  to a conditional probability  $\Pr[F|E]$ . For a discrete probability space, the conditional probability is defined as  $\Pr[F|E] = \frac{\Pr[F \cap E]}{\Pr[E]}$ . This definition necessitates that  $\Pr[E]$  be greater than zero to define the post-selection process properly.

In practical quantum experiments, post-selection is sometimes employed after an experiment to substitute for communication during the experiment. This is achieved by post-selecting the communicated value into a constant.

## 2.3 Postulates of Quantum mechanics

In this section, we will use the mathematical formalism developed in 2.2 to provide the statement followed by a comprehensive elucidation of the fundamental axioms of quantum mechanics. These postulates establish a vital bridge between the physical reality we observe and the mathematical structure of quantum mechanics.

### 2.3.1 Postulate 1: State Space, Describing the state of a system

*Each isolated physical system corresponds to a Hilbert space  $\mathcal{H}$ , the system's state space. The state of the system at any given time  $t$ , represented by a ray in  $\mathcal{H}$ , captures the complete description of the system.*

A 'ray' refers to an equivalence class of vectors differing only by a non-zero complex scalar, **global phase**. By convention, we can choose a representative vector from this class denoted as  $|\psi\rangle$ , with a norm of one,  $\langle\psi|\psi\rangle = 1$ , called a **state vector**, to represent quantum states where the vector's phase lacks physical relevance. Thus,  $|\psi\rangle$  and  $e^{i\alpha}|\psi\rangle$  describe the same state, as  $|e^{i\alpha}| = 1$ . We call any linear combination  $\sum_i a_i |\psi_i\rangle$ , a **superposition** of states  $|\psi_i\rangle$  where each corresponding complex scalar  $a_i$  is the probability amplitude that quantifies the contribution of the state to the overall superposition. Considering two states  $|\phi\rangle$  and  $|\psi\rangle$ , their linear superposition can form a new state,  $a|\psi\rangle + b|\phi\rangle$  since every ray corresponds to a possible state. The **relative phase** difference in this superposition is significant, as we can differentiate  $a|\psi\rangle + b|\phi\rangle$  from  $a|\psi\rangle + e^{i\alpha}b|\phi\rangle$ , but not  $e^{i\alpha}(a|\psi\rangle + b|\phi\rangle)$

**Schrödinger picture:** A quantum mechanical system's state is conveyed through a complex wavefunction  $\varphi(x, t)$ , which more abstractly is represented as a state vector (ket)  $|\psi\rangle$ , described above.

We can either measure a quantum state or let it evolve in time, and we will explore these in further postulates.

### 2.3.2 Measurement on the system

#### 2.3.2.1 Postulate 2: Observables, Describing physical quantities

*Each measurable physical quantity,  $\mathcal{A}$ , is depicted by a Hermitian operator  $\mathbf{A}$  on state space  $\mathcal{H}$ .*

In the framework established by John von Neumann [47], the act of measuring a physical system is conceptualized as the application of a self-adjoint (hermitian) operator within the corresponding Hilbert space, which is called an **observable**. These correspond to physical quantities of interest in quantum mechanics, such as position, momentum, energy, and spin. Hermitian operators are unique because they always have real eigenvalues, as shown in (2.2.3.4). These real eigenvalues are what we observe as possible results when we measure these observables. As an observable,  $\mathbf{A}$ 's eigenvectors constitute an orthonormal basis for  $\mathcal{H}$ , ensuring that measurements of  $\mathbf{A}$  correspond to eigenvalues of  $\mathbf{A}$ . The correspondence between hermitian

operators and physically meaningful observables is not universal, as discussed in references [48]. Certain observables do not necessitate the existence of non-trivial hermitian operators. E.g., the concept of mass is not represented as a non-trivial operator.

Quantum observables often exhibit a characteristic known as **complementarity**, which means certain observable pairs cannot be measured simultaneously if they are non-commutative (2.2.3.3), i.e.  $[\mathbf{A}, \mathbf{B}] \neq 0$ . Measuring  $\mathbf{A}$  first impacts the quantum state in such a manner that it influences the subsequent measurement of  $\mathbf{B}$ , and the reverse is also true. When dealing with quantum observables, those associated with commuting operators are termed **compatible**. An example of compatible observables is the momentum measured along different axes, like the x-axis and y-axis, as in the case of the Stern Gerlach experiment. In contrast, observables tied to non-commuting operators are labeled as incompatible or complementary. A classic example of this is the position and momentum measured along the same axis, demonstrating the **uncertainty principle**.

If different states of a quantum mechanical system result in the same measured energy, these states are described as being **degenerate**. According to the **Born rule**, the probability of observing a particular eigenvalue  $\lambda$  (assuming it is non-degenerate) is given by  $|\langle \lambda | \psi \rangle|^2$ , where  $|\lambda\rangle$  is the eigenvector associated with  $\lambda$ . In cases where the eigenvalue  $\lambda$  is degenerate, the probability is determined by  $\langle \psi | P_\lambda | \psi \rangle$ , where  $P_\lambda$  denotes the projection onto the eigenspace associated with  $\lambda$ .

### 2.3.2.2 Postulate 3: Projective Measurement

*Quantum measurements are characterized by a set  $\{M_n\}$  of measurement operators, acting on the state space of the measured system. The index  $n$  denotes the possible outcomes of the measurement. For a system in state  $|\psi\rangle$  immediately before measurement, the probability of observing outcome  $n$  is*

$$p(n) = \langle \psi | M_n^\dagger M_n | \psi \rangle = \|M_n |\psi\rangle\|^2, \quad (2.18)$$

*and the post-measurement state of the system becomes*

$$\frac{M_m |\psi\rangle}{\sqrt{\langle \psi | M_m^\dagger M_m | \psi \rangle}}. \quad (2.19)$$

The measurement operators satisfy the completeness relation

$$\sum_m M_m^\dagger M_m = I, \quad (2.20)$$

which ensures the total probabilities sum to one:

$$1 = \sum_m p(m) = \sum_m \langle \psi | M_m^\dagger M_m | \psi \rangle. \quad (2.21)$$

This equation's validity for all  $|\psi\rangle$  is equivalent to the completeness relation, which is more straightforward to verify, hence its inclusion in the postulate.

Spectral decomposition facilitates the association of probability measures with the observable values in a given quantum state, denoted as  $\psi$ . This approach implies that the possible measurement outcomes of an observable  $A$  are determined by its spectrum. The expectation of  $A$  in a state represented by a normalized vector  $\psi$  in a Hilbert space  $H$  is calculated using  $\langle\psi|A|\psi\rangle$ . Representing  $\psi$  in the eigenbasis of  $A$ , the probability of detecting an eigenvalue is the squared magnitude of the corresponding eigenvector component. Collectively, these principles, known as the **Born rule** and the state update or collapse rule, offer a comprehensive depiction of quantum measurement processes.

A projective measurement in a given space, characterized by  $m$  distinct outcomes, involves a set of projectors  $P_1, \dots, P_m$ . These projectors act on the same space and collectively add up to the identity operator,  $\sum_{j=1}^m P_j = I$ . Each projector  $P_i$  is orthogonal to the others, signified by  $P_i P_j = 0$  for  $i \neq j$ . The projector  $P_j$  focuses on a subspace  $V_j$  of the total Hilbert space  $V$ . Any state  $|\phi\rangle$  in  $V$  can uniquely be expressed as  $|\phi\rangle = \sum_{j=1}^m |\phi_j\rangle$  where  $|\phi_j\rangle = P_j |\phi\rangle$  is part of  $V_j$ . Due to the orthogonality of the projectors, the subspaces  $V_j$  and the states  $|\phi_j\rangle$  are also orthogonal.

It's important to note that the specific projector  $P_j$  applied during a measurement is not predetermined but is governed by a probability distribution. However, if the measured state  $|\phi\rangle$  is completely within one of the subspaces  $V_j$ , then the measurement outcome is assured  $j$ . For example, consider a projective measurement in the computational basis on an  $N$ -dimensional state. Here,  $m = N$  and each projector  $P_j$  corresponds to  $|j\rangle\langle j|$ . Thus,  $P_j$  projects onto the state  $|j\rangle$  in the subspace  $V_j \subseteq V$ , which is one-dimensional and spanned by  $|j\rangle$ . If we have a state  $|\phi\rangle = \sum_{j=0}^{N-1} \alpha_j |j\rangle$ , applying this measurement yields outcome  $j$  with probability  $|\alpha_j|^2$ , and the state collapses to  $\frac{\alpha_j}{|\alpha_j|} |j\rangle$ . Here, the norm-1 factor  $\frac{\alpha_j}{|\alpha_j|}$  can be disregarded as it holds no physical significance, leading us to the final state  $|j\rangle$ .

Beyond the standard orthonormal basis, we might consider an alternative orthonormal basis  $B$  consisting of states  $|\psi_0\rangle, \dots, |\psi_{N-1}\rangle$ , and define a projective measurement using the projectors  $P_j = |\psi_j\rangle\langle\psi_j|$ . Applying this measurement to  $|\phi\rangle$  results in outcome  $j$  with probability  $|\langle\phi|\psi_j\rangle|^2$ . If  $|\phi\rangle$  is identical to one of the basis vectors  $|\psi_j\rangle$ , then the measurement outcome is  $j$  with certainty.

**Schrödinger Picture, continuous, nondegenerate spectrum:** The act of measuring a physical quantity  $\mathcal{A}$  in a state  $|\psi\rangle$  yields probabilities for specific eigenvalues  $a_n$  (in discrete spectra) or  $\alpha$  (in continuous spectra) of the corresponding observable  $\mathbf{A}$ . This probability is quantified as  $\partial P(\alpha) = |\langle\alpha|\psi\rangle|^2 d\alpha$ .

### 2.3.3 Postulate 4: Time Evolution of system

The time evolution of an isolated quantum system in state  $|\psi_0\rangle$  at an initial time  $t_0$ , to its state  $|\psi_t\rangle$  at a later time  $t$ , can be described by a unitary transformation. This is represented by a unitary operator  $U_{t,t_0}$  that is only dependent on the time instances  $t_0$  and  $t$  acting as:

$$|\psi_t\rangle = \mathbf{U}_{t,t_0} |\psi_0\rangle \quad (2.22)$$

For a quantum state transformation to preserve the probabilistic interpretation of quantum mechanics, the operation  $\mathbf{U}$  must be unitary. A unitary matrix  $U$  satisfies  $U^{-1} = U^*$ , ensuring that the norm of vectors is preserved:

$$\sum_{j=0}^{N-1} |\alpha_j|^2 = 1. \quad (2.23)$$

This condition confirms that a unitary operation maps a norm-1 vector to another norm-1 vector (both with dimension  $N$ ). Note that the theory does not determine the exact state space or the quantum state of a specific system. It does not specify which unitary operators encapsulate the dynamics of real-world quantum systems. Non-measurement operations in quantum mechanics are reversible. By applying the inverse unitary operation  $U^{-1}$ , the original state  $|\varphi\rangle$  can be retrieved from  $|\psi\rangle$ , highlighting the reversible nature of quantum state transformations. In contrast, measurements are inherently irreversible, as the original quantum state cannot be reconstructed from the observed classical outcome.

These principles underscore the distinct nature of quantum state operations and their fundamental differences from classical transformations.

**Schrödinger Picture, Continuous-time evolution** *The Schrödinger equation governs the infinitesimal or continuous time evolution of the state of a closed quantum system*

$$i\hbar \frac{\partial |\psi(t)\rangle}{\partial t} = \mathbf{H} |\psi(t)\rangle. \quad (2.24)$$

Where,  $|\psi(t)\rangle = \int \psi(x,t) |x\rangle dx$ ,  $|x\rangle$  are position eigenstates forming a complete basis. Any state vector can be expressed as a superposition of these eigenstates.  $\mathbf{H}$  is the Hamiltonian of the closed system, which is a Hermitian operator.

### 2.3.4 Postulate 5: Composite Systems

*The state space of a composite physical system is formed by the tensor product of the state spaces of its component systems.*

For systems  $A$  and  $B$  with Hilbert spaces  $\mathcal{H}_A$  and  $\mathcal{H}_B$  respectively, the Hilbert space of the composite system  $AB$  is  $\mathcal{H}_A \otimes \mathcal{H}_B$ , assuming component system  $A$  is in state  $|\psi\rangle_A \in \mathcal{H}_A$  and component system  $B$  in  $|\phi\rangle_B \in \mathcal{H}_B$ . The composite state of the combined system  $AB$  is thus  $|\psi\rangle_A \otimes |\phi\rangle_B$ .

The tensor product space  $\mathcal{H} = \mathcal{H}_A \otimes \mathcal{H}_B$  forms an  $NM$ -dimensional space when considering an orthonormal basis  $|0\rangle, \dots, |N-1\rangle$  in  $\mathcal{H}_A$  and another basis  $|0\rangle, \dots, |M-1\rangle$  in  $\mathcal{H}_B$ , spanned by the set  $\{|i\rangle \otimes |j\rangle \mid i \in \{0, \dots, N-1\}, j \in \{0, \dots, M-1\}\}$ . A general state in  $\mathcal{H}$  can be expressed as  $\sum_{i=0}^{N-1} \sum_{j=0}^{M-1} \alpha_{ij} |i\rangle \otimes |j\rangle$ , representing a bipartite state, and similarly, tripartite states or more complex multipartite states can be formed in a Hilbert space that is the tensor product of three or more, smaller Hilbert spaces.

In the context of bipartite states, observables assume a more complex role. The tensor product operator  $M_A \otimes N_B$  operates by applying  $M_A$  to system A and  $N_B$  to system B, with its effect on the orthonormal basis  $|i, \mu\rangle_{AB}$  given by  $M_A \otimes N_B |i, \mu\rangle_{AB} = M_A |i\rangle_A \otimes N_B |\mu\rangle_B = \sum_{j, \nu} |j, \nu\rangle_{AB} (M_A)_{ji} (N_B)_{\nu\mu}$ . An operator that does not affect system B is represented as  $M_A \otimes I_B$ , and similarly, an operator acting trivially on system A is denoted as  $I_A \otimes N_B$ . The distinction between measuring observables  $A$  and  $B$  separately on the respective parts of a bipartite state versus measuring the joint observable  $A \otimes B$  lies in the outcomes: separate measurements yield individual outcomes for each part, whereas a joint measurement produces a single outcome.

## Entanglement in Composite Systems

Entanglement, a pivotal feature of composite quantum systems, represents quantum correlations between subsystems, exemplified by the Bell state  $(|00\rangle + |11\rangle)/\sqrt{2}$ . This state demonstrates that if the first subsystem is measured and observed as  $|0\rangle$ , the entire state collapses to  $|00\rangle$ , and similarly, observing  $|1\rangle$  collapses the state to  $|11\rangle$ . Such instant correlation, even when subsystems are spatially separated, underscores entanglement's non-local properties. In entangled systems, the state of the whole cannot be described as a product of the states of its parts; it is instead represented through a combination of multiple tensor products of the states belonging to its constituent subsystems, necessitating the use of density operator formalism for a single subsystem within an entangled system. In contrast, in scenarios devoid of quantum entanglement, the system's quantum state is identifiable as separable.

The Bell state, or EPR pair, is essential in quantum computation, exhibiting entanglement where parts of the system cannot be described independently. The measurement of one subsystem of a Bell state yields an outcome (either 0 or 1) with an equal probability of  $1/2$ , and the measurement of the second subsystem will always yield the same result as the first, signifying entangled states crucial for phenomena such as quantum teleportation and superdense coding. The Bell state and its correlations, highlighted in the landmark paper by Einstein, Podolsky, and Rosen (EPR) and further analyzed by John Bell, demonstrate that the correlations in such

quantum states exceed any possible correlation between classical systems, hinting at quantum mechanics' extraordinary potential for information processing.

## 2.4 Density Operator Formalism

The density matrix, or density operator formalism, is an essential tool in the fields of quantum mechanics and quantum information theory. It proves particularly useful when state vectors are insufficient due to incomplete knowledge of quantum systems. Density operators allow for the representation of **mixed states**, which are statistical mixtures of different pure states  $|\psi_k\rangle$  along with their corresponding probabilities  $p_k$ , satisfying  $\sum_k p_k = 1$ . **Pure states**, on the other hand, occur when the system's state is entirely known and can be represented by a single state vector.

It is crucial to distinguish between a statistical mixture and a superposition. A superposition state  $|\Psi\rangle = \sum_k c_k |\psi_k\rangle$  differs from a statistical mixture because an average state vector cannot represent it due to interference terms.

The density operator was introduced to describe ensembles of quantum states and provides an intrinsic characterization of quantum systems. This approach enables a description of quantum mechanics independent of state vectors, which is especially beneficial when we have incomplete information about a system's state. Density operators offer a more nuanced way to describe entangled states, especially in multipartite scenarios, providing a comprehensive view that state vectors alone cannot provide. They are particularly relevant for quantum systems in statistical ensembles, where each member might be in a distinct state.

### 2.4.1 General Properties of the Density Operator

An operator  $\rho$  is a density operator associated with some ensemble  $\{p_i, |\psi_i\rangle\}$  if and only if it satisfies the following conditions:

1. **Trace Condition:**  $\rho$  has trace equal to one,  $\text{tr}(\rho) = 1$ .
2. **Positivity Condition:**  $\rho$  is a positive operator.

Consider  $\rho = \sum_i p_i |\psi_i\rangle\langle\psi_i|$  as a density operator. The trace condition is verified since  $\text{tr}(\rho) = \sum_i p_i \text{tr}(|\psi_i\rangle\langle\psi_i|) = \sum_i p_i = 1$ . For any vector  $|\phi\rangle$  in the state space,  $\langle\phi|\rho|\phi\rangle = \sum_i p_i |\langle\phi|\psi_i\rangle|^2 \geq 0$ , thus satisfying the positivity condition. Conversely, if  $\rho$  is any operator satisfying these conditions and is positive, it must have a spectral decomposition  $\rho = \sum_j \lambda_j |j\rangle\langle j|$ , with orthogonal vectors  $|j\rangle$  and non-negative eigenvalues  $\lambda_j$ . From the trace condition,  $\sum_j \lambda_j = 1$ . Therefore, an ensemble  $\{\lambda_j, |j\rangle\}$  gives rise to  $\rho$ .

## 2.4.2 Density Operator Representations

**For Pure States:** Consider a pure state  $|\Psi\rangle = \sum_k c_k |u_k\rangle$ , where  $\{|u_k\rangle\}$  is an orthonormal basis. The density operator for this state is  $\rho = |\Psi\rangle\langle\Psi|$ , with matrix elements  $\rho_{mn} = \langle u_m | \rho | u_n \rangle = c_n^* c_m$ . The normalization condition  $\sum_k |c_k|^2 = 1$  leads to  $\text{Tr}(\rho) = 1$ . The expectation value of an observable  $\hat{O}$  is  $\langle \hat{O} \rangle = \langle \Psi | \hat{O} | \Psi \rangle = \sum_{n,m} c_n^* c_m \langle u_n | \hat{O} | u_m \rangle$ , which can also be expressed as  $\langle \hat{O} \rangle = \text{Tr}(\rho \hat{O})$ .

**For Mixed States:** The density operator for a statistical mixture of states  $|\psi_k\rangle$  is  $\rho = \sum_k p_k \rho_k = \sum_k p_k |\psi_k\rangle\langle\psi_k|$ . When measuring this mixed state, the probability of an outcome is a weighted sum of probabilities for each state. The density operator for mixed states is Hermitian, and its trace equals unity,  $\text{Tr}(\rho) = 1$ . The expectation value of any observable is  $\langle \hat{O} \rangle = \text{Tr}(\rho \hat{O})$ .

**For General State in  $\mathbb{C}^2$ :** For a 2-dimensional system (e.g., a spin-1/2 system), an arbitrary density operator in  $\mathbb{C}^2$  can be written as  $\rho = \frac{1}{2}(I + \vec{n} \cdot \vec{\sigma})$ , where  $\vec{n}$  is a real vector in  $\mathbb{R}^3$  and  $\vec{\sigma}$  are the Pauli matrices. The condition  $|\vec{n}| \leq 1$  ensures that  $\rho$  is a valid density operator, with pure states satisfying  $|\vec{n}| = 1$  and mixed states having  $|\vec{n}| < 1$ .

## 2.4.3 The Reduced Density Operator

The reduced density operator plays a crucial role in describing subsystems of a composite quantum system, making it an indispensable tool in analyzing such systems. Consider physical systems A and B, described by a density operator  $\rho_{AB}$ . The reduced density operator for system A is defined as  $\rho_A \equiv \text{tr}_B(\rho_{AB})$ , where  $\text{tr}_B$  is the partial trace over system B.

Although it is not immediately obvious, the reduced density operator  $\rho_A$  effectively describes the state of system A. The justification for this identification is that  $\rho_A$  yields correct measurement statistics for measurements on system A. Consider a product state  $\rho_{AB} = \rho \otimes \sigma$ , where  $\rho$  and  $\sigma$  are density operators for systems A and B, respectively. Then,  $\rho_A = \text{tr}_B(\rho \otimes \sigma) = \rho \text{tr}(\sigma) = \rho$ , intuitively matching our expectations. For the Bell state  $(|00\rangle + |11\rangle)/\sqrt{2}$ , with density operator  $\rho = \frac{1}{2}(|00\rangle\langle 00| + |11\rangle\langle 00| + |00\rangle\langle 11| + |11\rangle\langle 11|)$ , tracing out the second qubit yields  $\rho_1 = \text{tr}_2(\rho) = \frac{1}{2}(|0\rangle\langle 0| + |1\rangle\langle 1|) = I/2$ . This mixed-state outcome exemplifies the non-trivial nature of quantum entanglement: even though the joint state is pure and completely known, the subsystem can be in a mixed state.

## 2.5 Introduction to Quantum Computation

The arrangement of a physical system can hold important information, and manipulating this information on physical devices is essential for various computational tasks. As our universe fundamentally operates on a quantum mechanical level, the principles of computer science and information theory must be grounded in quantum physics. Transitioning from classical to quantum computing represents more than just an upgrade; it marks a paradigm shift. Quantum information, which involves encoding information in the quantum states of physical systems, possesses unique properties that are significantly different from traditional "classical" information. Furthermore, quantum computers, which utilize these quantum properties, have the potential to perform certain computations much more efficiently than state-of-the-art classical computers.

Our goal is to examine the distinct characteristics of quantum information in comparison to classical information. We will investigate how these unique features can be utilized to develop quantum algorithms that can solve specific problems faster than their classical counterparts. Unlike classical bits that remain as either 0 or 1, quantum bits or qubits take advantage of superposition, meaning they can occupy multiple states simultaneously. When entanglement is added to the mix, whereby qubits become interdependent regardless of distance, an exponential computational force is generated.

### 2.5.1 Quantum Bits (Qubits)

The quantum bit or qubit is the foundational unit of quantum computation and information. Unlike classical bits, which exist in definite states of 0 or 1, qubits operate under the principles of quantum mechanics, leading to unique properties and behaviors. A qubit can exist in a state of superposition, represented as  $|\psi\rangle = \alpha|0\rangle + \beta|1\rangle$ , where  $\alpha$  and  $\beta$  are complex numbers. This superposition implies that a qubit can be in a combination of the states  $|0\rangle$  and  $|1\rangle$ . The states  $|0\rangle$  and  $|1\rangle$  themselves are analogous to the classical 0 and 1, but in the quantum realm, they form an orthonormal basis in a two-dimensional complex vector space. Upon measuring a qubit, it doesn't reveal its superposition state. Instead, the measurement collapses the qubit into one of the basis states,  $|0\rangle$  or  $|1\rangle$ . The likelihood of each outcome is determined by the squared magnitudes of  $\alpha$  and  $\beta$ . Specifically, the probability of the qubit collapsing to  $|0\rangle$  is  $|\alpha|^2$  and to  $|1\rangle$  is  $|\beta|^2$ . It's important to note that  $|\alpha|^2 + |\beta|^2 = 1$ , ensuring the normalization of the qubit's state. In classical computing, bits are akin to a switch with distinct on and off states. However, due to their ability to exist in superpositions, Qubits can represent a continuum of states between  $|0\rangle$  and  $|1\rangle$ . This characteristic of qubits, allowing them to be in multiple states simultaneously until measured, is a departure from the binary nature of classical bits. The state of a qubit can be represented on the **Bloch sphere**, a geometric model where the points on the sphere's surface correspond to possible qubit states. This representation is particularly

helpful in visualizing the state of a single qubit and understanding quantum operations. While a qubit can theoretically encode an infinite amount of information due to its continuous nature, practical measurement limits this capacity. Measuring a qubit yields a single bit of classical information corresponding to either state  $|0\rangle$  or  $|1\rangle$ . The process of measurement alters the qubit's state, collapsing it to align with the measurement outcome. Consequently, despite the vast potential information a qubit may hold, only a single bit of information is extractable through measurement.

### 2.5.2 Multiple Qubits

Composite quantum systems extend the concepts of superposition and entanglement beyond the realm of single quantum subsystems, residing in a tensor product space that leads to more complex and powerful computational capabilities. Unlike classical computation, where two bits can represent four distinct states (00, 01, 10, and 11), a composite system consisting of two quantum subsystems can exist in a superposition of these four computational basis states:  $|00\rangle$ ,  $|01\rangle$ ,  $|10\rangle$ , and  $|11\rangle$ . The state of a two-subsystem composite is thus can be represented as  $|\psi\rangle = \alpha_{00}|00\rangle + \alpha_{01}|01\rangle + \alpha_{10}|10\rangle + \alpha_{11}|11\rangle$ , where  $\alpha_{xy}$  are complex coefficients (amplitudes) associated with each basis state, adhering to the normalization condition  $\sum_{x \in \{0,1\}^2} |\alpha_x|^2 = 1$  to ensure the total probability sums to one. This framework extends to larger composite systems, where a register of  $n$  quantum subsystems encompasses  $2^n$  basis states, allowing for the existence of superpositions within these states. Measuring a composite system in the computational basis results in one of the basis states, with probabilities determined by the corresponding amplitudes. For instance, measuring the entire two-subsystem state  $|\psi\rangle$  yields state  $|xy\rangle$  with probability  $|\alpha_{xy}|^2$ . A density operator can represent the state of a **multi-qubit system** by incorporating correlations among qubits. For example, the density operator for a two-qubit system is given by  $\rho_{AB} = \frac{1}{4}(I \otimes I + I \otimes \vec{r} \cdot \vec{\sigma} + \vec{s} \cdot \vec{\sigma} \otimes I + \sum_{i,j=1}^3 [T_{AB}]_{ij} \sigma_i \otimes \sigma_j)$ , where  $\vec{r}, \vec{s} \in \mathbb{R}^3$  and  $[T_{AB}]_{ij}$  is the correlation matrix.

### 2.5.3 Bloch Sphere Representation of Qubit States

The Bloch sphere is an invaluable tool in quantum mechanics for visualizing the states of a single qubit, effectively demonstrating superposition and state transformations in a two-dimensional complex space,  $\mathbb{C}^2$ . The Bloch sphere uses a three-dimensional unit sphere to represent qubit states. On this sphere, **Pure States** are points on the surface, each corresponding to a unique qubit state. **Mixed States** are found within the interior, representing statistical mixtures of pure states. A state on the Bloch sphere is defined by angles  $\theta \in [0, \pi]$  and  $\phi \in [0, 2\pi]$ . The general form of a state  $|\psi\rangle$  is:

$$|\psi\rangle = \cos\left(\frac{\theta}{2}\right) |0\rangle + e^{i\phi} \sin\left(\frac{\theta}{2}\right) |1\rangle, \quad (2.25)$$

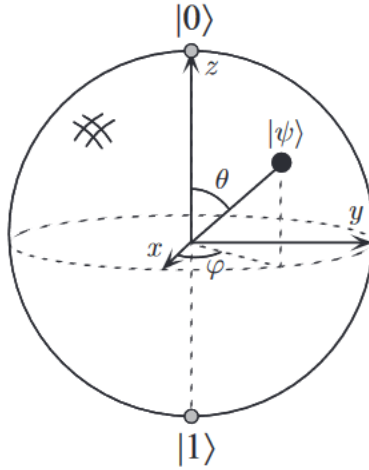


Figure 2.4: Bloch Sphere Representation

where  $|0\rangle$  and  $|1\rangle$  are the computational basis states. The Bloch vector  $\vec{n} \in \mathbb{R}^3$  describes a qubit state, with Pure States having  $|\hat{n}| = 1$  and Mixed States characterized by  $|\vec{n}| < 1$ . The density operator  $\rho = \frac{1}{2}(I + \vec{n} \cdot \vec{\sigma})$  is used for state definition, with  $\vec{\sigma}$  representing Pauli matrices. The **Maximally Mixed State** is at the center of the sphere, where  $|\hat{n}| = 0$ , and is represented as  $\rho = \frac{I}{2}$ . **Unitary Operations** are visualized as rotations of the Bloch vector on the sphere.

While effective for single-qubit states, the Bloch sphere does not easily generalize to higher-dimensional spaces or multi-qubit systems, where complex quantum phenomena like entanglement occur.

## 2.5.4 Quantum Gates

Quantum gates are fundamental components of quantum circuits, analogous to classical logic gates in digital computers. The evolution of any isolated quantum system preserves the norm and is reversible. Thus, it can be characterized through unitary operators. Below are some quantum gates relevant to this thesis:

## 2.5.5 Single-Qubit Gates

### 2.5.5.1 Pauli Gates (X, Y, Z)

#### Pauli Matrices

The Pauli matrices  $X$ (bit-flip),  $Y$ (phase-shift), and  $Z$ (phase-flip) are fundamental in the study and manipulation of qubit states in quantum computing. These matrices form a basis for

the space of  $2 \times 2$  Hermitian matrices, which are crucial for representing quantum operations that can be applied to single qubits. The set of Pauli matrices consists of three distinct matrices:

$$I = \begin{pmatrix} 1 & 0 \\ 0 & 1 \end{pmatrix}, \quad X = \begin{pmatrix} 0 & 1 \\ 1 & 0 \end{pmatrix}, \quad Y = \begin{pmatrix} 0 & -i \\ i & 0 \end{pmatrix}, \quad Z = \begin{pmatrix} 1 & 0 \\ 0 & -1 \end{pmatrix}.$$

The importance of the Pauli matrices in quantum computing can be summarized as follows: The Pauli matrices serve as a basis for all possible single-qubit quantum gates, which are unitary operators. Any  $2 \times 2$  unitary matrix describing a quantum operation on a single qubit can be expressed as a linear combination of the Pauli matrices and the identity matrix, with complex coefficients. This is because the Pauli matrices, along with the identity matrix, span the space of  $2 \times 2$  complex matrices. The Pauli matrices can directly manipulate quantum states. For example, the  $X$  matrix flips the amplitude between the  $|0\rangle$  and  $|1\rangle$  computational basis states, effectively performing a quantum bit flip. Similarly, the  $Z$  matrix flips the phase of the  $|1\rangle$  state while leaving the  $|0\rangle$  state unchanged, and the  $Y$  matrix applies a combination of bit and phase flip. They define different measurement bases. For instance, measuring in the  $Z$  basis corresponds to measuring the qubit in the standard computational basis ( $|0\rangle, |1\rangle$ ), whereas measuring in the  $X$  or  $Y$  basis involves first transforming the qubit state using the respective Pauli matrix and then measuring in the computational basis. Each matrix, denoted as  $P$ , is both unitary and Hermitian, leading to the property of being self-inverse ( $P^{-1} = P$ ). Consequently, their eigenvalues are confined to the set  $\{-1, 1\}$ . An interesting property is the anti-commutation of non-identity Pauli matrices: for any distinct  $P, Q \in \{X, Y, Z\}$ , it holds that  $PQ = -QP$ . Notably,  $Y$  can be expressed as  $Y = iXZ$ , and the product of any two distinct Pauli matrices has a zero trace.

## 2.5.6 Multi-Qubit Gates

### 2.5.6.1 Hadamard Gate (H)

The Hadamard gate acts on a single qubit and maps the basis states  $|0\rangle$  and  $|1\rangle$  to  $|+\rangle$  and  $|-\rangle$ , respectively. Its matrix representation is:

$$H = \frac{1}{\sqrt{2}} \begin{pmatrix} 1 & 1 \\ 1 & -1 \end{pmatrix}. \tag{2.26}$$

### 2.5.6.2 Controlled NOT Gate (CNOT)

The CNOT gate is a two-qubit operation where the second qubit (target) is flipped if and only if the first qubit (control) is in state  $|1\rangle$ . The matrix representation of the CNOT gate is:

$$\text{CNOT} = \begin{pmatrix} 1 & 0 & 0 & 0 \\ 0 & 1 & 0 & 0 \\ 0 & 0 & 0 & 1 \\ 0 & 0 & 1 & 0 \end{pmatrix}. \quad (2.27)$$

### 2.5.7 Universal Quantum Gates

Universal quantum gates are the quantum computing equivalent of universal gates in classical computing. In classical computing, a set of universal gates, such as NAND gates or NOR gates, can be combined in various ways to perform any possible computation—that is, any logical function can be implemented using just these gates. Similarly, A universal quantum gate set allows for the construction of any unitary operation on a quantum computer. Unitary operations are key in quantum mechanics, representing reversible transformations on the state space of qubits. They preserve the inner product, meaning they keep the total probability of outcomes as 1, which is essential for the physical realizability of quantum operations.

A popular example of a universal set is any set of single-qubit gates combined with the CNOT gate. The single-qubit gates allow for operations within the Bloch sphere on individual qubits, while the CNOT gate provides the ability to generate entanglement between qubits. Universal quantum gates are foundational to quantum computing, enabling the construction of arbitrary quantum algorithms and operations through the combination of a relatively small and manageable set of gates. This concept is pivotal for the design and implementation of quantum computers, as it ensures that, in principle, a quantum computer can perform any computation that quantum mechanics can describe.

### 2.5.8 Quantum Algorithms

Quantum algorithms are computational processes designed to utilize quantum mechanical phenomena—such as superposition, in which a quantum system exists in multiple states simultaneously; entanglement, a unique correlation between quantum particles regardless of distance; and quantum interference, the constructive or destructive pattern formation due to the phase properties of quantum states—to perform computations. These algorithms can operate on data encoded in qubits, the fundamental units of quantum information, to solve problems more efficiently than classical algorithms. At the heart of quantum computation is the principle of quantum interference, which allows a quantum algorithm to amplify the probabilities of correct answers while canceling out the probabilities of wrong ones. This principle is essential for the

operation of quantum algorithms, leveraging the coherent superposition of states in a quantum system to perform computational tasks. The probabilistic nature of quantum measurements means that outcomes are influenced by the interference pattern generated by the superposed states, making certain outcomes more likely than others based on the algorithm’s design.

According to [Shor](#), in his article [49], where he examines the question of why so few classes of quantum algorithms have been discovered, There are three classes of algorithms:

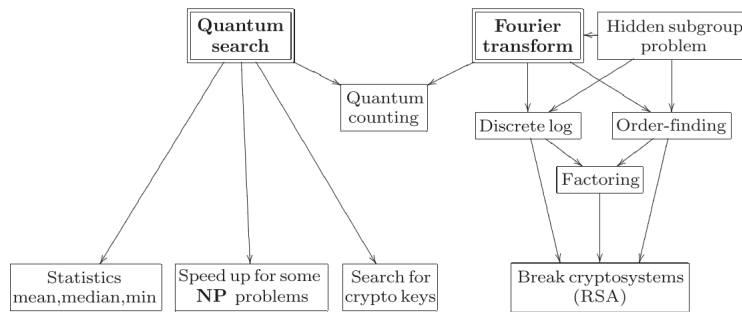


Figure 4.1. The main quantum algorithms and their relationships, including some notable applications.

Figure 2.5: main quantum algorithms and their relationships

- **Quantum algorithms based upon the Fourier transform:** The first class uses the Fourier transform to find periodicity. The Deutsch–Jozsa algorithm [50] is an example of this type of algorithm. The Deutsch-Jozsa algorithm is a quintessential example demonstrating quantum computing’s superiority over classical approaches for specific problem classes. It determines whether a given function is constant (the same output for all inputs) or balanced (equal numbers of inputs produce different outputs) with a single query to the function, using quantum parallelism. Classical approaches, in contrast, require at least  $N/2 + 1$  queries for a function with  $N$  possible inputs. But mainly, This class also contains the factoring and discrete logarithm algorithms [51], Simon’s algorithm [Simon 1997](the first member of this class to be discovered), and Hallgren’s algorithms for Pell’s equation and specific other number theory problems [Hallgren 2002]
- **Quantum search algorithms:** The second class contains Grover’s search algorithm, which can perform an exhaustive search of  $N$  items in  $\sqrt{N}$  time [52], and several extensions of this algorithm (see Grover and Sengupta [2002]). These extensions all have the general flavor of giving a square root improvement in the speed of optimization or search problems.
- **Quantum simulation:** Quantum simulation algorithms leverage quantum computers to model and simulate quantum systems themselves, an inherently complex task for classical computers due to the exponential growth of the system’s Hilbert space with the addition

of each particle. This class contains Feynman's original idea [Feynman 1982] of using quantum computers to speed up simulations of quantum physics. Hamiltonian needed to describe a particular physical system is a challenging problem

The implementation of quantum algorithms involves intricate control over quantum states and operations, demanding substantial computational resources and sophisticated error correction techniques. The complexity of developing practical quantum algorithms that outperform classical counterparts remains a formidable challenge, necessitating ongoing advancements in quantum computing technologies. Current quantum computing technologies face significant hurdles, such as high error rates in quantum operations and decoherence—a loss of quantum information to the environment. These challenges limit the size and complexity of quantum algorithms that can be reliably executed on today's quantum hardware.

## Chapter 3

### Noise in Quantum Systems and Search Algorithm

“An unproblematic state is a state without creative thought. Its other name is death.”

– David Deutsch, [The Beginning of Infinity](#)

“Quantum fluctuations are the monkeys that program the universe.”

– Seth Lloyd, [Programming the Universe](#)

In the previous chapter, our main focus has been on the behavior of quantum systems in isolation, without any harmful interactions with their external environment. Although that provided theoretical insights into the potential of these ideal systems for computational tasks, their practical applicability is limited by the fact that perfectly isolated systems do not exist in reality except for the universe itself. In reality, quantum systems are subject to external perturbations, which can manifest as noise within. Therefore, understanding and mitigating these noise effects are crucial for the development of practical quantum technologies. We begin this chapter by introducing quantum operations formalism, a comprehensive toolkit designed to model quantum noise effectively, and the dynamics of open quantum systems. Then, we will discuss and reformulate the axioms introduced in the previous chapter in terms of this mathematical formalism. Together with it, we cover an extensive range of topics, including quantum channels and generalized measurements. We talk about the role and effect of quantum noise in general before honing in on a specific model of noise: quantum depolarising channel noise. We then describe Grover’s search algorithm in an ideal setting before eventually ending with putting these pieces together to talk about depolarizing channel noise in Grover’s search algorithm.

## 3.1 Quantum Operations

Quantum operations’ formalism provides a comprehensive methodology to understand quantum states’ evolution in diverse situations, including stochastic changes similar to those displayed by classical states’ Markov processes. Density matrices denoted by  $\rho$  represent quantum states, similar to probability vectors that represent classical states. Quantum states evolve according to the transformation  $\rho' = E(\rho)$ , where  $E$  denotes a quantum operation that represents the dynamics of a state due to a physical process. The initial states, denoted by  $\rho$ , transition to final states, denoted by  $E(\rho)$ , due to this process, often requiring a normalization factor. Unitary transformations and measurements are examples of quantum operations where  $E(\rho) = U\rho U^\dagger$  and  $E_m(\rho) = M_m\rho M_m^\dagger$ , respectively.

The development of a general theory of quantum operations involves unitary evolution, measurement, and more general processes. Three distinct yet equivalent perspectives are employed to study this theory. The first perspective examines dynamics through the lens of system-environment interactions. Although this viewpoint has real-world applicability, it is mathematically cumbersome. The second perspective, known as the operator-sum representation, offers a robust mathematical framework for quantum operations, facilitating theoretical and computational analysis despite its abstract nature. The third perspective introduces a set of axioms, grounded in the physical rationale, that are expected to govern the dynamical maps in quantum mechanics. This axiomatic approach gives generality, such that quantum operations govern quantum dynamics under a vast array of scenarios. However, it lacks the computational ease of the second method and the tangible aspects of the first. These methodologies, taken together, offer a versatile toolkit for comprehending quantum noise and its ramifications.

### 3.1.1 System coupled to environment

In quantum mechanics, the concept of a system and its environment is fundamental. A system is typically a smaller part of the universe being studied, while the environment comprises everything else that interacts with the system. A Hilbert space can mathematically describe such a quantum system, and its state is represented by a density matrix living in this space.

To study the dynamics of an open quantum system, we can expect it to be a result of interactions between two entities: the principal system under examination and an environment. These two entities, when combined, form a closed quantum system. Imagine a scenario where our system, represented by the state  $\rho$ , is introduced into a mechanism that interacts with an environment. However, unlike the initial state  $\rho$ , the system’s final state, denoted as  $E(\rho)$ , may not be derivable through a unitary transformation from  $\rho$ . Initially, we assume that the combined state of the system and environment is separable and is represented as  $\rho \otimes \rho_{\text{env}}$ . Following the application of a transformation  $U$ , the system stops interacting with the environment. To isolate the system’s state post-interaction, we perform a partial trace over the

environment, yielding the system's reduced state as

$$E(\rho) = \text{Tr}_{\text{env}}[U(\rho \otimes \rho_{\text{env}})U^\dagger], \quad (3.1)$$

where  $\text{Tr}_{\text{env}}$  denotes the operation of tracing out the environmental degrees of freedom. Our analysis assumes that the system and its surroundings start as separate entities. Although quantum systems may interact with their environments, in practical settings, it's reasonable to assume that both start uncorrelated. Even when the initial state is not a pure product state between the system and its environment, the quantum operations framework can still manage the dynamics of quantum systems.

### 3.1.2 Operator-Sum representation

The operator-sum representation is an elegant way to capture the formalism of quantum operations. It is a direct re-articulation of eq.(3.1) but uses only operators acting within the principal system's Hilbert space. We start by assuming  $|e_k\rangle$  is an orthonormal basis for the environment's finite-dimensional state space, with the environment's initial state being  $|e_0\rangle\langle e_0|$ . With this assumption, eq.(3.1) can be reformulated as:

$$E(\rho) = \sum_k \langle e_k | U[\rho \otimes |e_0\rangle\langle e_0|] U^\dagger | e_k \rangle = \sum_k E_k \rho E_k^\dagger, \quad (3.2)$$

where  $E_k \equiv \langle e_k | U | e_0 \rangle$  acts as an operator on the principal system's state space. If the environment initiates in a mixed state, we can introduce an additional hypothetical system to purify the environment as discussed in (3.1.4.2). The hypothetical system does not affect the principal system's dynamics but serves as a useful calculative step. This representation, known as the operator-sum representation of  $E$ , with the set  $\{E_k\}$  being the operation elements or Kraus' operators for the quantum operation  $E$ , plays a crucial role and will frequently be used throughout the text.

The completeness relation is a critical constraint that these operation elements adhere to as it emerges from the requirement that  $E(\rho)$  has unit trace,  $\text{Tr}[E(\rho)] = 1$

$$\text{Tr} \left[ \sum_k E_k \rho E_k^\dagger \right] = \text{Tr} \left[ \sum_k E_k^\dagger E_k \rho \right] = 1. \quad (3.3)$$

Given that this relation holds for any  $\rho$ , it implies  $\sum_k E_k^\dagger E_k = \mathbb{I}$  which indicates that the quantum operations are trace-preserving. However, there exist non-trace-preserving quantum operations where  $\sum_k E_k^\dagger E_k \leq I$  characterizing processes that yield additional information about the operation through measurement. The operators  $\{M_{a\mu}\}$  adhere to the inequality constraint  $\sum_\mu M_{a\mu}^\dagger M_{a\mu} \leq I$ . Generalized measurements and quantum channels are special cases of this framework [53].

### 3.1.3 Axiomatic Formulas

We are now approaching quantum operations from a new perspective by establishing a set of axioms rooted in physical principles. This conceptual approach provides valuable insights through higher levels of abstraction. We assume that the quantum operation  $E$  transforms density operators from an initial space  $\mathcal{H}_1$  to density operators in a final space  $\mathcal{H}_2$ , following three foundational axioms.

1. As discussed previously, given the initial state  $\rho$ , the probability of process  $E$  occurring can be represented by the trace of  $E(\rho)$ , denoted as  $\text{Tr}[E(\rho)]$ . It is important to note that this probability is always between 0 and 1 for any state  $\rho$ .

Quantum operations, symbolized as  $E$ , transition quantum states with outcomes quantified by  $\text{Tr}(E(\rho))$ , the trace of the output state. In quantum channels,  $\text{Tr}(E(\rho)) = 1$  maintains the total probability, aligning with the probabilistic nature of quantum mechanics. However,  $\text{Tr}(E(\rho)) < 1$  implies selective measurement processes (or post-selection mechanisms) or non-trace-preserving operations, indicating lossy processes or conditional selections in quantum algorithms. This scenario necessitates normalization of  $E(\rho)$  by  $1/\text{Tr}(E(\rho))$  for further use, ensuring a valid quantum state. In summary,  $\text{Tr}(E(\rho)) < 1$  reflects selective or lossy quantum processes, requiring adjustment for continued application within quantum mechanics or computation.

2. **Linearity:** Quantum operations must be linear maps, implying that the evolution of a superposition of states is the superposition of the evolution of individual states.  $E$  is a convex-linear operator on density matrices. This means that if we have a set of probabilities  $\{p_i\}$  and a weighted sum of states  $\sum_i p_i \rho_i$ , applying the operation  $E$  will result in the weighted sum of the transformed states  $\sum_i p_i E(\rho_i)$ . For a state  $\rho_i$  prepared with probability  $p_i$ , its evolution is given by:

$$\rho' = \sum_i p_i E(\rho_i) = E \left( \sum_i p_i \rho_i \right). \quad (3.4)$$

3. **Completeness and Positivity:** Quantum operations must map valid quantum states to valid quantum states, which means that the operation must be completely positive (preserving the positivity of the density matrix) and trace-preserving (ensuring that the total probability is conserved).

Quantum operations are completely positive, remaining positive even when part of a larger system. If we have a positive operator  $A$  on system  $\mathcal{H}_1$  and  $E$  transforms density operators from  $\mathcal{H}_1$  to  $\mathcal{H}_2$ , then  $E(A)$  must also remain positive. Additionally, when we introduce a new system  $R$  of any size and perform the combined operation  $(\mathbb{I} \otimes E)(A)$  on the extended system  $R\mathcal{H}_1$ , the outcome must be positive for any positive operator  $A$  on  $R\mathcal{H}_1$ . Here,  $\mathbb{I}$  represents the identity operation on system  $R$ . Complete positivity is a

more stringent condition than positivity, illustrated by the non-complete positivity of the transpose map  $T$ .

A mapping  $E$  conforms to these axioms if it can be expressed through an operator-sum representation and thus bridges the gap between the axiomatic framework and our earlier discussions.

### 3.1.4 Revisiting the Postulates

The principles of quantum mechanics were initially formulated for closed systems. However, with our current understanding of open quantum systems, we reformulate the postulates of quantum mechanics in terms of the density operator to include both open and closed systems.  
:

#### Postulate 1: States

*Quantum states are represented by density operators,  $\rho$  which are non-negative and Hermitian operators within Hilbert space. They are normalized to have a trace of one.*

#### Postulate 2: Measurement

*These are described through positive operator-valued measures (POVMs), which are essentially collections of non-negative operators that sum to the identity operator. Quantum measurements are described by measurement operators  $\{M_m\}$ . For a system in state  $\rho$ , the probability of outcome  $m$  is:*

$$p(m) = \text{Tr}[M_m^\dagger M_m \rho], \quad (3.5)$$

*and the post-measurement state is:*

$$\frac{M_m \rho M_m^\dagger}{\text{Tr}[M_m^\dagger M_m \rho]}. \quad (3.6)$$

*The operators satisfy  $\sum_m M_m^\dagger M_m = \mathbb{I}$ .*

#### Generalized measurements

Generalized measurements extend the concept of measurement in quantum mechanics beyond the traditional framework of orthogonal projections. Instead of measuring in a specific basis that corresponds directly to the eigenstates of an observable, generalized measurements

allow for a broader class of measurement outcomes, which may not be associated with orthogonal states of the quantum system. This flexibility is crucial for capturing a wider variety of physical processes and interactions within quantum systems.

Consider a quantum system  $A$  described by a state vector  $|\psi\rangle_A$  in a Hilbert space. The interaction between the system  $A$  and a measurement apparatus (or another quantum system)  $B$  can be represented by a unitary transformation  $U$  on the composite system. Without restricting ourselves to the orthogonal basis of  $B$  or invoking specific physical models of measurement, we can analyze the outcome of the measurement process through the mathematical formalism of operators. Upon the application of  $U$ , the combined state of  $A$  and  $B$  evolves as:

$$U : |\psi\rangle_A \otimes |0\rangle_B \rightarrow \sum_a M_a |\psi\rangle_A \otimes |a\rangle_B, \quad (3.7)$$

where  $|0\rangle_B$  is the initial state of  $B$ ,  $|a\rangle_B$  are the basis states of  $B$  post-interaction, and  $M_a$  are operators acting on the state of  $A$ . These operators are derived from the interaction and effectively describe the transformation of  $A$ 's state dependent on the measurement outcome indexed by  $a$ . The measurement process projects the state of  $B$  onto one of its basis states  $|a\rangle_B$ , correlating the outcome with a corresponding transformation  $M_a$  of  $A$ . The post-measurement state of  $A$  is then given by  $M_a |\psi\rangle_A$ , up to normalization. Unitarity of  $U$  implies certain constraints on the operators  $M_a$ , most notably that they must satisfy the completeness relation:

$$\sum_a M_a^\dagger M_a = \mathbb{I}, \quad (3.8)$$

where  $\mathbb{I}$  is the identity operator on the state space of  $A$ . This relation ensures that the total probability of all possible outcomes of the measurement is 1, maintaining the probabilistic interpretation of quantum mechanics. In this context, the probability of obtaining a particular outcome  $a$  when measuring  $B$  is determined by the norm squared of the projected state of  $A$ ,  $\|M_a |\psi\rangle_A\|^2$ .

### Postulate 3: Evolution

*The evolution of a closed quantum system is described by a unitary transformation. If the system is in state  $\rho$  at time  $t_1$ , it transforms to state  $\rho' = U\rho U^\dagger$  at time  $t_2$  via a unitary operator  $U$ .*

The evolution over time is depicted by trace-preserving completely positive maps (TPCP maps). The temporal evolution of quantum states is governed by trace-preserving completely positive maps (TPCP maps).

### Quantum Channels

Quantum channels are fundamentally conceptualized as completely positive trace-preserving (CPTP) maps, serving as convex linear transformations that facilitate the transition of quantum

states in a system [54]. The initial state of a system, represented by the density operator  $\rho = |\psi\rangle\langle\psi|$ , undergoes a transformation through a linear mapping  $E$ , defined as:

$$E(\rho) = \sum_a M_a \rho M_a^\dagger. \quad (3.9)$$

These operations follow specific criteria ensuring the physical feasibility of such transformations. The completeness relation constrains the Kraus operators:

$$\sum_a M_a^\dagger M_a = I, \quad (3.10)$$

which guarantees the preservation of the total probability (trace preservation) through the channel. This mapping, characterized by the equation above, is referred to as a quantum channel. The term "channel" originates from the field of communication theory, suggesting the conceptual model of a sender transmitting the state  $\rho$  through a communication link, resulting in the recipient receiving an altered state  $E(\rho)$ . An alternative term, "superoperator," is also used to describe quantum channels, highlighting the transformation of operators by operators, as opposed to vector transformations. Additionally, these channels are known as **trace-preserving completely positive maps, or TPCP maps**, a designation that reflects specific properties of the transformation that will be clarified. The defining properties of a quantum channel include **Linearity**, **Hermiticity Preservation** (If an input state is Hermitian, i.e.  $\rho = \rho^\dagger$ , the output state will also be Hermitian), **Positivity Preservation** (For an input state that is positive i.e.  $\rho \geq 0$ ), the output state will also be positive, ensuring that the resulting probabilities are non-negative.), and **Trace Preservation**. The "completely positive" aspect of the term TPCP indicates that the channel not only maintains positivity for the states it directly acts upon but also when it is part of a larger system. This condition ensures that the physical validity of states is preserved even when the system is entangled with another and the channel is applied to only one part of the entangled system.

The representation described here is known as the operator-sum representation, and the  $\{M_a\}$  are identified as Kraus operators or operational elements of the channel. The operations are executed by a collection of operators known as Kraus operators  $\{M_a\}$ , with the quantum channel's action on a quantum state  $\rho$  given by the operator-sum representation. Moreover, the operator-sum representation of a quantum channel is not unique; varying sets of Kraus operators can equivalently describe the same quantum channel linked by a unitary transformation. This non-uniqueness permits diverse mathematical characterizations of the same physical phenomena.

Quantum channels extend beyond mere unitary evolution as delineated by the Schrödinger equation; they offer a generalized model for describing non-unitary evolution processes, including those involving decoherence and various forms of quantum noise.

	<b>Closed Quantum Systems</b>	<b>Open Quantum Systems</b>
State Representation	State vector	Density Matrix
Evolution	Unitary Transformation	Operator Sum Representation of Channels
Measurement	Projective Measurement	Positive Operator Valued Measurement (POVM)

Table 3.1: Summarising Closed Quantum Systems v/s Open Quantum Systems

## Postulate 4: Composite Systems

*The state space of a composite system is the tensor product of component state spaces. If system  $i$  is in state  $\rho_i$ , the joint state is  $\rho_1 \otimes \rho_2 \otimes \dots \otimes \rho_n$ .*

The concepts of density operators and partial trace are important in understanding the dynamics of composite quantum systems. In addition to these foundational tools, advanced techniques such as the Schmidt decomposition and purifications are significant and useful in enhancing our understanding of quantum systems.

### 3.1.4.1 Schmidt Decomposition

In the case of a bipartite AB system with a pure state  $|\psi\rangle$ , there exist sets of orthonormal states,  $|i_A\rangle$  for subsystem A and  $|i_B\rangle$  for subsystem B, that enable the expression of  $|\psi\rangle$  as a sum  $\sum_i \lambda_i |i_A\rangle |i_B\rangle$ . The coefficients  $\lambda_i$  are non-negative real numbers (Schmidt coefficients) that satisfy the condition  $\sum_i \lambda_i^2 = 1$ . This is known as the Schmidt decomposition.

### 3.1.4.2 Purification

Purification involves the conceptualization of an auxiliary system R when analyzing a quantum state  $\rho_A$  of a given quantum system A. A joint pure state  $|AR\rangle$  can then be constructed for the composite AR system, ensuring that the mixed state  $\rho_A$  emerges as the reduced state of system A upon performing a partial trace over system R. The process of introducing the notion of a reference system R to associate mixed states with corresponding pure states is crucial in the mathematical framework for analyzing quantum states, although R is considered a hypothetical system with no direct physical manifestation.

This framework allows for either the open-system or closed-system perspective to be viewed as the foundational approach to quantum theory, depending on preference. We have demonstrated how to derive the open-system principles from those of closed systems. Conversely, beginning with open-system concepts, we find that pure states emerge as special cases (extremal points) within the set of density operators, highlighting that any density operator can be 'purified' within a larger system. Furthermore, the framework naturally incorporates orthogonal measurements and unitary evolution. Every POVM measurement can be realized through

orthogonal measurements in a larger space, and all TPCP maps can be extended to isometric transformations in a higher-dimensional Hilbert space. This interplay supports the concept often referred to as the "church of the larger Hilbert space," which posits that any open system can be part of a greater, encompassing closed system.

## 3.2 Quantum Noise

Quantum computers face greater susceptibility to noise and imperfections than traditional digital computers. The inevitable interaction between the device and its environment leads to decoherence, adversely affecting the encoded quantum information. Density matrices are pivotal in studying the effects of decoherence, a common phenomenon in practical quantum computing where systems interact with their environment. Strategies must be devised to mitigate these challenges in order to realize the practical application of quantum computers. Noise is an unwanted disturbance that affects a quantum system, and it is closely related to decoherence. Decoherence occurs when a quantum system interacts with its environment, causing it to become entangled with its surroundings and leading to a loss of fragile quantum properties such as superposition and phase coherence. Noise can come from various sources, including environmental factors, imperfect hardware, and interactions with external fields.

When the quantum system is not isolated from its surroundings, the background noise causes the quantum states to lose coherence rapidly over time. This degradation limits the ability to perform complex calculations and maintain desired quantum states. Thus, quantum computing research is focused on minimizing noise and decoherence through error correction techniques, quantum error correction codes, and fault-tolerant quantum computing methods. These methods aim to improve the stability of quantum states, suppress the negative effects of noise, and enable reliable quantum computation in the presence of environmental disturbances.

Understanding the impact of noise on quantum systems is crucial for comprehending the role of the environment in their evolution. To model these environmental interactions, we can use quantum channels, as defined in 3.2.1. These channels are Trace-preserving Completely Positive (TPCP) linear maps such that  $\Lambda$  gives:  $\rho \rightarrow \sum_i K_i \rho K_i^\dagger$ , where the  $K_i$ 's are the Kraus operators associated with the state's evolution. Researchers have explored the effect of noise on various quantum properties, including entanglement [7][8] and correlation [9], from both closed and open system perspectives [10].

## 3.2.1 Modeling Noise as a Quantum Depolarizing Channel

### 3.2.1.1 Generalised Depolarizing Channel

The quantum depolarizing channel is a prevalent model for representing quantum noise, characterized as a CPTP map,  $\Lambda_q$ , with a single parameter,  $q$  [55]. It transforms a quantum state  $\rho$  in a  $d$ -dimensional space into a mixture of itself and the maximally mixed state,  $\frac{\mathbb{I}_d}{d}$ , as expressed by:

$$\Lambda_q(\rho) = q\rho + \frac{(1-q)}{d}\mathbb{I}_d. \quad (3.11)$$

The parameter  $q$  in  $\Lambda_q$  must conform to a certain range to ensure complete positivity [56]:

$$\frac{-1}{d^2 - 1} \leq q \leq 1. \quad (3.12)$$

### 3.2.1.2 Depolarizing Channel Noise Model

The  $\mathcal{D}_t$  channel, a specific instance of the generalized qudit depolarizing channel from (3.11), affects a  $d$ -dimensional quantum state  $\rho$  with a parameter  $0 < t < 1$  to yield the output,

$$\mathcal{D}_t(\rho) = (1-t)\frac{\mathbb{I}_d}{d} + t\rho. \quad (3.13)$$

Here,  $1-t$  symbolizes the depolarizing probability of the channel, while  $t$  indicates the likelihood of the state  $\rho$  being preserved. This depolarizing channel model is widely used to simulate quantum noise [25], represented by,

$$\mathcal{D}_t(\rho) = t\rho + \frac{1-t}{d^2} \sum_{i=1}^{d^2} U_i \rho U_i^\dagger. \quad (3.14)$$

In this representation,  $\{U_i\}_{i=1}^{d^2}$  signifies a set of unitary operators forming an orthonormal basis in the space of  $d \times d$  matrices, utilized consistently in this paper.

The depolarizing channel can be depicted using operator-sum representation with Kraus operators [54]. In a  $d$ -dimensional space, it is formulated as:

$$\mathcal{D}_t(\rho) = \sum_{i=0}^{d^2} D_i \rho D_i^\dagger, \quad (3.15)$$

where  $D_i$  are defined with  $D_0 = \sqrt{t}\mathbb{I}_d$  and  $D_i = \frac{1}{\sqrt{d(1-t)}}U_i$  for  $i = 1, \dots, d^2$ , and  $U_i$  are orthogonal unitary operators.

A notable attribute of this channel is its commutative property when sequentially applied. Using two channels,  $\mathcal{D}_{t_1}$  and  $\mathcal{D}_{t_2}$ , with preservation probabilities  $t_1$  and  $t_2$ , the result is a single depolarizing channel, irrespective of the application sequence, with a combined state preservation probability of  $t_1 t_2$ :

$$\mathcal{D}_{t_2}(\mathcal{D}_{t_1}(\rho)) = \mathcal{D}_{t_1}(\mathcal{D}_{t_2}(\rho)) = (1-t_1 t_2)\frac{\mathbb{I}_d}{d} + t_1 t_2 \rho. \quad (3.16)$$

In some contexts, this model might be considered overly pessimistic. Often, further information about the channel's physical properties can be obtained through various estimation techniques. The use of the depolarizing channel as a noise model is mainly advisable when there is limited knowledge about the actual physical channel. It can be presented as follows:

$$\mathcal{D}_t(\rho) := (1 - t)\rho_d + t\frac{\mathbb{I}_d}{d}\text{Tr}[\rho_d], \quad (3.17)$$

where it acts on states  $\rho$  in a  $d$ -dimensional Hilbert space.

For certain calculations, it is useful to consider quantum channels within the broader context of all linear operators on a given Hilbert space, not just density matrices, as will be seen in [A.3](#). The inclusion of  $\text{Tr}[\rho]$  in the channel's definition ensures linearity. If the input is guaranteed to have a unit trace, then the  $\text{Tr}[\rho]$  term becomes superfluous.

The depolarizing channel has been pivotal in channel identification studies [\[57\]](#), in exploring channel capacity enhancements through indefinite causal order [\[27\]](#), and in analytical comparisons of various channel probing methods [\[58\]](#).

### 3.2.1.3 Error probability $e$ and its relation with the channel parameter $t$

The channel parameter  $t$  for a quantum channel  $\mathcal{D}_t$  is different from the probability of retaining the original state of the register  $(1 - e)$  (where  $e$  is the probability of getting an erroneous state output, i.e., not equal to the input state)

We are denoting the preservation probability as  $\bar{e} = 1 - e$ . The expression for the generalized depolarizing channel in terms of probability  $\bar{e}$ :

$$\begin{aligned} \mathcal{D}_{\bar{e}}(\rho) &= \bar{e}\rho + \frac{1 - \bar{e}}{d^2 - 1} \sum_{i=1}^{d^2-1} U_i \rho U_i^\dagger \\ &= \bar{e}\rho - \left( \frac{1 - \bar{e}}{d^2 - 1} \cdot \mathbb{U}_0 \rho \mathbb{U}_0^\dagger \right) + \frac{1 - \bar{e}}{d^2 - 1} \sum_{i=1}^{d^2-1} U_i \rho U_i^\dagger + \left( \frac{1 - \bar{e}}{d^2 - 1} \cdot \mathbb{U}_0 \rho \mathbb{U}_0^\dagger \right) \\ &= \left( \bar{e} - \frac{1 - \bar{e}}{d^2 - 1} \right) \rho + \frac{1 - \bar{e}}{d^2 - 1} \sum_{i=0}^{d^2-1} U_i \rho U_i^\dagger \quad (\because \mathbb{U}_0 = \mathbb{I}) \end{aligned} \quad (3.18)$$

We know that  $\frac{1}{d^2} \sum_{i=1}^{d^2} U_i \rho U_i^\dagger = \text{Tr}(\rho) \frac{\mathbb{I}}{d} = \frac{1}{d^2} \sum_{i=0}^{d^2-1} U_i \rho U_i^\dagger$

$$\mathcal{D}_{\bar{e}}(\rho) = \underbrace{\left( \bar{e} - \frac{1 - \bar{e}}{d^2 - 1} \right)}_t \rho + \underbrace{\left( \left( \frac{1 - \bar{e}}{d^2 - 1} \right) d^2 \right)}_{1-t} \text{Tr}(\rho) \frac{\mathbb{I}}{d} \quad (3.19)$$

We can verify this by checking if the total probability comes to be 1, as follows:

$$\begin{aligned} \left( \bar{e} - \frac{1 - \bar{e}}{d^2 - 1} \right) + \left( \frac{1 - \bar{e}}{d^2 - 1} \right) d^2 &= \frac{(d^2 \bar{e} - \bar{e} - 1 + \bar{e}) + (d^2 - d^2 \bar{e})}{d^2 - 1} \\ &= \frac{(d^2 - 1)}{d^2 - 1} = 1 \end{aligned}$$

$$\begin{aligned}
\text{Thus, } \quad & \left( \bar{e} - \frac{1 - \bar{e}}{d^2 - 1} \right) = t \\
& \left( \frac{(d^2 - 1)\bar{e} - (1 - \bar{e})}{d^2 - 1} \right) = t \\
& \left( \frac{d^2\bar{e} - 1}{d^2 - 1} \right) = t
\end{aligned} \tag{3.20}$$

Applying Probability constraints gives us the range of the parameter as discussed earlier

$$\begin{aligned}
\bar{e} &= \frac{(d^2 - 1)t + 1}{d^2} \\
0 < \bar{e} < 1 &\implies 0 < \left( \frac{(d^2 - 1)t + 1}{d^2} \right) < 1 \\
0 < (d^2 - 1)t + 1 < d^2 &\implies -1 < (d^2 - 1)t < (d^2 - 1) \\
\frac{-1}{(d^2 - 1)} < t < 1 &
\end{aligned} \tag{3.21}$$

It works the other way around as well, whereby the definition given above, a generic depolarizing channel in terms of parameter  $t$ , is

$$\begin{aligned}
\mathcal{D}_t(\rho) &= t\rho + (1 - t) \text{Tr}[\rho] \frac{\mathbb{I}}{d} \\
&= t\rho + \frac{1 - t}{d^2} \sum_{i=1}^{d^2} U_i \rho U_i^\dagger \\
&= t\rho + \frac{1 - t}{d^2} U_{d^2} \rho U_{d^2}^\dagger + \frac{1 - t}{d^2} \sum_{i=1}^{d^2-1} U_i \rho U_i^\dagger \\
&= \left( t + \frac{1 - t}{d^2} \right) \rho + \frac{1 - t}{d^2} \sum_{i=1}^{d^2-1} U_i \rho U_i^\dagger \\
&= \underbrace{\left( \frac{(d^2 - 1)t + 1}{d^2} \right)}_{\bar{e}} \rho + \underbrace{\frac{1 - t}{d^2}}_{\frac{1 - \bar{e}}{d^2 - 1}} \sum_{i=1}^{d^2-1} U_i \rho U_i^\dagger
\end{aligned}$$

It can be verified that  $\frac{1-t}{d^2} = \frac{1-\bar{e}}{d^2-1}$

$$\begin{aligned}
\frac{1 - \bar{e}}{d^2 - 1} &= \frac{1 - \left( \frac{(d^2 - 1)t + 1}{d^2} \right)}{d^2 - 1} \\
&= \frac{d^2 - (d^2 - 1)t - 1}{d^2(d^2 - 1)} \\
&= \frac{\cancel{(d^2 - 1)} + \cancel{(d^2 - 1)}t}{d^2 \cancel{(d^2 - 1)}} \\
&= \frac{1 - t}{d^2}
\end{aligned}$$

### 3.2.1.4 Total vs Local Depolarizing Channel

The Total Depolarizing Channel is a noise model that transforms an  $n$ -qubit state  $\rho$  into a maximally mixed state  $\frac{\mathbb{I}}{d}$  with a specified probability  $e$ . Conversely, with probability  $1 - e$ , the state  $\rho$  remains unaffected. This channel can be represented as:

$$\mathcal{D}_T(\rho) = \begin{cases} \frac{\mathbb{I}}{d}, & \text{with probability } e, \\ \rho, & \text{with probability } 1 - e. \end{cases} \quad (3.22)$$

This introduces a stochastic element to the evolution of the quantum state, making the noise model significant in scenarios where a state might completely lose its coherence with a certain likelihood.

In contrast, the Local Depolarizing Channel acts on each qubit of an  $n$ -qubit state  $\rho$  independently. It applies the depolarizing channel to each qubit, resulting in the transformation:

$$\varepsilon(\rho) = \varepsilon_1(\rho, e) \circ \varepsilon_2(\rho, e) \circ \dots \circ \varepsilon_n(\rho, e), \quad (3.23)$$

where  $\varepsilon_i(\rho, e)$  is the depolarizing channel acting on the  $i$ -th qubit, and  $e$  represents the error probability. Thus, this noise model systematically alters each qubit's state, leading to a more uniformly modified quantum state compared to the TDCh.

### 3.2.1.5 Complete vs. Partial Depolarizing Channel

We will be omitting the need to specify that the channel is partially depolarizing because a completely depolarizing channel is a special case of the partially depolarizing channel when the error parameter  $e = 1$  and always maps any input state to the maximally mixed state  $\frac{\mathbb{I}}{d}$  and thus doesn't need to be specified unless necessary.

## 3.3 Ideal Grover's Quantum Search Algorithm

Grover's algorithm, a pioneering quantum search method, significantly enhanced the efficiency of searching within an unstructured data set. Demonstrating optimal performance in identifying a specific element from an unsorted database of  $N$  items, it requires only  $k_{Gr} = \lceil \frac{\pi}{4} \sqrt{N} \rceil$  queries to the oracle [59, 60]. The search problem is formulated as follows: We are given a search domain comprising  $N = 2^n$  quantum states, where  $n$  is the number of qubits in the Hilbert space ( $\mathcal{H} = \mathbb{C}^{2^n}$ ). Within this set, an unknown target state is concealed. An oracle, or black box, is available, which can confirm whether a given state is the target. The goal is to pinpoint this target state with maximum accuracy while reducing the number of steps involved.

**Algorithm:** Firstly, the elements in the unstructured database of  $N$  items are indexed from  $[0, N - 1]$ . Here,  $N = 2^n$ , and  $n \in \mathbb{Z}_+$  signifies the qubit count in the register. The quantum states in the register are used to represent each database entry, denoted as  $\{|0\rangle, |1\rangle, \dots, |N - 1\rangle\}$ . A selection function  $f$ , inputting a state  $|x\rangle$  where  $x \in [0, N - 1]$ , outputs 1 if the state fulfills the search criteria and 0 otherwise. This function can be likened to an unstructured database query, with its domain representing the indices of the database.

$$f = \begin{cases} 0 & \text{if } x \text{ is not the desired state,} \\ 1 & \text{if } x \text{ is the desired state.} \end{cases} \quad (3.24)$$

The target state is represented as  $|\tau\rangle$ , and the algorithm aims to locate this specific index  $\tau$ . To interact with a function  $f$ , Grover's algorithm utilizes a quantum oracle-black box, represented by the unitary operator  $O_\tau$ . This operator acts on a quantum state as:

$$O_\tau|x\rangle = (-1)^{f(x)}|x\rangle.$$

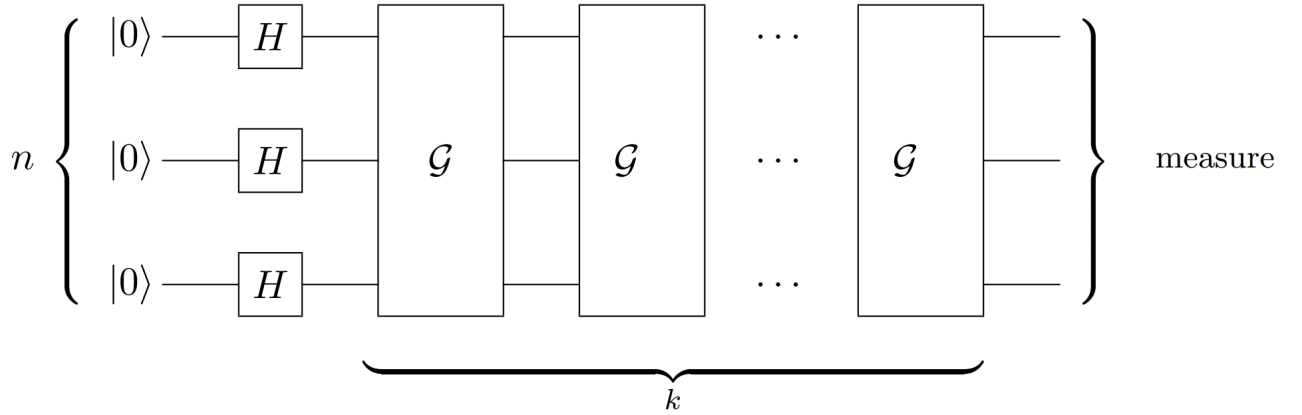


Figure 3.1: The Grover search algorithm with  $k$  Grover iterations

The algorithm is depicted as a schematic diagram in fig (3.1). Initially, a superposition of  $N$  quantum states is created through the application of a Hadamard transformation ( $H$ ),

$$|s\rangle = \frac{1}{\sqrt{N}} \sum_{x=0}^{N-1} |x\rangle. \quad (3.25)$$

Subsequently, the algorithm prescribes repetitive applications of a quantum subroutine termed the Grover iteration or Grover operator  $\mathcal{G}$ . A circuit diagram describing this Grover operator  $\mathcal{G}$  as a combination of Oracle function and diffusion operator is given in Fig.(3.3)

Each **Grover iteration**  $\mathcal{G}$  includes:

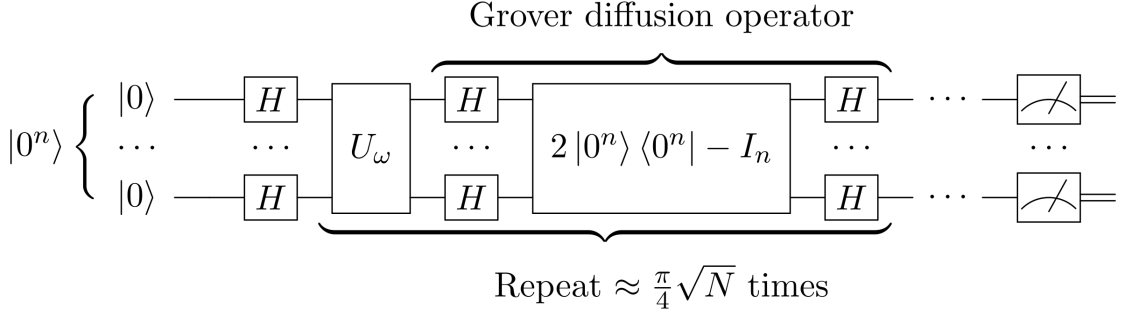


Figure 3.2: Quantum circuit representation of Grover's algorithm (The Grover oracle  $U_\omega$  flips the sign of  $|s\rangle$  if it is the marked element.) **By Fawly - Own work, CC BY-SA 4.0**

- Implementation of the oracle operator  $O_\tau = 2|t\rangle\langle t| - \mathbb{I}$ .
- Activation of the diffusion operator  $\delta$ , which conducts a rotation around the state  $|s\rangle$ . The expression for  $\delta$  is:

$$\delta = -H^{\otimes n}(2|0\rangle\langle 0| - I)H^{\otimes n} = 2|s\rangle\langle s| - \mathbb{I}$$

- Execution of measurements in the canonical basis on each qubit, where the target state is likely to be observed.

**State Evolution and Success Probability:** The algorithm state after  $k$  iterations of applying the oracle and diffusion operators is given by:

$$\rho(k) = \mathcal{G}^k \rho(0) (\mathcal{G}^\dagger)^k, \quad (3.26)$$

where  $\mathcal{G} = \delta O_\tau$  and  $\rho(0) = |s\rangle\langle s|$ . The resulting density operator is  $\rho(k) = |s_k\rangle\langle s_k|$ , with

$$\begin{aligned} |s_k\rangle &= \sin\left((2k+1)\sin^{-1}\frac{1}{\sqrt{N}}\right)|\tau\rangle \\ &+ \cos\left((2k+1)\sin^{-1}\frac{1}{\sqrt{N}}\right)|1-\tau\rangle, \end{aligned}$$

where,  $|1-\tau\rangle = \frac{1}{\sqrt{N-1}} \sum_{\substack{i=0 \\ i \neq \tau}}^{N-1} |i\rangle$  (3.27)

Thus, the probability of successfully locating the target element after  $k$  steps is

$$P(k) = \sin^2\left((2k+1)\sin^{-1}\frac{1}{\sqrt{N}}\right). \quad (3.28)$$

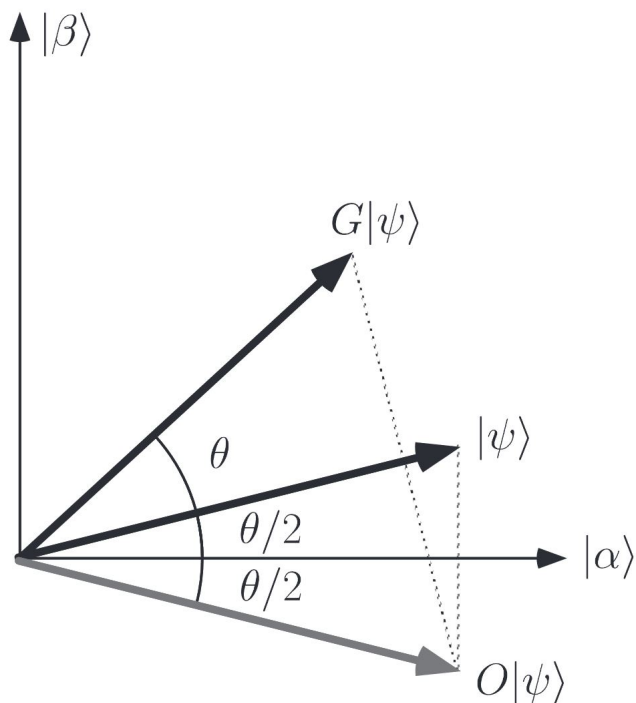


**Figure 3.3: Geometric Picture for the working of Grover's Search algorithm:**

Grover's search algorithm employs a geometric approach to find a marked item within an unsorted database efficiently. Initially, the quantum state  $|\psi\rangle$  is positioned at an angle  $\theta/2$  relative to the state  $|\alpha\rangle$ , which is orthogonal to  $|\beta\rangle$ , the superposition of all potential solutions. The process begins with an oracle operation  $O$ , which reflects  $|\psi\rangle$  about  $|\alpha\rangle$ , producing a new state  $O|\psi\rangle$ . Following this, the Grover diffusion operator,  $2|\psi\rangle\langle\psi| - I$ , reflects  $O|\psi\rangle$  about  $|\psi\rangle$ , yielding the state  $G|\psi\rangle$ . Each Grover iteration  $G$  effectively rotates the state vector  $|\psi\rangle$  by an angle  $\theta$  towards  $|\beta\rangle$ . Repeated iterations amplify the probability amplitude of the correct solution states. After roughly  $\mathcal{O}(\sqrt{N/M})$  iterations, where  $N$  is the total number of states and  $M$  is the number of solutions, the state vector approaches  $|\beta\rangle$ . At this point, measuring the quantum state on a computational basis yields a solution with high probability. The algorithm's efficiency is notable because the angle  $\theta$  is proportional to  $\sqrt{M/N}$ , resulting in significantly fewer iterations compared to classical search methods.

### 3.4 Influence of Noise on Grover’s Quantum Search Algorithm

Grover’s quantum search algorithm, discussed briefly in the previous section, constitutes an oracle-based method designed to search an unordered database efficiently. In its ideal form, this algorithm showcases a remarkable quadratic acceleration compared to the classical brute-force search. Nonetheless, this advantage significantly diminishes when the oracle encounters faults [13, 14] or when the algorithm operates in an environment of noise [15]. Local error models hold significance as they reflect the impact of gate errors on any practical implementation of a quantum circuit.

In this section, we can delve briefly into investigating the impact of a known noise rate on Grover’s search algorithm, looking into prior research conducted in [11, 12]. It is specifically using the error model associated with a **total partial depolarizing channel noise**. Many studies have been conducted to explore the effect of the depolarizing channel on Grover’s search algorithm. These studies have shown that this noise can significantly reduce the algorithm’s performance, indicating the need to maintain the integrity of the oracle mechanism and reduce external disturbances to ensure optimal operational efficiency.

In quantum systems, interaction with the environment is inevitable, particularly during processes like gate applications or state preparation, leading to the introduction of errors and noise. The effect of such environmental factors on quantum algorithms has been extensively studied [61, 62]. Grover’s quantum search algorithm, an oracle-based technique, is known for its efficient searching capabilities in an unordered database, demonstrating a quadratic speedup over traditional brute-force search methods [52]. However, this advantage diminishes when the oracle is faulty [14] or in noisy environments [63]. Investigations into partial depolarizing and dephasing noise models have been conducted by *Vrana et al.*. Besides the total depolarizing error model, which affects the entire quantum register, *Cohn et al.* also explored a local depolarizing error model that affects each qubit in the register individually with a certain probability, reflecting gate errors in quantum circuit implementations.

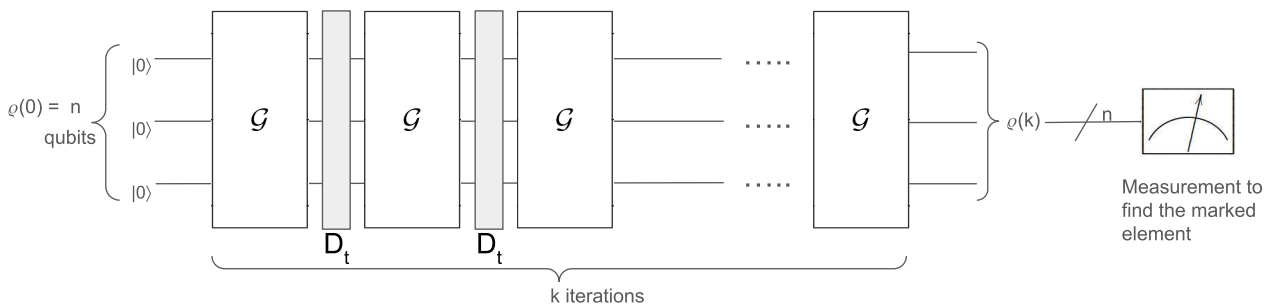


Figure 3.4: This figure illustrates the effect of noise on the Grover operator  $\mathcal{G}$ , shown by the shaded bar. Measurement at the end evaluates the impact of noise on the operator’s success probability.

This section provides an overview of the known noise rate’s impact on Grover’s algorithm. Errors occurring between successive quantum gate operations can be effectively modeled by depolarizing channels  $\mathcal{D}_t$ . This model simulates continuous exposure to noise in quantum computing and the random nature of error occurrence. The depolarizing noise replaces the entire  $n$ -qubit quantum register with a maximally mixed state with a probability  $t$  between each oracle invocation. This model, acting correlated across the entire quantum register, is akin to a noisy oracle and can be quite pessimistic in some cases. Quantum error correction techniques [54, 64] are notably ineffective against partial depolarizing or dephasing noises, which affect the quantum computer as a whole. Such collective disturbances are comparable to the quantum system experiencing a sudden ‘flash’ of noise, such as laser fluctuations or external magnetic field interference, common in moderately sized quantum computers.

### 3.4.1 State Evolution with Error

The process involves the sequential use of the Grover operator  $\mathcal{G}$  and the subsequent application of the depolarizing channel error  $\mathcal{D}_t$ . The depolarizing channel error commutes with any unitary operation when acting on the system [11]. Hence, in the noisy Grover’s algorithm, the resultant state after noise application is expressed as  $(\mathcal{D}_t\mathcal{G})^k(\rho)$ , where  $\mathcal{G}(\rho)$  is defined by  $\mathcal{G}(\rho) = ((\mathbb{I}_d - 2|\psi\rangle\langle\psi|)O_\tau)\rho((\mathbb{I}_d - 2|\psi\rangle\langle\psi|)O_\tau)^\dagger$ . Therefore, after ‘ $k$ ’ iterations, the state evolves as:

$$\rho(k, t) = t^k \rho(k) + (1 - t^k) \frac{I}{d}, \quad (3.29)$$

where  $\rho(k)$  is as in eq.(3.26).

### 3.4.2 Success Probability

The probability of successfully identifying the target index  $\tau$  in the oracle is determined by:

$$P(k, (1 - t), d) = \frac{1}{d} \sum_{x=1}^d \langle \tau | (\mathcal{D}_t\mathcal{G})^k (|\psi\rangle\langle\psi|) | \tau \rangle. \quad (3.30)$$

This expression represents the success probability after  $k$  iterations for an input space  $\rho$  of dimension  $d = 2^n$ , with  $d$  as the total number of possible oracles. The parameter  $(1 - t)$  indicates the depolarizing noise strength during the algorithm, with  $t$  as the channel parameter for the total, partial depolarizing channel at each step (refer to 3.17). This formulation averages the success probability over all  $d$  oracles, assuming equal likelihood, contrasting with methodologies that focus on the minimal success probability. This average success approach aligns with perspectives in references like [59], differing from the minimal success probability method seen in [54, 65].

$$\begin{aligned}
P(1, (1-t), d) &= \frac{1}{d} \sum_{x=1}^d \langle x | (\mathcal{D}_t \mathcal{G}_x)(\rho) | x \rangle \\
&= t \cdot P(1, 0, d) + (1-t) \frac{1}{d} \quad [ \because P(k, 0, d) \text{ as in 3.28} ] \\
&= t \cdot \sin \left( (2(1) + 1) \arcsin \left( \frac{1}{\sqrt{d}} \right) \right) + (1-t) \frac{1}{d}. \tag{3.31}
\end{aligned}$$

For the noise above model, the process  $(DpGx)^k$  can be expanded into  $2^k$  distinct histories, with each term positively contributing. By retaining the noise-free component  $t\rho$  in each segment, a lower bound for success probability  $P(k, (1-t), d)$  is given by:

$$P(k, (1-t), d) \geq t^k \sin^2 \left( (2k + 1) \arcsin \frac{1}{\sqrt{d}} \right). \tag{3.32}$$

With partial depolarizing noise, the exact success probability is computable [12]. Omitting  $2^k - 1$  terms results in  $\frac{1}{d}(1-t)^m(t)^{k-m}$ , where  $m$  is the number of noise occurrences in  $k$  iterations. Summing these terms, which total  $1 - t^k$ , gives the precise probability for this model as,

$$P(k, (1-t), d) = (1-t^k) \frac{1}{d} + t^k \sin^2 \left( (2k + 1) \arcsin \frac{1}{\sqrt{d}} \right). \tag{3.33}$$

## Chapter 4

### Investigating Noisy Grover’s Search using Quantum Switches

“All fiction that does not violate the laws of physics is fact”

– David Deutsch, [The Beginning of Infinity](#)

“Creativity is just connecting things... A lot of people in our industry haven’t had very diverse experiences. So, they don’t have enough dots to connect, and they end up with very linear solutions without a broad perspective on the problem. The broader one’s understanding of the human experience, the better design we will have.”

– Steve Jobs, [In a 1995 Wired article](#)

In this chapter, we build on the foundations laid in the previous chapters and explore the use of quantum switches to mitigate noise in Grover’s search algorithm. We start with a brief on indefinite causal order before introducing the quantum device central to our study, called quantum switches, and talk about its functioning and mathematical formalism used for calculations. Quantum channels put in a superposition of order using quantum switches leads to what we will often refer to as **switched channels with indefinite causal order** [66, 67], and we will be introducing two frameworks utilizing these switched channels. We set up some background and assumptions underlying the two proposed switched channel frameworks for noisy Grover’s search algorithm before getting into the state evolution and success probability of the algorithm under each framework. For this study, we will be using the total, partial depolarising channel discussed in (3.4) for modeling the quantum noise, contrasting the success probabilities of Grover’s algorithm on a search space of 4 qubits or  $2^4$  elements with and without the application of quantum switches for both the frameworks for upto  $k = 3$  iterations.

## 4.1 Quantum Switch

The quantum switch is a novel quantum primitive that has attracted attention due to the various advantages it can provide in different subfields of quantum information over processes with well-defined causal orders.

### 4.1.1 Introduction to Indefinite Causal Order

The concept of causal order is a fundamental aspect of daily experience, where events are perceived as occurring in a fixed order. However, quantum physics proposes the existence of nonclassical causal structures where the order of events is indefinite. In particular, the process matrix formalism extends quantum mechanics laws to accommodate processes with indefinite causal order. This allows for the generation of superpositions of causal orders by controlling the causal order between two operations with a quantum degree of freedom in a superposition. Quantum theory allows the combination of communication channels in novel ways, creating a quantum superposition of different configurations. This theory allows the order of channel application to be entangled with a control system known as a **quantum superposition of orders**. Besides, quantum theory also permits the formation of unusual configurations that are not compatible with any underlying model where the order is definite. The **quantum switch** is a canonical example of a process with indefinite causal order. It is studied using a framework that distinguishes whether a process is compatible with a fixed causal order or not. The ability to combine communication channels in a superposition of orders can enhance various tasks, such as testing properties of quantum channels, playing non-local games, and reducing communication complexity.

### 4.1.2 Mathematical Formulation of Quantum Switch

In this subsection, we discuss the implementation of quantum switches in general. As mentioned before in eq.(3.15), the action of a quantum channel  $\mathcal{N}$  on an input state  $\rho$  can be expressed using the Kraus representation, or operator-sum representation, formulated as  $\mathcal{N}(\rho) = \sum_i K_i \rho K_i^\dagger$ , where  $\{K_i\}$  denotes the set of Kraus operators for  $\mathcal{N}$ . Consider two quantum channels,  $\mathcal{N}_1$  and  $\mathcal{N}_2$ ; they can operate either concurrently or sequentially. The concurrent operation is represented as  $\mathcal{N}_1 \otimes \mathcal{N}_2$ . In contrast, sequential operations can be arranged in two ways:  $\mathcal{N}_1$  followed by  $\mathcal{N}_2$  (notated as  $\mathcal{N}_2 \circ \mathcal{N}_1$ ) or  $\mathcal{N}_2$  followed by  $\mathcal{N}_1$  (notated as  $\mathcal{N}_1 \circ \mathcal{N}_2$ ). If the sequence of these channels is fixed, only one of the sequences, either  $\mathcal{N}_2 \circ \mathcal{N}_1$  or  $\mathcal{N}_1 \circ \mathcal{N}_2$ , is permissible. However, the sequence in which two channels operate can be rendered indefinite using an ancillary system, namely the control qubit ( $\rho_c$ ) [25, 27, 68],  $\rho_c = |c\rangle\langle c|$  where  $\sqrt{\theta}|0\rangle + \sqrt{\bar{\theta}}|1\rangle$ . With  $\rho_c$  set to the  $|0\rangle\langle 0|$  state, the  $\mathcal{N}_2 \circ \mathcal{N}_1$  arrangement affects the state  $\rho$ , while  $\mathcal{N}_1 \circ \mathcal{N}_2$  comes into play when  $\rho_c$  is in the  $|1\rangle\langle 1|$  state. If  $\{K_i^{(1)}\}$  represent the Kraus

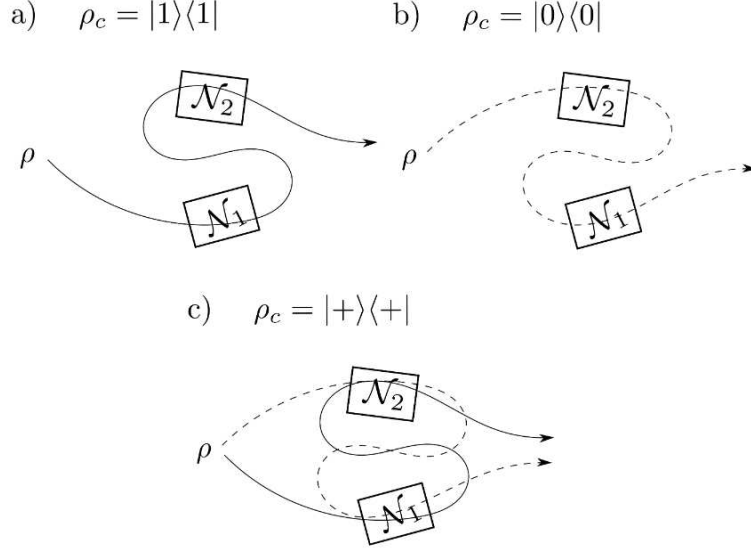


Figure 4.1: *Fixed order vs superposition of orders.* (a) A quantum particle, prepared in the state  $\rho$ , goes first through channel  $\mathcal{N}_1$  and then through channel  $\mathcal{N}_2$ . This configuration is associated with the state  $\rho_c = |1\rangle\langle 1|$  of a control qubit, in which the choice of order is encoded. (b) The quantum particle goes first through  $\mathcal{N}_2$  and then through  $\mathcal{N}_1$ . This alternative configuration is associated with the qubit state  $\rho_c = |0\rangle\langle 0|$ . (c) The quantum switch creates a superposition of the two configurations (a) and (b). It takes a control qubit in a superposition state, such as  $\rho_c = |+\rangle\langle +|$ , and correlates the order of the two channels with the state of the qubit.

operators for  $\mathcal{N}_1$  and  $\{K_j^{(2)}\}$  for  $\mathcal{N}_2$ , the generalized Kraus operator can be expressed as

$$\mathcal{W}_{ij} = K_j^{(2)} \circ K_i^{(1)} \otimes |0\rangle\langle 0| + K_i^{(1)} \circ K_j^{(2)} \otimes |1\rangle\langle 1|, \quad (4.1)$$

where  $K_i^{(1)}$  is the  $i^{\text{th}}$  Kraus operator of channel  $\mathcal{N}_1$  and  $K_j^{(2)}$  is the  $j^{\text{th}}$  Kraus operator of channel  $\mathcal{N}_2$ ; and  $|0\rangle\langle 0|_c, |1\rangle\langle 1|_c$  are the projectors associated with the native basis of  $|c\rangle$ . Thus, we can describe the cumulative evolution of the combined system as follows:

$$\mathcal{S}(\mathcal{N}_1, \mathcal{N}_2)(\rho \otimes \rho_c) = \sum_{i,j} \mathcal{W}_{ij}(\rho \otimes \rho_c) \mathcal{W}_{ij}^\dagger. \quad (4.2)$$

This arrangement, in which the order of application of the two channels is coherently controlled, captures the operation of the quantum switch. It can be thought of as a higher order map that takes two channels  $\mathcal{N}_1, \mathcal{N}_2$  as inputs and gives the superposition of their orders as outputs depending upon the choice of the control qubit  $|c\rangle$ . Expanding upon this quantum operation, it evolves into the following form:

$$\begin{aligned} \mathcal{S}(\rho \otimes \rho_c) &= \mathcal{S}_{00}(\rho) \otimes \langle 0|\rho_c|0\rangle |0\rangle\langle 0|_c + \mathcal{S}_{01}(\rho) \otimes \langle 0|\rho_c|1\rangle |0\rangle\langle 1|_c \\ &+ \mathcal{S}_{10}^\dagger(\rho) \otimes \langle 1|\rho_c|0\rangle |1\rangle\langle 0|_c + \mathcal{S}_{11}(\rho) \otimes \langle 1|\rho_c|1\rangle |1\rangle\langle 1|_c, \end{aligned} \quad (4.3)$$

Superoperators are defined as:

$$\mathcal{S}_{00}(\rho) = \sum_{i,j} K_j^{(2)} K_i^{(2)} \rho K_i^{(1)\dagger} K_j^{(2)\dagger}, \quad (4.4)$$

$$\mathcal{S}_{01}(\rho) = \sum_{i,j} K_j^{(2)} K_i^{(1)} \rho K_j^{(2)\dagger} K_i^{(1)\dagger}, \quad (4.5)$$

$$\mathcal{S}_{11}(\rho) = \sum_{i,j} K_i^{(1)} K_j^{(2)} \rho K_j^{(2)\dagger} K_i^{(1)\dagger}. \quad (4.6)$$

In this schema,  $\mathcal{S}_{00}(\rho)$  characterizes the quantum operation effected by a sequential application of two channels in a fixed causal order (1) to (2), whereas  $\mathcal{S}_{11}(\rho)$  aligns with the order (2) to (1). On the contrary,  $\mathcal{S}_{01}(\rho)$  represents a unique coupling term intrinsic to the quantum switch, representing an indefinite causal order between the two channels. Upon integrating the control qubit in a superposed state  $|\psi_c\rangle = \sqrt{p_c}|0\rangle + \sqrt{1-p_c}|1\rangle$ , with  $p_c$  ranging between 0 and 1, into this framework, the operation transforms into:

$$\begin{aligned} \mathcal{S}(\rho \otimes \rho_c) &= p_c \mathcal{S}_{00}(\rho) \otimes |0\rangle\langle 0|_c + (1-p_c) \mathcal{S}_{11}(\rho) \otimes |1\rangle\langle 1|_c \\ &+ \sqrt{(1-p_c)p_c} \left[ \mathcal{S}_{01}(\rho) \otimes |0\rangle\langle 1|_c + \mathcal{S}_{01}^\dagger(\rho) \otimes |1\rangle\langle 0|_c \right]. \end{aligned} \quad (4.7)$$

This results in entanglement between the input qubit in state  $\rho$  and the control qubit in state  $\rho_c$ , culminating in the joint state  $\mathcal{S}(\rho \otimes \rho_c)$ , which can be used to extract information by measuring either the input or the control qubit. The way the switched channel works, especially during entangling and disentangling operations, is mathematically described using reduced density operators obtained by performing partial trace operation over one of the qubits.

Focusing initially on the input qubit, the measurement process is governed by the reduced density operator  $\rho_{\text{input}} = \text{Tr}_{\text{control}} \mathcal{S}(\rho \otimes \rho_c) = \mathcal{S}_{00}(\rho)$  or  $\mathcal{S}_{11}(\rho)$ . This operation simulates the outcome as if the input qubit went through a sequence of operations with a defined causal order, making the superposition of causal orders irrelevant. This scenario, while simpler, does not exploit the full potential of the quantum switch. The alternative, though, where we measure the control qubit while leaving the input as is, reveals the unique capabilities afforded by the quantum switch. The reduced density operator for the control qubit,  $\rho_{\text{control}} = \text{Tr}_{\text{input}} \mathcal{S}(\rho \otimes \rho_c)$ , manifests as

$$\rho_{\text{control}} = p_c |0_c\rangle\langle 0_c| + (1-p_c) |1_c\rangle\langle 1_c| + \text{Tr}[\mathcal{S}_{01}(\rho)] \sqrt{p_c(1-p_c)} (|1_c\rangle\langle 0_c| + |0_c\rangle\langle 1_c|), \quad (4.8)$$

where  $\text{Tr}[\mathcal{S}_{01}(\rho)]$  captures the dependency on the channel parameters introduced by channels  $\mathcal{N}(\cdot)$ .

To analyze the information processed by the switched channel, one can measure the control qubit in the Fourier basis  $\{|+\rangle, |-\rangle\}$ , using the measurement operators  $\{\mathbb{I}_d \otimes |+\rangle\langle +|, \mathbb{I}_d \otimes |-\rangle\langle -|\}$  within the combined Hilbert space. This measurement projects the control qubit into either state  $|+\rangle$  or  $|-\rangle$ , rendering the input qubit in an unnormalized conditional state defined as:

$$\rho^{(\pm)} = {}_c \langle \pm | \mathcal{S}(\rho \otimes \rho_c) | \pm \rangle_c = \frac{1}{2} \mathcal{S}_{00}(\rho) \pm \sqrt{(1-p_c)p_c} \mathcal{S}_{01}(\rho), \quad (4.9)$$

Where the operation outcomes' probabilities are given by the traces  $P_{\text{control}}^{(\pm)} = \text{Tr}[\rho^{(\pm)}]$ . When initializing the input qubit in a specific state  $\rho$ , the trace outcomes are represented as:

$$\text{Tr}[\rho^{(\pm)}] = \frac{1}{2} \text{Tr} \left[ \frac{1}{2} \mathcal{S}_{00}(\mathbb{I}_d) \pm \sqrt{(1-p_c)p_c} \mathcal{S}_{01}(\mathbb{I}_2) \right]. \quad (4.10)$$

As observed by [Ebler \*et al.\*](#), The dependence of certain states on  $\rho$  allows the receiver to extract valuable information from the target system. By applying the post-selection method on the outcomes  $|+\rangle$  and  $|-\rangle$ , the noisy channel generalization of the quantum superpositions of time evolutions proposed by [Aharonov \*et al.\*](#) can be generated in terms of the Kraus operators given in eq.(4.1).

Performing post-selection ensures that non-zero information can be extracted from the target system of interest after measurement in the Fourier basis  $\{|+\rangle, |-\rangle\}$ . This could be seen from the conditional state evolved as in eq.(4.9), which will lose the off-diagonal terms when considered as an ensemble after measurement. Post-selection is traditionally done by taking many samples of the measurement (without post-selection) and discarding the ones that didn't meet the selection criteria. However, current state-of-the-art hardware is developing more fine-grained controls for doing mid-circuit conditionals [70]. It is important to note that this sampling is a resource-heavy operation depending on the conditional probability of the ensemble and needs to be taken into account when comparing the success probabilities.

## 4.2 Application of Quantum Switch to Grover Search Algorithm

In this section, we develop two theoretical frameworks to explore and demonstrate the potential of quantum switches to mitigate noise accumulating in iterations of the Grover search algorithm. For this, we assume the resultant noise at every iteration to be originating in discrete steps within the iteration such that it can be modeled as a composition of two depolarising channels. The differences between the two frameworks become relevant only at the end of the first Grover iteration, where we first get the following choice: either (1) making a measurement and post-selection now to trace out the switch correlated with the input state so that input to the next iteration is just the input state after first Grover iteration or (2) postponing the measurement and post-selection till the end of the algorithm, such that the input to the next iteration will be the joint state of the input state correlated with the control qubit. This distinction will become clear as we further this discussion, but before delving into the specifics of each framework, we will establish and elaborate on certain assumptions common to both frameworks.

**First Iteration: (k=1):** Let us look at the first iteration of Grover's search algorithm running on an unstructured database. The input system will be an  $n$ -qubit system, represented by a  $d$  dimensional qudit system where  $d = 2^n$ . This is because a one-to-one mapping exists between the  $n$ -qubit system and  $d = 2^n$  level qudit system. We model the noise in the iteration as a composition of two total depolarizing channel errors  $(1 - \sqrt{t})$ .

Thus, if we consider  $t$  to be the channel parameter for the depolarizing channel, we can model noise in the first iteration as a channel,

$$\mathcal{D}_t(\rho) = t\rho + (1-t)\text{Tr}[\rho]\frac{\mathbb{I}_d}{d} = \mathcal{D}_{\sqrt{t}}(\mathcal{D}_{\sqrt{t}}(\rho)). \quad (4.11)$$

This resultant noise could be assumed to be a combination of two identical depolarizing channel noises, each with channel parameter  $\sqrt{t}$ , error probability  $1 - \sqrt{t}$ . These noises can be expressed as the channel,

$$\mathcal{D}_{\sqrt{t}}(\rho) = \sqrt{t}\rho + (1 - \sqrt{t})\text{Tr}[\rho]\frac{\mathbb{I}_d}{d} = \sum_{i=0}^{d^2} K_i \rho K_i^\dagger. \quad (4.12)$$

Here the set of Kraus operators,  $\{K_i\}$ , for the above channel will be,  $K_0 = t^{\frac{1}{4}}\mathbb{I}_d$  and  $K_i = \sqrt{\frac{(1 - \sqrt{t})}{d^2}}U_i$  where  $\{i = 1, 2, \dots, d^2\}$ . Thus, we can express the Kraus operators of the switch  $\mathcal{S}$  as,

$$\begin{aligned} \mathcal{W}_{ij} &= K_i K_j \otimes |0\rangle\langle 0| + K_j K_i \otimes |1\rangle\langle 1| \\ &= \frac{(1 - \sqrt{t})}{d^2} \left( U_i U_j \otimes |0\rangle\langle 0| + U_j U_i \otimes |1\rangle\langle 1| \right), \end{aligned} \quad (4.13)$$

for  $i, j = 0, 1, 2, \dots, d^2$ . Here,  $\{K_i\}$  and  $\{K_j\}$  are Kraus operators for the two identical channels given in (4.12). Suppose that the control system is fixed to the state,  $\rho_c = |c\rangle\langle c|$ , where,  $|c\rangle = \sqrt{\theta}|0\rangle + \sqrt{\bar{\theta}}|1\rangle$ . We prepare the  $n$ -qubit system, which is input to Grover's search, in the state  $\rho(0)$ , which can be considered a  $d$  dimensional qudit system. Now, in an ideal case scenario without noise, it is straightforward that after applying the oracle operator  $O_\tau$  and diffusion operator  $k$  times, the result is  $\rho(k) = \mathcal{G}^k \rho(0) (\mathcal{G}^\dagger)^k$ , where the Grover operator  $\mathcal{G} = \delta O_\tau$ . Thus, after the first Grover iteration, the system's state is supposed to be  $G\rho(0)G^\dagger = \rho(1)$ . But, If we consider the noise as in eq.(4.11), the resultant state can be denoted by,

$$\mathcal{D}_t(\rho(1)) = t\rho(1) + (1-t)\text{Tr}[\rho(1)]\frac{\mathbb{I}_d}{d} = \mathcal{D}_{\sqrt{t}}(\mathcal{D}_{\sqrt{t}}(\rho(1))). \quad (4.14)$$

Now, If we consider a quantum switch applied on these two decomposed channels, the resultant state  $\mathcal{S}(\mathcal{D}_{\sqrt{t}}, \mathcal{D}_{\sqrt{t}})(\rho(1) \otimes \rho_c)$  is given by,

$$\mathcal{S}(\mathcal{D}_{\sqrt{t}}, \mathcal{D}_{\sqrt{t}})(\rho(1) \otimes \rho_c) = \sum_{i,j=0}^{d^2} \mathcal{W}_{ij}(\rho(1) \otimes \rho_c) \mathcal{W}_{ij}^\dagger \quad (4.15)$$

$$\begin{aligned} &= \sum_{i,j=0}^{d^2} \left\{ (K_i K_j \otimes |0\rangle \langle 0| + K_j K_i \otimes |1\rangle \langle 1|) (\rho(1) \otimes \rho_c) (K_i K_j \otimes |0\rangle \langle 0| + K_j K_i \otimes |1\rangle \langle 1|)^\dagger \right\} \\ &= \sum_{i,j=0}^{d^2} \left\{ \left( K_i K_j \rho(1) K_j^\dagger K_i^\dagger \otimes \theta |0\rangle \langle 0| \right) + \left( K_i K_j \rho(1) K_i^\dagger K_j^\dagger \otimes \sqrt{\theta \bar{\theta}} |0\rangle \langle 1| \right) \right. \\ &\quad \left. + \left( K_j K_i \rho(1) K_j^\dagger K_i^\dagger \otimes \sqrt{\theta \bar{\theta}} |1\rangle \langle 0| \right) + \left( K_i K_j \rho(1) K_j^\dagger K_i^\dagger \otimes \bar{\theta} |1\rangle \langle 1| \right) \right\} \end{aligned} \quad (4.16)$$

$$\begin{aligned} \mathcal{S}(\mathcal{D}_{\sqrt{t}}, \mathcal{D}_{\sqrt{t}})(\rho(1) \otimes \rho_c) &= (1 - \sqrt{t})^2 \left( \text{Tr}[\rho(1)] \frac{\mathbb{I}_d}{d} \otimes (\theta |0\rangle \langle 0| + \bar{\theta} |1\rangle \langle 1|) \right. \\ &\quad \left. + \frac{\rho(1)}{d^2} \otimes (\sqrt{\theta \bar{\theta}} |0\rangle \langle 1| + \sqrt{\theta \bar{\theta}} |1\rangle \langle 0|) \right) \\ &\quad + 2\sqrt{t}(1 - \sqrt{t}) \left( \text{Tr}[\rho(1)] \frac{\mathbb{I}_d}{d} \otimes \rho_c \right) + t(\rho(1) \otimes \rho_c). \end{aligned} \quad (4.17)$$

For more detailed calculations, refer to Appendix A.1. The quantum switch facilitates the transfer of information not only within the input system  $\rho$  or the control system  $\rho_c$  but primarily through the correlations established between the output system and the control. These quantum correlations are crucial for the successful transfer of information. If the control qubit experiences decoherence within the computational basis  $\{|0\rangle, |1\rangle\}$ , the information becomes entirely inaccessible. However, for our study, we assume the control system will be noiseless for the duration of our investigation. Finally, we measure the control qubit in the basis  $\{|+\rangle, |-\rangle\}$ , and these measurements yield conditional states.

## 4.2.1 Framework 1, $F_\xi$ : Measurement after every iteration

In the schematic diagram fig.(4.2), we show the action of the Grover operator, along with switched noisy total depolarising channels in the first framework. Notice the measurement and post-selection after each iteration.

### 4.2.1.1 State Evolution with Error

In this framework, we measure the basis  $\{|+\rangle, |-\rangle\}$  at the end of every iteration. The state of the system at the end of the first iteration is given by,

$$\rho_\xi(1)^\pm = \frac{\langle \pm | \mathcal{S}(\mathcal{D}_{\sqrt{t}}, \mathcal{D}_{\sqrt{t}})(\rho(1) \otimes \rho_c) | \pm \rangle}{\text{Tr} \left[ \langle \pm | \mathcal{S}(\mathcal{D}_{\sqrt{t}}, \mathcal{D}_{\sqrt{t}})(\rho(1) \otimes \rho_c) | \pm \rangle \right]}. \quad (4.18)$$

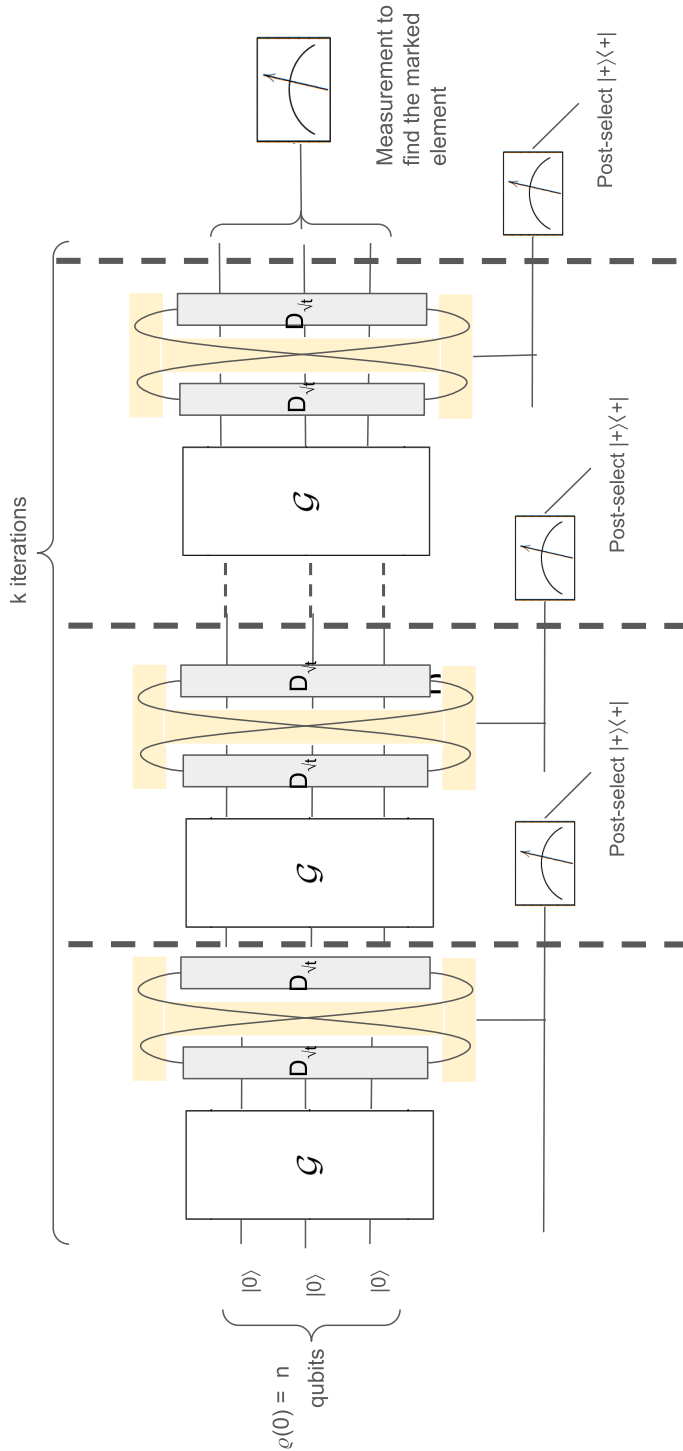


Figure 4.2: Framework 1 ( $F_\xi$ ): The figure depicts the application of switch to Grover’s search algorithm (modeled by the Grover operator  $\mathcal{G}$ ) to mitigate the noise that arises because of the total depolarizing channel. The channel is the ash-colored bar, while the yellow region represents the switch. The dotted line indicates that the post-selection happens at every step, which is specific to this framework.

Here,  $\xi$  in the subscript denotes the stepwise switched channel framework. If we substitute  $t$  as 0, in eq.(4.17), it yields the same results as [25], which uses completely depolarizing channels for demonstrating enhancement in communication. However, in the case of Grover's search algorithm, we will consider  $t$  as the variable parameter for our analysis later. The density matrix after measurement in the basis  $\{|+\rangle, |-\rangle\}$  is given by eq.(4.18),

$$\rho_\xi(1)^{(\pm)} = N/M, \quad (4.19)$$

where,

$$N = \frac{1}{2} \left\{ \left( t \pm 2\sqrt{\theta\bar{\theta}} \left( \left( \frac{1-\sqrt{t}}{d} \right)^2 + t \right) \right) \rho(1) + \left( (1-t) \pm 2\sqrt{\theta\bar{\theta}} 2\sqrt{t}(1-\sqrt{t}) \right) \text{Tr}[\rho(1)] \frac{\mathbb{I}_d}{d} \right\}$$

and

$$M = \frac{1}{2} \left\{ \left( t \pm 2\sqrt{\theta\bar{\theta}} \left( \left( \frac{1-\sqrt{t}}{d} \right)^2 + t \right) \right) + \left( (1-t) \pm 2\sqrt{\theta\bar{\theta}} 2\sqrt{t}(1-\sqrt{t}) \right) \right\}$$

Now we have,

$$\rho_\xi(1)^+ = f_\xi(t)\rho(1) + (1 - f_\xi(t))\frac{I}{d}. \quad (4.20)$$

where,

$$f_\xi(t) = \frac{\left( \frac{1-\sqrt{t}}{d} \right)^2 + 2t}{\left( \frac{1+(t-2\sqrt{t})(1-d^2)}{d^2} + 1 \right)}. \quad (4.21)$$

#### 4.2.1.2 Success Probability

For this switched channel framework, we have the success probability  $P_\xi$  for Grover's search algorithm assisted by this switched channel framework as,

$$P_\xi(1, (1-t), d) = f_\xi(t)P(1, 0, d) + \frac{(1 - f_\xi(t))}{d}.$$

**Generalisation to  $k$  iterations:** Previously, we have shown how the framework behaves when there is only 1 iteration. We extend this to  $k$  iterations. In other words, if we do post-selection measurement at the  $k^{th}$  step, then the final success probability is given by,

$$P_\xi(k, (1-t), d) = (f_\xi(t))^k P(k, 0, d) + \frac{1 - (f_\xi(t))^k}{d}.$$

Here, in this framework, we take a measurement (without disturbing the output state after every iteration) and then do a post-selection, which is a resource-heavy operation. This, in turn, also destroys the correlation between the switch and the state at every step, and we can keep resetting the same quantum state as a switch repeatedly until the end of the algorithm. So, we will be proposing a better framework in the next subsection.

We plot the fig.(4.3) comparing the success probability of the switched model of framework 1 and the success probability of the noisy Grover iteration when there is no switch (we take  $d = 2^4$  as an example. The switch gives some advantages in restoring the probability for the first iteration. However, the noise gradually reduces the advantage as the algorithm undergoes further iterations.

## 4.2.2 Framework 2, $F_\omega$ : Measurement at the end

In the schematic diagram fig.(4.4), we show the action of the Grover operator, along with switched noisy total depolarising channels in the second framework. Notice the measurement and post-selection at the end of the algorithm on the complete joint state combining the input state with  $k$  quantum switches, where  $k$  is the number of Grover iterations the state has traversed through. Our previous framework for analyzing the system after each Grover's search iteration involved performing measurements and post-selections at every step. So, the gain in the probability of success may be attributed to the state's post-selection. However, we have now adopted a different approach for the second framework to circumvent this. In this new framework that we propose in this section, we see the cumulative effect of  $k$  switches after  $k$  iterations by measuring them on the Hadamard basis at the very end. Instead of measuring and post-selecting the control qubit after each iteration, we use multiple quantum switches and hold off on these actions until the end of all iterations. By doing so, the system can undergo a sequence of Grover search iterations without intermediate collapse, which may result in dynamics different from those of the first framework.

### 4.2.2.1 Analysing the output state obtained after the first iteration

Before we go into the details of this framework, we start with analyzing the output obtained after the first iteration, which will be common in both. The result above demonstrates a dependence on the parameter  $\theta$  of the control qubit  $|c\rangle$ , solely through the coherent indefiniteness [38] denoted as  $\sqrt{\theta\bar{\theta}}$  in eq.(4.17). It is apparent that the optimal choice for the maximum switch setting, i.e  $2\sqrt{\theta\bar{\theta}} = 1$ , proves to be advantageous across all values of  $t$  and dimensions  $d$ . Notably, any positive degree of indefiniteness ( $\theta > 0$ ) proves advantageous, signifying that increased indefiniteness yields enhanced benefits. Moreover, it becomes evident that maximum indefiniteness ( $\theta = \frac{1}{2}$ ,  $2\sqrt{\theta\bar{\theta}} = 1$ ) provides the most favorable conditions for this purpose. This

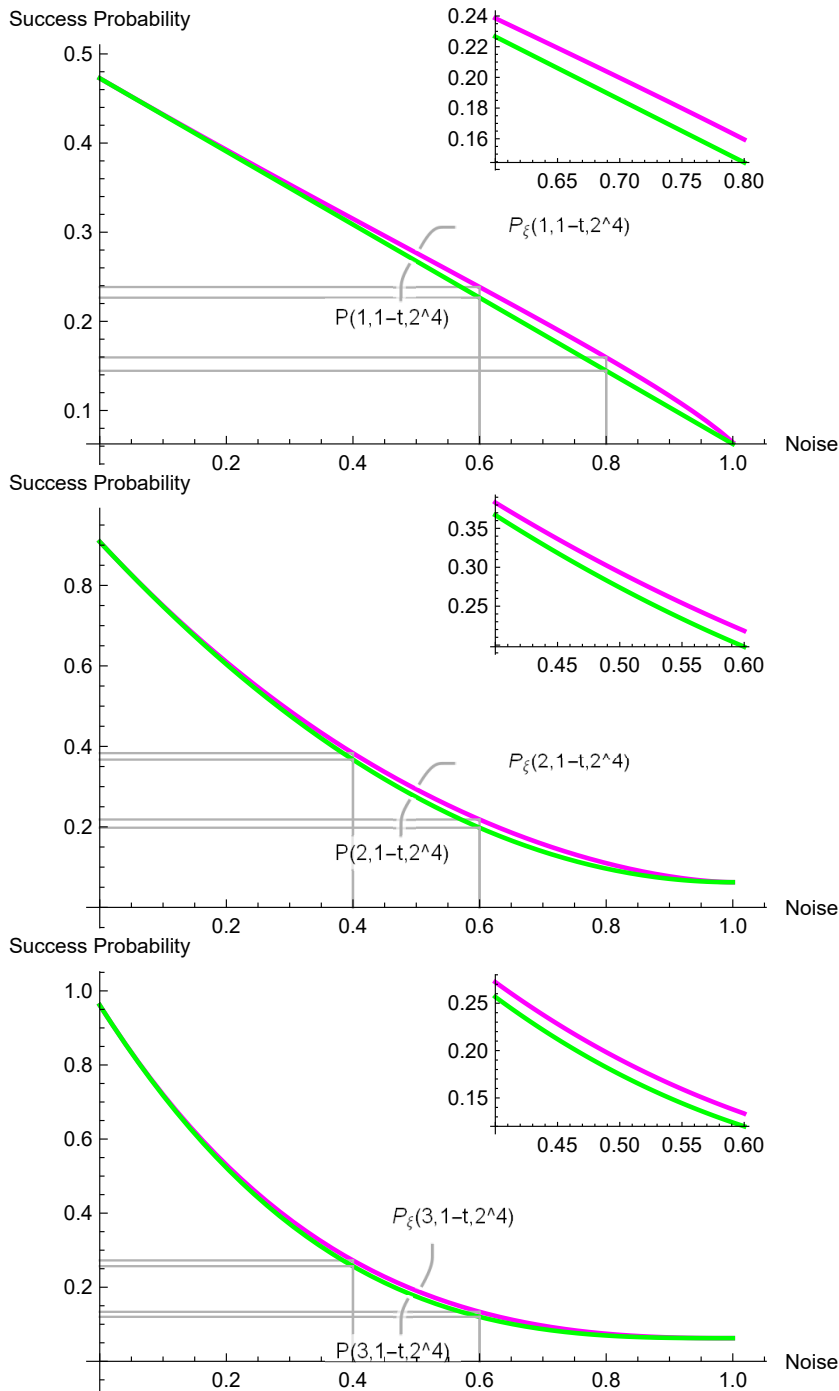


Figure 4.3: These plots show the effect of noise strength  $(1 - t)$  on the success probability of finding the target element in the search space in Noisy Grover's search algorithm. We are taking the search space to be  $d = 2^4$ , and thus the algorithm should stop at  $k_G r = \frac{\pi}{4} \sqrt{16} = \pi \approx 3$  iterations. The Plots from left to right show these variations for different iterations:  $k = 1$  (top-left),  $k = 2$  (top-right), and  $3$  (bottom-left). Here, the green curve represents the Success probability without using any switches, and the magenta curve represents the success probability on applying switches as described in fig.4.2

output  $\mathcal{S}(\mathcal{D}_{\sqrt{t}}, \mathcal{D}_{\sqrt{t}})(\rho(1) \otimes \rho_c)$  in eq.( 4.17 ) can be rearranged as:

$$\begin{aligned}
& \mathcal{S}(\mathcal{D}_{\sqrt{t}}, \mathcal{D}_{\sqrt{t}})(\rho(1) \otimes \rho_c) \\
&= \left\{ t\rho(1) + (1-t)\text{Tr}[\rho(1)]\frac{\mathbb{I}_d}{d} \right\} \otimes (\theta|0\rangle\langle 0| + \bar{\theta}|1\rangle\langle 1|) \\
&+ \left\{ \left( \left( \frac{1-\sqrt{t}}{d} \right)^2 + t \right) \rho(1) + 2\sqrt{t}(1-\sqrt{t})\text{Tr}[\rho(1)]\frac{\mathbb{I}_d}{d} \right\} \\
&\otimes \sqrt{\theta\bar{\theta}}(|0\rangle\langle 1| + |1\rangle\langle 0|). \tag{4.22}
\end{aligned}$$

The term  $(1-t)\text{Tr}[\rho]\frac{\mathbb{I}_d}{d} + t\rho(1)$  in eq.(4.17) represents the output after first iteration corresponding to the parameter  $\theta$  under the scenario where the channel order remains entirely definite ( $\theta = 0$  or  $1$ ). Meanwhile, the second term in eq.(4.17) signifies the additional information gained due to any degree of ICO ( $\theta > 0$  or  $< 1$ ). These observations emphasize that within the context of Grover's search algorithm, the quantum switch functions as a mitigator of noise by facilitating more information transfer.

#### 4.2.2.2 Block Matrix Notation

In the pursuit of a more concise representation of states within the framework of switched quantum channels, we introduce a set of notations that capture the essence of recursive operations on quantum states. This formalism is rooted in the structure of block matrices and the operations defined on them, which are pivotal for understanding the dynamics of quantum states under the influence of noise and control mechanisms.

Consider a block matrix  $A$ , composed of  $2^k \times 2^k$  blocks, with each block  $A_{ij}$  being a  $d \times d$  matrix. This structure enables a fine-grained representation of quantum operations on multipartite states. To facilitate the analysis of such operations, we define the element-wise trace operation,  $\text{Tr}_{d \times d}(A)$ , which transforms  $A$  into a new  $2^k \times 2^k$  matrix  $T$ . Each element  $T_{ij}$  of  $T$  is obtained by taking the trace of the corresponding  $d \times d$  block  $A_{ij}$  in  $A$ . Formally, this operation is expressed as:

$$\text{Tr}_{d \times d}(A) = T \quad \text{where} \quad T_{ij} = \text{Tr}[A_{ij}] \quad \forall i \text{ in } 1, 2, \dots, M \text{ and } j \text{ in } 1, 2, \dots, N. \tag{4.23}$$

To further this discourse, we introduce specific parameters that describe the effects of certain quantum operations on states. The parameters  $r_\rho$  and  $r_{\mathbb{I}}$  are defined as:

$$r_\rho = \left( \frac{1-\sqrt{t}}{d} \right)^2 + t, \quad r_{\mathbb{I}} = 2\sqrt{t}(1-\sqrt{t}), \tag{4.24}$$

where  $\sqrt{t}$  is the noise parameter related to the depolarising channel  $\mathcal{D}_{\sqrt{t}}$ . Similarly, we define  $f_\rho$  and  $f_{\mathbb{I}}$  to maintain symmetry in our notations:

$$f_\rho = t, \quad f_{\mathbb{I}} = (1-t). \tag{4.25}$$

Building upon these definitions, we define and examine the action of a fictitious operation  $\mathcal{F}$  on the joint quantum state  $\rho_\omega$  consisting of the original  $d$ -dimensional input state correlated with the  $k$  switches, which is represented as:

$$\mathcal{F}(\rho_\omega) = \left( (1-t) \text{Tr}_{d \times d}[\rho_\omega] \frac{\mathbb{I}_d}{d} + t\rho_\omega \right), \quad (4.26)$$

demonstrating how the operation mixes the state with its trace over the identity matrix. Likewise, another operation  $\mathcal{R}$  is characterized by:

$$\mathcal{R}(\rho_\omega) = \left\{ \left( \left( \frac{1-\sqrt{t}}{d} \right)^2 + t \right) \rho_\omega + 2\sqrt{t}(1-\sqrt{t}) \text{Tr}_{d \times d}[\rho_\omega] \frac{\mathbb{I}_d}{d} \right\}, \quad (4.27)$$

Which highlights the recursive application of operations with a clear dependency on the parameter  $t$ . These operations are then utilized in the construction of a concise representation of the more complex switch operation  $\mathcal{S}$ , acting on a tensor product of input states and the control qubit.

Thus, we can represent the expression for  $\mathcal{S}(\mathcal{D}_{\sqrt{t}}, \mathcal{D}_{\sqrt{t}})(\rho(1) \otimes \rho_c)$   $\rho(1) \otimes \rho_c$ , given in eq.(4.22), in a block matrix form to illustrate the resulting entangled state. The operation is written as:

$$\mathcal{S}(\mathcal{D}_{\sqrt{t}}, \mathcal{D}_{\sqrt{t}})(\rho(1) \otimes \rho_c) = \begin{bmatrix} \theta \mathcal{F}(\rho(1)) & \sqrt{\theta \bar{\theta}} \mathcal{R}(\rho(1)) \\ \sqrt{\theta \bar{\theta}} \mathcal{R}(\rho(1)) & \bar{\theta} \mathcal{F}(\rho(1)) \end{bmatrix}, \quad (4.28)$$

where  $\theta$  and  $\bar{\theta} = 1 - \theta$  denote the coefficients that modulate the effect of operations  $\mathcal{F}$  and  $\mathcal{R}$  on the state. In further text, we will be using shorthand to write this output as:

$$\rho_{\omega,1}(1) = \mathcal{S}(\mathcal{D}_{\sqrt{t}}, \mathcal{D}_{\sqrt{t}})(\rho(1) \otimes \rho_c) \quad (4.29)$$

Here, the  $\omega$  in subscript highlights this second framework where we make measurements at the end. The integer after that (1 in this case) denotes the number of switches correlated to the input state. The integer in the bracket denotes the number of Grover iterations applied on the search space, the input state.

$$\rho_{\omega,1}(1) = \mathcal{S}(\mathcal{D}_{\sqrt{t}}, \mathcal{D}_{\sqrt{t}})(\rho(1) \otimes \rho_c) = \begin{bmatrix} \theta \mathcal{F}(\rho(1)) & \sqrt{\theta \bar{\theta}} \mathcal{R}(\rho(1)) \\ \sqrt{\theta \bar{\theta}} \mathcal{R}(\rho(1)) & \bar{\theta} \mathcal{F}(\rho(1)) \end{bmatrix}. \quad (4.30)$$

This representation not only captures the interaction between different components of the state but also ensures that the output is a valid density matrix, adhering to the principles of quantum mechanics. By adopting these notations and operations, we delve into the intricate behavior of quantum systems under a variety of influences, laying a foundation for further exploration of their properties and the development of strategies for noise mitigation in quantum algorithms. This notation not only streamlines the representation of quantum states but also elucidates the recursive nature of the operations applied to them.

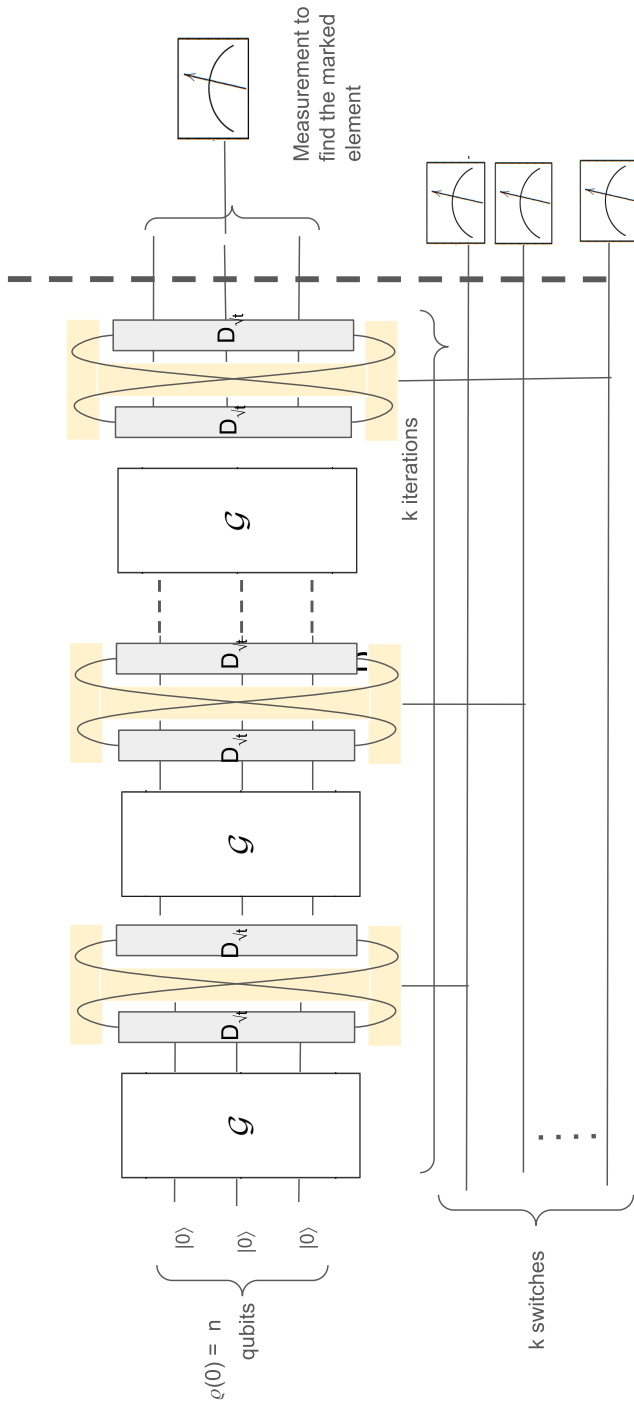


Figure 4.4: The figure depicts the application of the switch to Grover's search algorithm (modeled by the Grover operator  $\mathcal{G}$ ). The channel is the ash-colored bar, while the yellow region represents the switch. The dotted line at the end indicates that the post-selection happens at the very end, which is specific to this particular framework. Here, we take a register of  $k$  switches, thus allowing us to preserve the system and switch correlation until the end.

### 4.2.2.3 State Evolution with Error

Here, we use a register containing  $k$  switches, and it should be noted that this framework is identical to the previous framework for the first iteration because we're measuring the control state after the first iteration in the previous framework. The stark departure from the previous framework can be noticed if we look at further iterations where we will consider the quantum state consisting of the output after the first iteration ( $\rho_1(1)$ ) and the control state ( $\rho_{c_1}$ ) as the input to the next noisy Grover iteration. This contrasts with the previous framework, where we measure the control state and perform post-selection, thus destroying the correlation between the input state and the quantum switch. We are only able to calculate the states obtained by running Grover's Search Algorithm in this framework till  $k = 3$  as the matrix calculations blow up exponentially with the number of iterations.

**Second Iteration ( $k = 2$ ):** We know the action of the switched noisy channels from the first iteration. This output, where the state representing the search space is now correlated with the first switch  $\rho_{c_1}$ , will be the input to the next iteration. Thus, unlike the first framework where in the next iteration,  $\mathcal{G}$  is applied again on the search space  $\rho_{xi}(1)$ , after the switch is traced out, in this framework, the next Grover iteration will act as  $(\mathcal{G} \otimes \mathbb{I}_d)$  on  $\rho_{\omega,1}(1)$  to make sure only the search space goes through the Grover iteration ( $\mathcal{G}$ ). Following the notation defined in 4.30, We denote this output as  $\rho_{\omega,1}(2)$ . After this, the noise acting on this iteration will be a combination of  $(\mathcal{D}_{\sqrt{t}} \otimes \mathbb{I}_d)$ , as discussed earlier 4.14.

Here, We assume the quantum switches are noiseless for the time scale we're considering. Now, we use another switch  $\rho_{c_2}$  to put these noisy channels in superposition as We apply the noise,  $(\mathcal{D}_{\sqrt{t}} \otimes \mathbb{I}_d)$  because the switch is noiseless. We can express the Kraus operators of the switch with two identical noise  $(\mathcal{D}_{\sqrt{t}} \otimes \mathbb{I}_d)$ .

$$\begin{aligned} \mathcal{W}_{ij}^{(2)} &= (K_i \otimes \mathbb{I}_d)(K_j \otimes \mathbb{I}_d) \otimes |0\rangle\langle 0| + (K_i \otimes \mathbb{I}_d)(K_j \otimes \mathbb{I}_d) \otimes |1\rangle\langle 1| \\ &= (K_i K_j \otimes \mathbb{I}_d) \otimes |0\rangle\langle 0| + (K_j K_i \otimes \mathbb{I}_d) \otimes |1\rangle\langle 1| \end{aligned} \quad (4.31)$$

$$\rho_{\omega,2}(2) = \mathcal{S} \left( \mathcal{D}_{\sqrt{t}} \otimes \mathbb{I}_d, \mathcal{D}_{\sqrt{t}} \otimes \mathbb{I}_d \right) (\rho_{\omega,1}(2) \otimes \rho_{c_2}) = \sum_{i,j=0}^{d^2} \mathcal{W}_{ij}^{(2)} (\rho_{\omega,1}(2) \otimes \rho_c) \mathcal{W}_{ij}^\dagger \quad (4.32)$$

We know the action of the switched noisy channels from the  $k = 1$  iteration if we apply the same action recursively; for  $k = 2$ , we get this.

$$\begin{aligned}
\rho_{\omega,2}(2) = & \left\{ \underbrace{f_{\rho} \begin{bmatrix} \theta \mathcal{F}(\rho(2)) & \sqrt{\theta \bar{\theta}} \mathcal{R}(\rho(2)) \\ \sqrt{\theta \bar{\theta}} \mathcal{R}(\rho(2)) & \bar{\theta} \mathcal{F}(\rho(2)) \end{bmatrix}}_{f_{\rho}(\cdot)+} + \underbrace{f_{\mathbb{I}} \frac{\mathbb{I}_d}{d} \otimes \begin{bmatrix} \theta \text{Tr}[\mathcal{F}(\rho(2))] & \sqrt{\theta \bar{\theta}} \text{Tr}[\mathcal{R}(\rho(2))] \\ \sqrt{\theta \bar{\theta}} \text{Tr}[\mathcal{R}(\rho(2))] & \bar{\theta} \text{Tr}[\mathcal{F}(\rho(2))] \end{bmatrix}}_{f_{\mathbb{I}} \frac{\mathbb{I}_d}{d} \otimes \text{Tr}_{d \times d}[\cdot]} \right\} \\
& \otimes (\theta |0\rangle \langle 0| + \bar{\theta} |1\rangle \langle 1|) \\
& + \left\{ \underbrace{r_{\rho} \begin{bmatrix} \theta \mathcal{F}(\rho(2)) & \sqrt{\theta \bar{\theta}} \mathcal{R}(\rho(2)) \\ \sqrt{\theta \bar{\theta}} \mathcal{R}(\rho(2)) & \bar{\theta} \mathcal{F}(\rho(2)) \end{bmatrix}}_{r_{\rho}(\cdot)+} + \underbrace{r_{\mathbb{I}} \frac{\mathbb{I}_d}{d} \otimes \begin{bmatrix} \theta \text{Tr}[\mathcal{F}(\rho(2))] & \sqrt{\theta \bar{\theta}} \text{Tr}[\mathcal{R}(\rho(2))] \\ \sqrt{\theta \bar{\theta}} \text{Tr}[\mathcal{R}(\rho(2))] & \bar{\theta} \text{Tr}[\mathcal{F}(\rho(2))] \end{bmatrix}}_{r_{\mathbb{I}} \frac{\mathbb{I}_d}{d} \otimes \text{Tr}_{d \times d}[\cdot]} \right\} \\
& \otimes \sqrt{\theta \bar{\theta}} (|0\rangle \langle 1| + |1\rangle \langle 0|) \tag{4.33}
\end{aligned}$$

$$\begin{aligned}
\rho_{\omega,2}(2) = & \left\{ f_{\rho} \rho_{\omega,1}(2) + f_{\mathbb{I}} \frac{\mathbb{I}_d}{d} \otimes \text{Tr}_{d \times d}[\rho_{\omega,1}(2)] \right\} + \otimes (\theta |0\rangle \langle 0| + \bar{\theta} |1\rangle \langle 1|) \\
& + \left\{ r_{\rho} \rho_{\omega,1}(2) + r_{\mathbb{I}} \frac{\mathbb{I}_d}{d} \otimes \text{Tr}_{d \times d}[\rho_{\omega,1}(2)] \right\} \otimes \sqrt{\theta \bar{\theta}} (|0\rangle \langle 1| + |1\rangle \langle 0|) \tag{4.34}
\end{aligned}$$

See Appendix A.3, for detailed calculation. We can use eqn.(4.30) and eqn.(4.24) and expand the previous notation of  $\mathcal{F}$  and  $\mathcal{R}$  to write the above result as:

$$\rho_{\omega,2}(2) = \begin{bmatrix} \theta \mathcal{F}_{(2)}(\rho_{\omega,1}(2)) & \sqrt{\theta \bar{\theta}} \mathcal{R}_{(2)}(\rho_{\omega,1}(2)) \\ \sqrt{\theta \bar{\theta}} \mathcal{R}_{(2)}(\rho_{\omega,1}(2)) & \theta \mathcal{F}_{(2)}(\rho_{\omega,1}(2)) \end{bmatrix}, \tag{4.35}$$

where the matrix in eq.(4.35) is a  $4d$ -dimensional block matrix which is again analogous to matrix in eq.(4.26). Now, if we want to stop the algorithm at this stage and analyze the state for success probability, we will need to make the measurement, assuming the quantity  $2\sqrt{\theta \bar{\theta}} = 1$  for maximum indefiniteness as discussed before

$$\begin{aligned}
\rho_{\omega}(2) &= \frac{(\langle + |^{\otimes 2} \rho_{\omega,2}(2) | + \rangle^{\otimes 2})}{\text{Tr}[\langle + |^{\otimes 2} \rho_{\omega,2}(2) | + \rangle^{\otimes 2}]} \\
&= f_{\omega,2}(t) \rho(2) + (1 - f_{\omega,2}(t)) \text{Tr}[\rho] \frac{\mathbb{I}}{d}, \tag{4.36}
\end{aligned}$$

where,

$$\begin{aligned}
f_{\omega,2}(t) = & \frac{(f_{\rho} + r_{\rho})^2 \left( (f_{\rho} + r_{\rho})^2 + (f_{\mathbb{I}} + r_{\mathbb{I}}) \right)}{\left( (1 + r_{\rho} + r_{\mathbb{I}}) + (f_{\rho} + r_{\rho}) \right)^{-1}} \tag{4.37}
\end{aligned}$$

**Extending the output state to  $k^{\text{th}}$  iteration:** The quantum operation applied to the output of  $(k-1)^{\text{th}}$  (input to the  $k^{\text{th}}$  iteration will be  $(\mathbb{I}_d \otimes G D_t) \rho_{\omega,k-1}(k) (D_t^{\dagger} G^{\dagger} \otimes \mathbb{I}_d^{\dagger})$ . If we apply that action recursively, (as the input of the  $k^{\text{th}}$  iteration is the same as the output of the  $(k-1)^{\text{th}}$  iteration)

At the  $k^{\text{th}}$  iteration, the state/system will be a  $2^k * 2^n = 2^{k+n}$  dimensional matrix. In terms of the number of terms, there will be  $2^k * 2^k = 2^{k+k} = 4^k$  terms. To study the accumulated error at the  $k^{\text{th}}$  iteration, we will need to consider taking the state obtained after measurement and post-selection of all the  $k$  control states correlated with the output state after  $k$  iterations. Here we can start unpacking the block matrices  $\mathcal{F}$  and  $\mathcal{R}$ :

$$\mathcal{F}(\rho_{\omega,k-1}(k)) = f_{\rho} \underbrace{(\rho_{\omega,k-1}(k))}_{2^{k-1}d\text{-dimensional}} + f_{\mathbb{I}} \underbrace{\frac{\mathbb{I}_d}{d}}_{d\text{-dimensional}} \otimes \underbrace{\text{Tr}_{d \times d}[\rho_{\omega,k-1}(k)]}_{2^{k-1}\text{-dimensional}}. \quad (4.38)$$

$$\mathcal{R}(\rho_{\omega,k-1}(k)) = r_{\rho} \underbrace{(\rho_{\omega,k-1}(k))}_{2^{k-1}d\text{-dimensional}} + r_{\mathbb{I}} \underbrace{\frac{\mathbb{I}_d}{d}}_{d\text{-dimensional}} \otimes \underbrace{\text{Tr}_{d \times d}[\rho_{\omega,k-1}(k)]}_{2^{k-1}\text{-dimensional}}. \quad (4.39)$$

We get a recursive relation using the above substitutions in (4.38) and (4.39). Again, for concise representation, we introduce a notation called block trace, which applies trace on all the  $2 \times 2$  block matrices in the matrix. It leads to a matrix that is half the size of the input matrix, again keeping in line with the exponential nature of the calculations. We will reduce the matrix's dimension by half with each step.

$$\begin{aligned} (\langle + |^{\otimes k} \rho_{\omega,k}(k) | + \rangle^{\otimes k}) &= (\langle + |^{\otimes k}) \begin{bmatrix} \theta \mathcal{F}(\rho_{\omega,k-1}(k)) & \sqrt{\theta \bar{\theta}} \mathcal{R}(\rho_{\omega,k-1}(k)) \\ \sqrt{\theta \bar{\theta}} \mathcal{R}(\rho_{\omega,k-1}(k)) & \bar{\theta} \mathcal{F}(\rho_{\omega,k-1}(k)) \end{bmatrix} (| + \rangle^{\otimes k}) \\ &= (\langle + |^{\otimes k-1}) (\mathcal{F}(\rho_{\omega,k-1}(k))) (| + \rangle^{\otimes k-1}) + 2\sqrt{\theta \bar{\theta}} (\langle + |^{\otimes k-1}) (\mathcal{R}(\rho_{\omega,k-1}(k))) (| + \rangle^{\otimes k-1}) \end{aligned} \quad (4.40)$$

We can write this as  $M_k(\rho_{\omega,k}(k))$  where  $M_k$  denotes the measurement operation  $(| + \rangle^{\otimes k})$ . This trivial notation will again help us appreciate the recursive nature of the evolution:

$$\begin{aligned} M_k(\rho_{\omega,k}(k)) &= (\langle + |^{\otimes k}) \rho_k(k) (| + \rangle^{\otimes k}), = \frac{1}{2} \left\{ (f_{\rho} + 2\sqrt{\theta \bar{\theta}} r_{\rho}) M_{k-1}(\rho_{\omega,(k-1)}(k)) + (f_{\mathbb{I}} + 2\sqrt{\theta \bar{\theta}} r_{\mathbb{I}}) \right. \\ &\quad \left. (\mathbb{I}_d \otimes \langle + |^{\otimes k-1} \otimes \text{Tr}_{d \times d}(\rho_{\omega,k-1}(k)) \otimes | + \rangle^{\otimes k-1}) \right\}. \end{aligned} \quad (4.41)$$

Using this generalization, we can recursively obtain the third iterations as follows:

$$\begin{aligned} M_3(\rho_{\omega,3}(3)) &= \frac{1}{2} (f_{\rho} + 2\sqrt{\theta \bar{\theta}}) M_2(\rho_2(3)) \\ &+ \frac{1}{2} (f_{\mathbb{I}} + 2\sqrt{\theta \bar{\theta}}) \frac{\mathbb{I}_d}{d} (\langle + |^{\otimes 2} \text{Tr}_{d \times d}(\rho_{\omega,2}(3)) | + \rangle^{\otimes 2}), \\ M_2(\rho_2(3)) &= \frac{1}{2} (f_{\rho} + 2\sqrt{\theta \bar{\theta}}) M_1(\rho_1(3)) \\ &+ \frac{1}{2} (f_{\mathbb{I}} + 2\sqrt{\theta \bar{\theta}}) \frac{\mathbb{I}_d}{d} (\langle + | \text{Tr}_{d \times d}(\rho_2(3)) | + \rangle), \\ M_1(\rho_1(3)) &= \frac{1}{2} (f_{\rho} + 2\sqrt{\theta \bar{\theta}}) M_0(\rho_0(3)) \\ &+ \frac{1}{2} (f_{\mathbb{I}} + 2\sqrt{\theta \bar{\theta}}) \frac{\mathbb{I}_d}{d} \text{Tr}_{d \times d}(\rho_0(3)). \end{aligned} \quad (4.42)$$

Here,  $M_0(\rho_0(2)) = \rho_3$  and  $\text{Tr}_{d \times d}(\rho_3) = \text{Tr}(\rho_3) = 1$ .

#### 4.2.2.4 Success Probability

If we simplify and abstract out the expression for the unnormalized output state after measurement and post-selection obtained by eqn. (4.41) as:

$$(\text{coefficient of } \rho)\rho + \frac{(\text{coefficient of } \frac{\mathbb{I}_d}{d})}{d}\mathbb{I}_d, \quad (4.43)$$

We can calculate the success probability in a similar way to the first framework, where success probability can be written as:

$$\frac{(\text{coefficient of } \rho)}{(\text{coefficient of } \rho) + (\text{coefficient of } \frac{\mathbb{I}_d}{d})}P(k, 0, d) + \frac{(\text{coefficient of } \frac{\mathbb{I}_d}{d})}{(\text{coefficient of } \rho) + (\text{coefficient of } \frac{\mathbb{I}_d}{d})}\frac{1}{d}, \quad (4.44)$$

Thus, we can write the success probability for the first three iterations in terms of the parameter  $t$  as,

$$P_\omega(1, (1-t), d) = P_\xi(1, (1-t), d) = (f_\xi(t))P(1, 0, d) + \frac{1 - f_\xi(t)}{d}, \quad (4.45)$$

$$\begin{aligned} & P_\omega(2, (1-t), d) \\ &= \frac{\left(\left(\frac{1-\sqrt{t}}{d}\right)^2 + 2t\right)^2}{\left(\left(\left(\frac{1-\sqrt{t}}{d}\right)^2 + 2t\right)^2 + (1 + 2(1-\sqrt{t})\sqrt{t} - t)\left(1 + \frac{1}{d^2}(1-\sqrt{t})^2 + 2(1-\sqrt{t})\sqrt{t} + 3t\right)\right)}P(2, 0, d) \\ &+ \frac{(1 + 2(1-\sqrt{t})\sqrt{t} - t)\left(1 + \frac{1}{d^2}(1-\sqrt{t})^2 + 2(1-\sqrt{t})\sqrt{t} + 3t\right)}{\left(\left(\left(\frac{1-\sqrt{t}}{d}\right)^2 + 2t\right)^2 + (1 + 2(1-\sqrt{t})\sqrt{t} - t)\left(1 + \frac{1}{d^2}(1-\sqrt{t})^2 + 2(1-\sqrt{t})\sqrt{t} + 3t\right)\right)}\frac{1}{d}. \end{aligned} \quad (4.46)$$

$$\begin{aligned} & P_\omega(3, (1-t), d) \\ &= \frac{\left(\left(\frac{1-\sqrt{t}}{d}\right)^2 + 2t\right)^3}{\left(\left(\left(\frac{1-\sqrt{t}}{d}\right)^2 + 2t\right)^3 + (1 + 2(1-\sqrt{t})\sqrt{t} - t)\left(1 + \frac{1}{2d^2}(1-\sqrt{t})^2 + 2(1-\sqrt{t})\sqrt{t} + 3t + \left(\frac{1}{d^2}(1-\sqrt{t})^2 + 2t\right)^2\right)\right)}P(3, 0, d) \\ &+ \frac{(1 + 2(1-\sqrt{t})\sqrt{t} - t)\left(1 + \frac{1}{2d^2}(1-\sqrt{t})^2 + 2(1-\sqrt{t})\sqrt{t} + 3t + \left(\frac{1}{d^2}(1-\sqrt{t})^2 + 2t\right)^2\right)}{\left(\left(\left(\frac{1-\sqrt{t}}{d}\right)^2 + 2t\right)^3 + (1 + 2(1-\sqrt{t})\sqrt{t} - t)\left(1 + \frac{1}{2d^2}(1-\sqrt{t})^2 + 2(1-\sqrt{t})\sqrt{t} + 3t + \left(\frac{1}{d^2}(1-\sqrt{t})^2 + 2t\right)^2\right)\right)}\frac{1}{d}. \end{aligned} \quad (4.47)$$

Here, we plot the fig.(4.5) comparing the success probability of the switched channel framework 2 and the success probability of the noisy Grover iteration when there is no switch as the

noise  $(1 - t)$  varies across  $x$ -axis. Just like fig.(4.3), it is again clear that the switch is giving an advantage in terms of restoring the success probability for the first and subsequent  $k = 2$  and  $k = 3$  (we take  $d = 2^4$  as an example). Ideally, the algorithm is supposed to stop after  $k_{Gr} = \frac{\pi}{4}\sqrt{2^4} = \pi \approx 3$  iterations, and we can see how an increase in noise can drastically bring down the success probability from 1. This can be prevented using the switched channel framework 2 proposed in this section, which allows the system to tolerate more noise while keeping the success probability within an acceptable range.

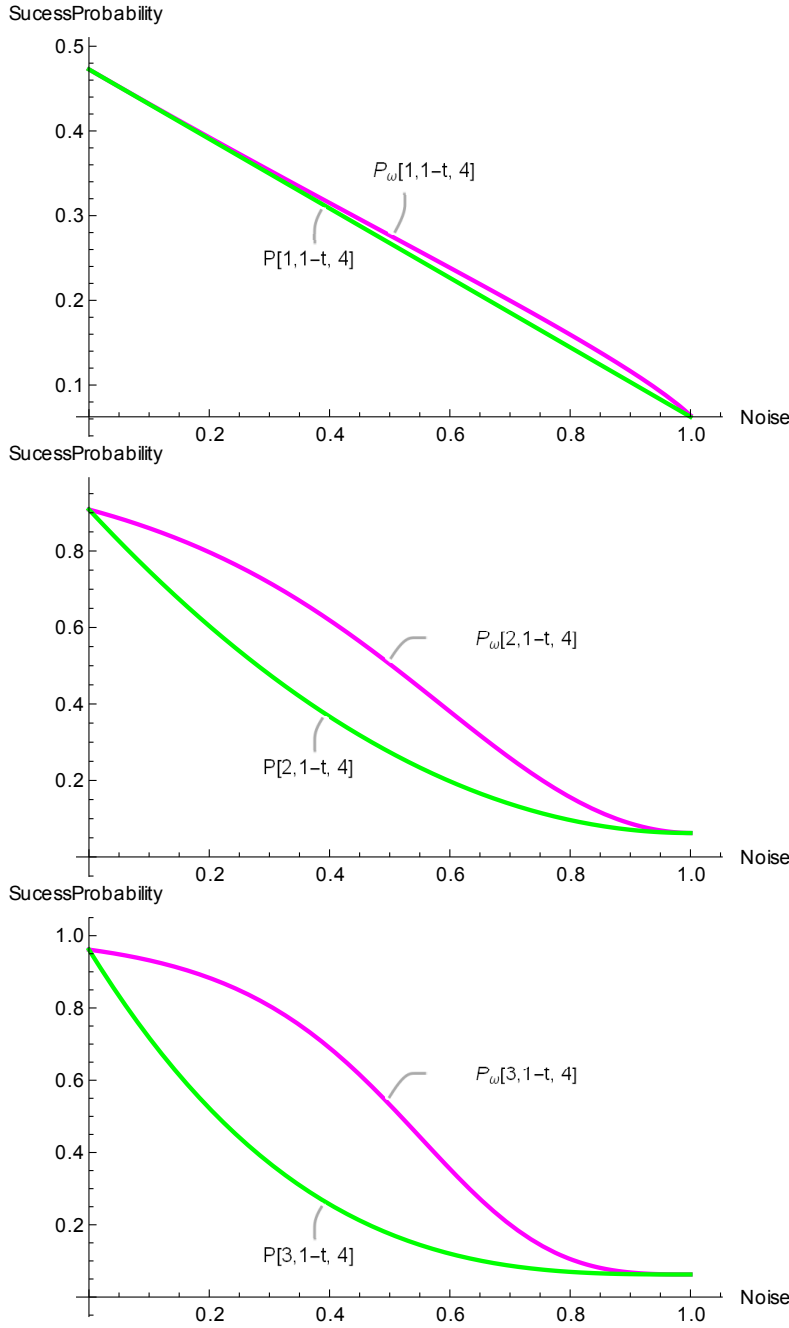


Figure 4.5: These plots show the effect of noise strength  $(1 - t)$  on the success probability of finding the target element in the search space in Noisy Grover's search algorithm. We are taking the search space to be  $d = 2^4$ , and thus the algorithm should stop at  $k_{Gr} = \frac{\pi}{4}\sqrt{16} = \pi \approx 3$  iterations. The Plots from left to right show these variations for different iterations:  $k = 1$  (top-left),  $k = 2$  (top-right), and  $3$  (bottom-left). Here, the green curve represents the Success probability without using any switches, and the magenta curve represents the success probability on applying switches as described in fig.4.4

## Chapter 5

### Summary and Future Prospects

“The whole [scientific] process resembles biological evolution. A problem is like an ecological niche, and a theory is like a gene or a species which is being tested for viability in that niche”

– David Deutsch, [The Fabric of Reality](#)

“..In other words, if you can’t win the game, change the rules.”

– Eric Schmidt, [The New Digital Age](#)

In the current landscape of quantum computing, where researchers are proposing new algorithms more frequently, there is a shift in focus from the anticipation of a fault-tolerant quantum computer towards the reality of noisy intermediate-scale quantum (NISQ) devices. Thus, going back to the fundamental algorithms like Shor’s algorithm, Deutsch’s algorithm, and Grover’s search algorithm introduced in the late part of the previous century and trying to tackle the problem of noise and decoherence in these, as we scale them, is becoming more and more relevant.

Quantum searching was first discovered in the context of searching an unsorted database of size  $N$  in  $\sqrt{N}$  steps. In contrast to other quantum algorithms, which are stand-alone algorithms for specific problems, quantum searching has found application in designing numerous other important algorithms. Grover’s search algorithm is widely applicable in various domains, including statistics. It can quickly extract the minimum element [71] and compute averages like mean [72] and median [73] from unordered data sets, which would otherwise take longer on classical computers. It is also useful for solving NP-complete problems [74], such as exhaustive searches [75] and constraint satisfaction problems [76]. In quantum computing, Grover’s algorithm is used to solve black-box problems like element distinctness [75] and collision problems [77]. It is a valuable tool in cryptography, particularly in breaking encryption through brute-force attacks [78]. The Grover oracle is even used for key search in AES [79]. The concept of Grover coin/Grover walk has also been introduced and used in random walks to demonstrate

Iteration	Noisy	F1	F2
1	$t$	$f_{\xi}(t)$	$f_{\xi}(t)$
2	$t^2$	$f_{\xi}(t)^2$	$\frac{f_{\xi}(t)^2}{\left(\left(\left(\frac{1-\sqrt{t}}{d}\right)^2 + 2t\right)^2 + (1+2(1-\sqrt{t})\sqrt{t}-t)\left(1+\frac{1}{d^2}(1-\sqrt{t})^2+2(1-\sqrt{t})\sqrt{t}+3t\right)\right)}$
3	$t^3$	$f_{\xi}(t)^3$	$\frac{f_{\xi}(t)^3}{\left(\left(\left(\left(\frac{1-\sqrt{t}}{d}\right)^2 + 2t\right)^3 + (1+2(1-\sqrt{t})\sqrt{t}-t)\left(1+\frac{1}{2d^2}(1-\sqrt{t})^2+2(1-\sqrt{t})\sqrt{t}+3t+\left(\frac{1}{d^2}(1-\sqrt{t})^2+2t\right)^2\right)\right)}$

Table 5.1: Coefficient of  $\rho$  of Grover’s search algorithm across up to 3 iterations for. Success probability can be calculated using

its advantages [80].

Despite all these potential usages and applications, we have been unable to implement Grover’s search algorithm at a practical scale as its efficacy is notably compromised when faced with scenarios involving a non-ideal oracle [13, 14] or in the presence of environmental quantum noise [15].

Our research aimed to investigate whether quantum switches can reduce the negative impact of noise in Grover’s search algorithm, specifically when used with depolarizing channel noise. We explored this by separating the total noise in a particular iteration into two or more parts and placing them in superposition. This technique can be particularly useful when error-correction methods are costly and complex, as it provides an alternative method to mitigate the effects of noise. In our work, we presented two switched-channel frameworks for achieving this goal. The first framework involved tracing out the quantum switch by measuring at every step in the  $\{|+\rangle, |-\rangle\}$  basis and post-selecting  $|+\rangle$ . The second framework delayed the measurement and post-selection until the end of the algorithm run. Our study showed that both frameworks produced a positive difference in success probability compared to a noisy Grover’s search algorithm. However, the second framework provided a marked improvement in success probability compared to the noisy scenario. A summary of our results is shown in table 5.1. Therefore, our research suggests that quantum switches can be a useful tool for reducing the effects of noise in Grover’s search algorithm, and the second framework can be particularly effective in achieving this goal.

It was found that creating a superposition of a channel with another copy of itself can result in gaining the Shannon theoretic advantage. This result may seem paradoxical because exchanging two uses of the same channel would not have any observable effect in any ordinary quantum circuit. The reason for this paradox is that noisy quantum channels can be seen as a random mixture of different processes corresponding to different Kraus operators. The

advantage of self-switching arises because some of these processes do not commute with each other. Therefore, a quantum control on the order offers a non-trivial resource. It is important to note that no self-switching effect arises for quantum channels that admit a Kraus decomposition consisting of mutually commuting operators.

However, it's important to note that the practical implementation of these error mitigation techniques using quantum switches is still a significant challenge and an active area of research. Some of the key challenges include:

- **Precise control over quantum operations:** Implementing quantum switches requires precise control over the coherence and timing of quantum operations, which can be difficult to achieve with current quantum hardware.
- **Scalability:** As the size of the search space ( $N$ ) increases, the complexity of implementing indefinite causal order and quantum switches may grow rapidly, potentially limiting the scalability of these techniques.
- **Error models:** The effectiveness of these techniques in mitigating errors may depend on the specific error models and noise processes present in the quantum hardware used to implement Grover's algorithm. In this study, we have analyzed depolarising noise as a worst-case scenario noise. There have been similar studies on other models of noise in Grover's search algorithm that can also be analyzed in the context of switched channel frameworks.

As given in [Vrana \*et al.\*](#), quantum search is only one such problem fitting the framework and definition of a fault-ignorant quantum algorithm. Since we have not used any specific property of Grover's search algorithm, We can make a case for other iterative quantum algorithms with unitary operators, in general, that are susceptible to noise accumulation like Variational Quantum Algorithms (VQAs), quantum phase estimation algorithms [81].

While significant progress has been made in studying indefinite causal order and its applications using quantum switches, several challenges and opportunities for further research remain. The physical realization of quantum switches with low error rates and high controllability is crucial for their successful integration into larger quantum systems like ours. Additionally, exploring the fundamental limits [82] associated with indefinite causal order and quantum switches is an important direction for future investigation. Understanding the constraints and potential advantages of manipulating causal order will contribute to developing optimal strategies for noise mitigation, algorithm design, and the utilization of indefinite causal order in various quantum computing tasks.

## Appendix A

### Detailed Calculations

#### A.1 Calculations for the first iteration ( $k = 1$ ) in noisy Grover's Search with Algorithm with quantum switch

For  $k = 1$ , we have  $\mathcal{S}(\mathcal{D}_{\sqrt{t}}, \mathcal{D}_{\sqrt{t}})(\rho \otimes \rho_c)$ . Now, by expanding the inputs in the expression, we have

1. The depolarising channel noise represented as  $\mathcal{D}_{\sqrt{t}}$

$$\begin{aligned}
 \mathcal{D}_{\sqrt{t}}(\rho) &= \sqrt{t}\rho + (1 - \sqrt{t})\text{Tr}[\rho]\frac{\mathbb{I}_d}{d} \\
 &= \sqrt{t}\rho + (1 - \sqrt{t})\frac{1}{d^2}\sum_{i=1}^{d^2}U_i\rho U_i^\dagger \quad \text{using, } \frac{1}{d^2}\sum_{i=1}^{d^2}U_i\rho U_i^\dagger = \text{Tr}[\rho]\frac{\mathbb{I}_d}{d} \\
 &= \frac{(1 - \sqrt{t})}{d^2}\left(\frac{\sqrt{t}d^2}{1 - \sqrt{t}}\mathbb{I}_d\rho\mathbb{I}_d^\dagger + \sum_{i=1}^{d^2}U_i\rho U_i^\dagger\right) \\
 &= \frac{(1 - \sqrt{t})}{d^2}\left(U_0\rho U_0^\dagger + \sum_{i=1}^{d^2}U_i\rho U_i^\dagger\right) \quad \text{taking, } U_0 = \sqrt{\frac{\sqrt{t}d^2}{1 - \sqrt{t}}}\mathbb{I}_d \\
 &= \frac{(1 - \sqrt{t})}{d^2}\sum_{i=0}^{d^2}U_i\rho U_i^\dagger \tag{A.1}
 \end{aligned}$$

Using,  $K_0 = \sqrt{\frac{(1 - \sqrt{t})}{d^2}}U_0 = \sqrt[4]{t}\mathbb{I}_d$  and  $K_i = \sqrt{\frac{(1 - \sqrt{t})}{d^2}}U_i$  where  $\{i = 1, 2, \dots, d^2\}$ . We have the set of Kraus operators  $\{K_i\}$  for  $\mathcal{D}_{\sqrt{t}}$

$$\mathcal{D}_{\sqrt{t}}(\rho) = \sum_{i=0}^{d^2}K_i\rho K_i^\dagger \tag{A.2}$$

2. The control qubit represented as denoted by  $\rho_c$

$$\begin{aligned}\rho_c &= |c\rangle\langle c| \quad \text{where, } |c\rangle = \sqrt{\theta}|0\rangle + \sqrt{\bar{\theta}}|1\rangle \\ &= \theta|0\rangle\langle 0| + \sqrt{\theta\bar{\theta}}|0\rangle\langle 1| + \sqrt{\theta\bar{\theta}}|1\rangle\langle 0| + \bar{\theta}|1\rangle\langle 1|\end{aligned}\tag{A.3}$$

3. The input search space after the application of the first Grover iteration, consisting of  $n$ -qubits  $\equiv 2^n$  dimensional qudit system denoted by  $\rho(1)$ .

We also note the following for later use

$$\frac{1}{d} \sum_{i=1}^{d^2} \text{Tr}[U_i^\dagger V] U_i = V,\tag{A.4}$$

$$\frac{1}{d^2} \sum_{i=1}^{d^2} U_i V U_i^\dagger = \text{Tr}[V] \frac{\mathbb{I}_d}{d},\tag{A.5}$$

Since the  $d^2$  unitary operators  $U_i$  are orthogonal to each other, they establish an orthonormal basis with respect to the Hilbert-Schmidt inner product. This basis is applicable to any  $d$ -dimensional linear operator  $V$ .

We can express the Kraus operators of the switch  $\mathcal{S}$  4.1:

$$\begin{aligned}\mathcal{W}_{ij} &= K_i K_j \otimes |0\rangle\langle 0| + K_j K_i \otimes |1\rangle\langle 1| \\ &= \frac{(1 - \sqrt{t})}{d^2} \left( U_i U_j \otimes |0\rangle\langle 0| + U_j U_i \otimes |1\rangle\langle 1| \right) \text{ for } i, j = 0, 1, 2 \dots d^2\end{aligned}\tag{A.6}$$

$$\begin{aligned}
\mathcal{S}(\mathcal{D}_{\sqrt{t}}, \mathcal{D}_{\sqrt{t}})(\rho(1) \otimes \rho_c) &= \sum_{i,j=0}^{d^2} \mathcal{W}_{ij}(\rho(1) \otimes \rho_c) \mathcal{W}_{ij}^\dagger \\
&= \sum_{i,j=0}^{d^2} \left\{ (K_i K_j \otimes |0\rangle \langle 0| + K_j K_i \otimes |1\rangle \langle 1|) (\rho(1) \otimes \rho_c) \right. \\
&\quad \left. (K_i K_j \otimes |0\rangle \langle 0| + K_j K_i \otimes |1\rangle \langle 1|)^\dagger \right\} \tag{A.7}
\end{aligned}$$

$$\begin{aligned}
&= \sum_{i,j=0}^{d^2} \left\{ (K_i K_j \rho(1) K_j^\dagger K_i^\dagger \otimes |0\rangle \langle 0| \rho_c |0\rangle \langle 0|) \right. \\
&\quad + (K_i K_j \rho(1) K_j^\dagger K_i^\dagger \otimes |0\rangle \langle 0| \rho_{c_1} |1\rangle \langle 1|) \\
&\quad + (K_i K_j \rho(1) K_j^\dagger K_i^\dagger \otimes |1\rangle \langle 1| \rho_{c_1} |0\rangle \langle 0|) \\
&\quad \left. + (K_i K_j \rho(1) K_j^\dagger K_i^\dagger \otimes |1\rangle \langle 1| \rho_{c_1} |1\rangle \langle 1|) \right\} \tag{A.8}
\end{aligned}$$

$$\begin{aligned}
\mathcal{S}(\mathcal{D}_{\sqrt{t}}, \mathcal{D}_{\sqrt{t}})(\rho(1) \otimes \rho_{c_1}) &= \sum_{i,j=0}^{d^2} \left\{ (K_i K_j \rho(1) K_j^\dagger K_i^\dagger \otimes \theta |0\rangle \langle 0|) \right. \\
&\quad + (K_i K_j \rho(1) K_j^\dagger K_i^\dagger \otimes \sqrt{\theta \bar{\theta}} |0\rangle \langle 1|) \\
&\quad + (K_i K_j \rho(1) K_j^\dagger K_i^\dagger \otimes \sqrt{\theta \bar{\theta}} |1\rangle \langle 0|) \\
&\quad \left. + (K_i K_j \rho(1) K_j^\dagger K_i^\dagger \otimes \bar{\theta} |1\rangle \langle 1|) \right\} \tag{A.9}
\end{aligned}$$

A.2 gives the Kraus operators. We will break this equation into four parts:

1. After fixing both  $i = j = 0$ , we have

$$\begin{aligned}
&\sum_{i=1}^{d^2} \sum_{j=1}^{d^2} \left\{ \left( \sqrt{\frac{1-\sqrt{t}}{d^2}} U_i \sqrt{\frac{1-\sqrt{t}}{d^2}} U_j \rho(1) \sqrt{\frac{1-\sqrt{t}}{d^2}} U_j^\dagger \sqrt{\frac{1-\sqrt{t}}{d^2}} U_i^\dagger \otimes \theta |0\rangle \langle 0| \right) \right. \\
&\quad + \left( \sqrt{\frac{1-\sqrt{t}}{d^2}} U_i \sqrt{\frac{1-\sqrt{t}}{d^2}} U_j \rho(1) \sqrt{\frac{1-\sqrt{t}}{d^2}} U_j^\dagger \sqrt{\frac{1-\sqrt{t}}{d^2}} U_i^\dagger \otimes \sqrt{\theta \bar{\theta}} |0\rangle \langle 1| \right) \\
&\quad + \left( \sqrt{\frac{1-\sqrt{t}}{d^2}} U_i \sqrt{\frac{1-\sqrt{t}}{d^2}} U_j \rho(1) \sqrt{\frac{1-\sqrt{t}}{d^2}} U_j^\dagger \sqrt{\frac{1-\sqrt{t}}{d^2}} U_i^\dagger \otimes \sqrt{\theta \bar{\theta}} |1\rangle \langle 0| \right) \\
&\quad \left. + \left( \sqrt{\frac{1-\sqrt{t}}{d^2}} U_i \sqrt{\frac{1-\sqrt{t}}{d^2}} U_j \rho(1) \sqrt{\frac{1-\sqrt{t}}{d^2}} U_j^\dagger \sqrt{\frac{1-\sqrt{t}}{d^2}} U_i^\dagger \otimes \bar{\theta} |1\rangle \langle 1| \right) \right\} \tag{A.10}
\end{aligned}$$

$$\begin{aligned}
&= \sum_{i=1}^{d^2} \sum_{j=1}^{d^2} \left( \frac{1 - \sqrt{t}}{d^2} \right)^2 \left( U_i U_j \rho(1) U_j^\dagger U_i^\dagger \otimes \theta |0\rangle \langle 0| + U_i U_j \rho(1) U_i^\dagger U_j^\dagger \otimes \sqrt{\theta \bar{\theta}} |0\rangle \langle 1| \right. \\
&\quad \left. + U_j U_i \rho(1) U_j^\dagger U_i^\dagger \otimes \sqrt{\theta \bar{\theta}} |1\rangle \langle 0| + U_j U_i \rho(1) U_i^\dagger U_j^\dagger \otimes \bar{\theta} |1\rangle \langle 1| \right) \quad (\text{A.11})
\end{aligned}$$

$$\begin{aligned}
&= \left( \frac{1 - \sqrt{t}}{d^2} \right)^2 \left( \sum_{i=1}^{d^2} \sum_{j=1}^{d^2} (U_i U_j \rho(1) U_j^\dagger U_i^\dagger \otimes \theta |0\rangle \langle 0|) \right. \\
&\quad + \sum_{i=1}^{d^2} \sum_{j=1}^{d^2} (U_i U_j \rho(1) U_i^\dagger U_j^\dagger \otimes \sqrt{\theta \bar{\theta}} |0\rangle \langle 1|) + \sum_{i=1}^{d^2} \sum_{j=1}^{d^2} (U_j U_i \rho(1) U_j^\dagger U_i^\dagger \otimes \sqrt{\theta \bar{\theta}} |1\rangle \langle 0|) \\
&\quad \left. + \sum_{i=1}^{d^2} \sum_{j=1}^{d^2} (U_j U_i \rho(1) U_i^\dagger U_j^\dagger \otimes \bar{\theta} |1\rangle \langle 1|) \right) \quad (\text{A.12})
\end{aligned}$$

$$\begin{aligned}
&= (1 - \sqrt{t})^2 \left\{ \frac{1}{d^2} \sum_{i=1}^{d^2} U_i \left( \frac{1}{d^2} \sum_{j=1}^{d^2} U_j \rho(1) U_j^\dagger \right) U_i^\dagger \otimes \theta |0\rangle \langle 0| \right. \\
&\quad + \frac{1}{d^2} \sum_{j=1}^{d^2} \left( \frac{1}{d^2} \sum_{i=1}^{d^2} U_i (U_j \rho(1)) U_i^\dagger \right) U_j^\dagger \otimes \sqrt{\theta \bar{\theta}} |0\rangle \langle 1| \\
&\quad + \frac{1}{d^2} \sum_{i=1}^{d^2} \left( \frac{1}{d^2} \sum_{j=1}^{d^2} U_j (U_i \rho(1)) U_j^\dagger \right) U_i^\dagger \otimes \sqrt{\theta \bar{\theta}} |1\rangle \langle 0| \\
&\quad \left. + \frac{1}{d^2} \sum_{j=1}^{d^2} U_j \left( \frac{1}{d^2} \sum_{i=1}^{d^2} U_i \rho(1) U_i^\dagger \right) U_j^\dagger \otimes \bar{\theta} |1\rangle \langle 1| \right\} \quad (\text{A.13})
\end{aligned}$$

$$\begin{aligned}
&= (1 - \sqrt{t})^2 \left\{ \frac{1}{d^2} \sum_{i=1}^{d^2} U_i \left( \text{Tr}(\rho(1)) \frac{\mathbb{I}_d}{d} \right) U_i^\dagger \otimes \theta |0\rangle \langle 0| + \frac{1}{d^2} \sum_{j=1}^{d^2} \left( \text{Tr}(U_j \rho(1)) \frac{\mathbb{I}_d}{d} U_j^\dagger \right) \otimes \sqrt{\theta \bar{\theta}} |0\rangle \langle 1| \right. \\
&\quad \left. + \frac{1}{d^2} \sum_{i=1}^{d^2} \left( \text{Tr}(U_i \rho(1)) \frac{\mathbb{I}_d}{d} U_i^\dagger \right) \otimes \sqrt{\theta \bar{\theta}} |1\rangle \langle 0| + \frac{1}{d^2} \sum_{j=1}^{d^2} U_j \left( \text{Tr}(\rho(1)) \frac{\mathbb{I}_d}{d} \right) U_j^\dagger \otimes \bar{\theta} |1\rangle \langle 1| \right\} \quad (\text{A.14})
\end{aligned}$$

$$\begin{aligned}
&= (1 - \sqrt{t})^2 \left\{ \text{Tr}[\rho] \frac{\mathbb{I}_d}{d} \otimes \theta |0\rangle \langle 0| + \frac{1}{d^2} \rho(1) \otimes \sqrt{\theta \bar{\theta}} |0\rangle \langle 1| \right. \\
&\quad \left. + \frac{1}{d^2} \rho(1) \otimes \sqrt{\theta \bar{\theta}} |1\rangle \langle 0| + \text{Tr}[\rho] \frac{\mathbb{I}_d}{d} \otimes \bar{\theta} |1\rangle \langle 1| \right\} \quad (\text{A.15})
\end{aligned}$$

2. fix  $i = 0, j \neq 0$ .

$$\begin{aligned}
&= \sum_{j=1}^{d^2} \left\{ \sqrt[4]{t} \mathbb{I}_d \sqrt{\frac{1-\sqrt{t}}{d^2}} U_j \rho(1) \sqrt{\frac{1-\sqrt{t}}{d^2}} U_j^\dagger \sqrt[4]{t} \mathbb{I}_d \otimes \theta |0\rangle \langle 0| \right. \\
&\quad + \sqrt[4]{t} \mathbb{I}_d \sqrt{\frac{1-\sqrt{t}}{d^2}} U_j \rho(1) \sqrt[4]{t} \mathbb{I}_d \sqrt{\frac{1-\sqrt{t}}{d^2}} U_j^\dagger \otimes \sqrt{\theta \bar{\theta}} |0\rangle \langle 1| \\
&\quad + \sqrt{\frac{1-\sqrt{t}}{d^2}} U_j \sqrt[4]{t} \mathbb{I}_d \rho(1) \sqrt{\frac{1-\sqrt{t}}{d^2}} U_j^\dagger \sqrt[4]{t} \otimes \sqrt{\theta \bar{\theta}} |1\rangle \langle 0| \\
&\quad \left. + \sqrt{\frac{1-\sqrt{t}}{d^2}} U_j \sqrt[4]{t} \mathbb{I}_d \rho(1) \sqrt[4]{t} \mathbb{I}_d \sqrt{\frac{1-\sqrt{t}}{d^2}} \otimes \bar{\theta} |1\rangle \langle 0| \right\} \tag{A.16}
\end{aligned}$$

$$\begin{aligned}
&= \sum_{j=1}^{d^2} \left( \sqrt{\frac{\sqrt{t}(1-\sqrt{t})}{d^2}} \right)^2 \left( U_j \rho(1) U_j^\dagger \otimes \theta |0\rangle \langle 0| + U_j \rho(1) U_j^\dagger \otimes \bar{\theta} |1\rangle \langle 1| \right. \\
&\quad \left. + U_j \rho(1) U_j^\dagger \otimes \sqrt{\theta \bar{\theta}} |0\rangle \langle 1| + U_j \rho(1) U_j^\dagger \otimes \sqrt{\theta \bar{\theta}} |1\rangle \langle 0| \right) \tag{A.17}
\end{aligned}$$

$$\begin{aligned}
&= \left( \frac{\sqrt{t}(1-\sqrt{t})}{d^2} \right) \sum_{j=1}^{d^2} \left( U_j \rho(1) U_j^\dagger \right. \\
&\quad \left. \otimes \left( \theta |0\rangle \langle 0| + \bar{\theta} |1\rangle \langle 1| + \sqrt{\theta \bar{\theta}} \left( |0\rangle \langle 1| + |1\rangle \langle 0| \right) \right) \right) \tag{A.18}
\end{aligned}$$

$$= \sqrt{t}(1-\sqrt{t}) \frac{1}{d^2} \sum_{j=1}^{d^2} \left( U_j \rho(1) U_j^\dagger \otimes \rho_c \right) = \sqrt{t}(1-\sqrt{t}) \text{Tr}[\rho] \frac{\mathbb{I}_d}{d} \otimes \rho_c \tag{A.19}$$

3. This is symmetric to [A.16](#) and will evaluate to the same value

$$= \sqrt{t}(1-\sqrt{t}) \text{Tr}[\rho] \frac{\mathbb{I}_d}{d} \otimes \rho_c \tag{A.20}$$

4. Finally, fix  $i \neq 0, j \neq 0$

$$\begin{aligned}
&= \sqrt[4]{t} \mathbb{I}_d \sqrt[4]{t} \mathbb{I}_d (\rho \otimes \rho_c) \sqrt[4]{t} \mathbb{I}_d \sqrt[4]{t} \mathbb{I}_d \\
&= t(\rho \otimes \rho_c) \tag{A.21}
\end{aligned}$$

Hence, [A.10](#)+[A.16](#)+[A.21](#)+[A.21](#)

$$\begin{aligned}
&\mathcal{S}(\mathcal{D}_{\sqrt{t}}, \mathcal{D}_{\sqrt{t}})(\rho(1) \otimes \rho_{c_1}) = \\
&(1-\sqrt{t})^2 \left( \text{Tr}[\rho] \frac{\mathbb{I}_d}{d} \otimes \left( \theta |0\rangle \langle 0| + \bar{\theta} |1\rangle \langle 1| \right) + \frac{\rho}{d^2} \otimes \left( \sqrt{\theta \bar{\theta}} \left( |0\rangle \langle 1| + |1\rangle \langle 0| \right) \right) \right) \\
&\quad + 2\sqrt{t}(1-\sqrt{t}) \text{Tr}[\rho] \left( \frac{\mathbb{I}_d}{d} \otimes \rho_c \right) + t(\rho \otimes \rho_c) \tag{A.22}
\end{aligned}$$

Collecting Terms, this output can also be written as:

$$\begin{aligned}
&= \left[ \left[ \left(1 - \sqrt{t}\right)^2 \left( \text{Tr}[\rho] \frac{\mathbb{I}_d}{d} \otimes \left( \theta |0\rangle \langle 0| + \bar{\theta} |1\rangle \langle 1| \right) + \frac{\rho}{d^2} \otimes \sqrt{\theta\bar{\theta}} \left( |0\rangle \langle 1| + |1\rangle \langle 0| \right) \right) \right] \right. \\
&\quad + \left[ 2\sqrt{t}(1 - \sqrt{t}) \text{Tr}[\rho] \frac{\mathbb{I}_d}{d} \otimes \left( \theta |0\rangle \langle 0| + \sqrt{\theta\bar{\theta}} \left( |0\rangle \langle 1| + |1\rangle \langle 0| \right) + \bar{\theta} |1\rangle \langle 1| \right) \right] \\
&\quad \left. + \left[ t\rho \otimes \left( \theta |0\rangle \langle 0| + \sqrt{\theta\bar{\theta}} \left( |0\rangle \langle 1| + |1\rangle \langle 0| \right) + \bar{\theta} |1\rangle \langle 1| \right) \right] \right] \\
&= \left(1 - \sqrt{t}\right)^2 \left( \text{Tr}[\rho] \frac{\mathbb{I}_d}{d} \otimes \left( \theta |0\rangle \langle 0| + \bar{\theta} |1\rangle \langle 1| \right) \right) + 2\sqrt{t}(1 - \sqrt{t}) \left( \text{Tr}[\rho] \frac{\mathbb{I}_d}{d} \otimes \left( \theta |0\rangle \langle 0| + \bar{\theta} |1\rangle \langle 1| \right) \right) \\
&\quad + t \left( \rho \otimes \left( \theta |0\rangle \langle 0| + \bar{\theta} |1\rangle \langle 1| \right) \right) + \frac{(1 - \sqrt{t})^2}{d^2} \left( \rho \otimes \sqrt{\theta\bar{\theta}} \left( |0\rangle \langle 1| + |1\rangle \langle 0| \right) \right) \\
&\quad + t \left( \rho \otimes \sqrt{\theta\bar{\theta}} \left( |0\rangle \langle 1| + |1\rangle \langle 0| \right) \right) + 2\sqrt{t}(1 - \sqrt{t}) \left( \text{Tr}[\rho] \frac{\mathbb{I}_d}{d} \otimes \sqrt{\theta\bar{\theta}} \left( |0\rangle \langle 1| + |1\rangle \langle 0| \right) \right) \\
&= \left( (1 - \sqrt{t})^2 + 2\sqrt{t}(1 - \sqrt{t}) \right) \text{Tr}[\rho] \frac{\mathbb{I}_d}{d} \otimes \left( \theta |0\rangle \langle 0| + \bar{\theta} |1\rangle \langle 1| \right) + (t)\rho \otimes \left( \theta |0\rangle \langle 0| + \bar{\theta} |1\rangle \langle 1| \right) \\
&\quad + \left( \left( \frac{1 - \sqrt{t}}{d} \right)^2 + t \right) \left( \rho \otimes \sqrt{\theta\bar{\theta}} \left( |0\rangle \langle 1| + |1\rangle \langle 0| \right) \right) \\
&\quad + 2\sqrt{t}(1 - \sqrt{t}) \left( \text{Tr}[\rho] \frac{\mathbb{I}_d}{d} \otimes \sqrt{\theta\bar{\theta}} \left( |0\rangle \langle 1| + |1\rangle \langle 0| \right) \right) \\
&= \left( (1 + t - 2t) \text{Tr}[\rho] \frac{\mathbb{I}_d}{d} \otimes \left( \theta |0\rangle \langle 0| + \bar{\theta} |1\rangle \langle 1| \right) + t\rho \otimes \left( \theta |0\rangle \langle 0| + \bar{\theta} |1\rangle \langle 1| \right) \right) \\
&\quad + \left( \left( \frac{1 - \sqrt{t}}{d} \right)^2 + t \right) \left( \rho \otimes \sqrt{\theta\bar{\theta}} \left( |0\rangle \langle 1| + |1\rangle \langle 0| \right) \right) \\
&\quad + 2\sqrt{t}(1 - \sqrt{t}) \left( \text{Tr}[\rho] \frac{\mathbb{I}_d}{d} \otimes \sqrt{\theta\bar{\theta}} \left( |0\rangle \langle 1| + |1\rangle \langle 0| \right) \right)
\end{aligned}$$

$$\begin{aligned}
&\mathcal{S}(\mathcal{D}_{\sqrt{t}}, \mathcal{D}_{\sqrt{t}})(\rho(1) \otimes \rho_{c_1}) \\
&= \left( (1 - t) \text{Tr}[\rho] \frac{\mathbb{I}_d}{d} + t\rho \right) \otimes \left( \theta |0\rangle \langle 0| + \bar{\theta} |1\rangle \langle 1| \right) \\
&\quad + \left\{ \left( \left( \frac{1 - \sqrt{t}}{d} \right)^2 + t \right) \rho + 2\sqrt{t}(1 - \sqrt{t}) \left( \text{Tr}[\rho] \frac{\mathbb{I}_d}{d} \right) \right\} \otimes \sqrt{\theta\bar{\theta}} \left( |0\rangle \langle 1| + |1\rangle \langle 0| \right)
\end{aligned} \tag{A.23}$$

Using notations introduced from eqn.(4.24) to (4.27)

$$\begin{aligned}
& \mathcal{S}(\mathcal{D}_{\sqrt{t}}, \mathcal{D}_{\sqrt{t}})(\rho(1) \otimes \rho_{c_1}) \\
&= \left( f_{\mathbb{I}} \text{Tr}[\rho] \frac{\mathbb{I}_d}{d} + t\rho \right) \otimes \left( \theta |0\rangle \langle 0| + \bar{\theta} |1\rangle \langle 1| \right) \\
&\quad + \left\{ r_{\rho} \rho + r_{\mathbb{I}} \text{Tr}[\rho] \frac{\mathbb{I}_d}{d} \right\} \otimes \sqrt{\theta\bar{\theta}} \left( |0\rangle \langle 1| + |1\rangle \langle 0| \right) \\
&= \begin{bmatrix} \theta \left( f_{\rho} \rho + f_{\mathbb{I}} \text{Tr}[\rho] \frac{\mathbb{I}_d}{d} \right) & \sqrt{\theta\bar{\theta}} \left( r_{\rho} \rho + r_{\mathbb{I}} \text{Tr}[\rho] \frac{\mathbb{I}_d}{d} \right) \\ \sqrt{\theta\bar{\theta}} \left( r_{\rho} \rho + r_{\mathbb{I}} \text{Tr}[\rho] \frac{\mathbb{I}_d}{d} \right) & \bar{\theta} \left( f_{\rho} \rho + f_{\mathbb{I}} \text{Tr}[\rho] \frac{\mathbb{I}_d}{d} \right) \end{bmatrix} \tag{A.24}
\end{aligned}$$

$$= \begin{bmatrix} \theta \mathcal{F}(\rho(1)) & \sqrt{\theta\bar{\theta}} \mathcal{R}(\rho(1)) \\ \sqrt{\theta\bar{\theta}} \mathcal{R}(\rho(1)) & \bar{\theta} \mathcal{F}(\rho(1)) \end{bmatrix} \tag{A.25}$$

Thus we have 3 ways [A.22](#), [A.23](#), [A.25](#) to write the output for  $\mathcal{S}(\mathcal{D}_{\sqrt{t}}, \mathcal{D}_{\sqrt{t}})(\rho(1) \otimes \rho_{c_1})$

## A.2 Measurement of the system

$$\rho_{\xi}(1) = \frac{\langle \pm | \mathcal{S}(\mathcal{D}_{\sqrt{t}}, \mathcal{D}_{\sqrt{t}})(\rho(1) \otimes \rho_c) | \pm \rangle}{\text{Tr} \left[ \langle \pm | \mathcal{S}(\mathcal{D}_{\sqrt{t}}, \mathcal{D}_{\sqrt{t}})(\rho(1) \otimes \rho_c) | \pm \rangle \right]} \tag{A.26}$$

Calculating the numerator, N:

$$\begin{aligned}
& \langle \pm | \left[ \left\{ t\rho(1) + (1-t)\text{Tr}[\rho(1)] \frac{\mathbb{I}_d}{d} \right\} \otimes \left( \theta |0\rangle \langle 0| + \bar{\theta} |1\rangle \langle 1| \right) \right. \\
& \quad \left. + \left\{ \left( \left( \frac{1-\sqrt{t}}{d} \right)^2 + t \right) \rho(1) + 2\sqrt{t}(1-\sqrt{t})\text{Tr}[\rho(1)] \frac{\mathbb{I}_d}{d} \right\} \otimes \sqrt{\theta\bar{\theta}} \left( |0\rangle \langle 1| + |1\rangle \langle 0| \right) \right] | \pm \rangle \tag{A.27}
\end{aligned}$$

$$\begin{aligned}
&= \frac{1}{2} \left( t\rho(1) + (1-t)\text{Tr}[\rho(1)] \frac{\mathbb{I}_d}{d} \right) + \frac{1}{2} \left( \pm 2\sqrt{\theta\bar{\theta}} \left\{ \left( \left( \frac{1-\sqrt{t}}{d} \right)^2 + t \right) \rho(1) + 2\sqrt{t}(1-\sqrt{t})\text{Tr}[\rho(1)] \frac{\mathbb{I}_d}{d} \right\} \right) \\
&= \frac{1}{2} \left\{ t\rho(1) + (1-t)\text{Tr}[\rho(1)] \frac{\mathbb{I}_d}{d} \pm 2\sqrt{\theta\bar{\theta}} \left( \left( \left( \frac{1-\sqrt{t}}{d} \right)^2 + t \right) \rho(1) \pm 2\sqrt{\theta\bar{\theta}} \left( 2\sqrt{t}(1-\sqrt{t})\text{Tr}[\rho(1)] \frac{\mathbb{I}_d}{d} \right) \right) \right\} \\
&= \frac{1}{2} \left\{ \left( t \pm 2\sqrt{\theta\bar{\theta}} \left( \left( \frac{1-\sqrt{t}}{d} \right)^2 + t \right) \right) \rho(1) + \left( (1-t) \pm 2\sqrt{\theta\bar{\theta}} 2\sqrt{t}(1-\sqrt{t}) \right) \text{Tr}[\rho(1)] \frac{\mathbb{I}_d}{d} \right\} \tag{A.28}
\end{aligned}$$

Calculating the denominator, M:

$$\text{Tr} \left[ \frac{1}{2} \left( \left( \pm 2\sqrt{\theta\bar{\theta}} \left( \frac{(1-\sqrt{t})^2}{d^2} + t \right) + t \right) \rho(1) + \left( (1-t) \pm 2\sqrt{\theta\bar{\theta}}(2\sqrt{t}(1-\sqrt{t})) \right) \frac{\mathbb{I}_d}{d} \right) \right] \quad (\text{A.29})$$

$$\begin{aligned} &= \frac{1}{2} \left\{ \text{Tr} \left[ \left( \pm 2\sqrt{\theta\bar{\theta}} \left( \frac{(1-\sqrt{t})^2}{d^2} + t \right) + t \right) \rho(1) \right] + \text{Tr} \left[ \left( (1-t) \pm 2\sqrt{\theta\bar{\theta}}(2\sqrt{t}(1-\sqrt{t})) \right) \frac{\mathbb{I}_d}{d} \right] \right\} \\ &= \frac{1}{2} \left\{ \left( \pm 2\sqrt{\theta\bar{\theta}} \left( \frac{(1-\sqrt{t})^2}{d^2} + t \right) + t \right) + \left( (1-t) \pm 2\sqrt{\theta\bar{\theta}}(2\sqrt{t}(1-\sqrt{t})) \right) \right\} \end{aligned} \quad (\text{A.30})$$

Because  $\text{Tr}[\rho(1)] = \text{Tr}[\frac{\mathbb{I}_d}{d}] = 1$ . Thus, the density matrix after measurement in Fourier basis is:

$$\frac{\frac{1}{2} \left\{ \left( t \pm 2\sqrt{\theta\bar{\theta}} \left( \left( \frac{1-\sqrt{t}}{d} \right)^2 + t \right) \right) \rho(1) + \left( (1-t) \pm 2\sqrt{\theta\bar{\theta}}(2\sqrt{t}(1-\sqrt{t})) \right) \text{Tr}[\rho(1)] \frac{\mathbb{I}_d}{d} \right\}}{\frac{1}{2} \left\{ \left( \pm 2\sqrt{\theta\bar{\theta}} \left( \frac{(1-\sqrt{t})^2}{d^2} + t \right) + t \right) + \left( (1-t) \pm 2\sqrt{\theta\bar{\theta}}(2\sqrt{t}(1-\sqrt{t})) \right) \right\}} \quad (\text{A.31})$$

For  $\theta = 0$  or  $(1-\theta) = \bar{\theta} = 0$

$$= \frac{1}{2} \left( t^2 \rho(1) + (1-t^2) \frac{\mathbb{I}_d}{d} \right)$$

For maximum superposition in the switch,  $\theta = (1-\theta) = \bar{\theta} = \frac{1}{2}$ . Taking the  $|+\rangle$  component of the measurement. **Post Selection** and Correcting based on the + or - part of the measurement

$$\frac{\left( 2t + \left( \frac{1-\sqrt{t}}{d} \right)^2 \right) \rho(1) + \left( (1-t) + 2\sqrt{t}(1-\sqrt{t}) \right) \text{Tr}[\rho(1)] \frac{\mathbb{I}_d}{d}}{\left( \frac{(1-\sqrt{t})^2}{d^2} + 2t \right) + \left( (1-t) + (2\sqrt{t}(1-\sqrt{t})) \right)} \quad (\text{A.32})$$

$$\begin{aligned} &= \frac{\left( 2t + \left( \frac{1-\sqrt{t}}{d} \right)^2 \right) \rho(1) + \left( (1-t) + 2\sqrt{t}(1-\sqrt{t}) \right) \text{Tr}[\rho(1)] \frac{\mathbb{I}_d}{d}}{\frac{(1-\sqrt{t})^2}{d^2} + (1-t + 2\sqrt{t})} \\ &= \frac{\left( 2t + \left( \frac{1-\sqrt{t}}{d} \right)^2 \right) \rho(1) + \left( (1-t) + 2\sqrt{t}(1-\sqrt{t}) \right) \text{Tr}[\rho(1)] \frac{\mathbb{I}_d}{d}}{\frac{1-2\sqrt{t}+t+(1-t+2\sqrt{t})d^2}{d^2}} \\ &= \frac{\left( 2t + \left( \frac{1-\sqrt{t}}{d} \right)^2 \right)}{\frac{1+(-2\sqrt{t}+t)+(t-2\sqrt{t})(-d^2)+d^2}{d^2}} \rho(1) + \frac{\left( (1-t) + 2\sqrt{t}(1-\sqrt{t}) \right) \text{Tr}[\rho(1)] \frac{\mathbb{I}_d}{d}}{\frac{1+(-2\sqrt{t}+t)+(t-2\sqrt{t})(-d^2)+d^2}{d^2} d} \end{aligned} \quad (\text{A.33})$$

$$f_\xi(t) \rho(1) + (1-f_\xi(t)) \text{Tr}[\rho(1)] \frac{\mathbb{I}_d}{d} \quad (\text{A.34})$$

$$f_\xi(t) = \frac{\left( \frac{1-\sqrt{t}}{d} \right)^2 + 2t}{\left( \frac{1+(t-2\sqrt{t})(1-d^2)}{d^2} + 1 \right)} \quad (\text{A.35})$$

### A.3 Calculations for next iterations ( $k > 1$ ) in Grover's Search Algorithm with the second framework

After the first iteration, the switched depolarizing channel's output in block form,

$$\rho_{\omega,1}(1) = \mathcal{S}(\mathcal{D}_{\sqrt{t}}, \mathcal{D}_{\sqrt{t}})(\rho(1) \otimes \rho_c) = \begin{bmatrix} \theta \mathcal{F}(\rho(1)) & \sqrt{\theta \bar{\theta}} \mathcal{R}(\rho(1)) \\ \sqrt{\theta \bar{\theta}} \mathcal{R}(\rho(1)) & \bar{\theta} \mathcal{F}(\rho(1)) \end{bmatrix}. \quad (\text{A.36})$$

Now, this is input for the next iteration,  $k = 2$

$$\begin{aligned} (\mathcal{G} \otimes \mathbb{I}_d) \rho_{\omega,1}(1) (\mathcal{G} \otimes \mathbb{I}_d)^\dagger &= \left( \mathcal{G} \otimes \begin{bmatrix} 1 & 0 \\ 0 & 1 \end{bmatrix} \right) \rho_{\omega,1}(1) \left( \mathcal{G}^\dagger \otimes \begin{bmatrix} 1 & 0 \\ 0 & 1 \end{bmatrix} \right) \\ &= \begin{bmatrix} \mathcal{G} & 0 \\ 0 & \mathcal{G} \end{bmatrix} \rho(1) \begin{bmatrix} \mathcal{G}^\dagger & 0 \\ 0 & \mathcal{G}^\dagger \end{bmatrix} \\ &= \begin{bmatrix} \mathcal{G} & 0 \\ 0 & \mathcal{G} \end{bmatrix} \begin{bmatrix} \theta \mathcal{F}(\rho(1)) & \sqrt{\theta \bar{\theta}} \mathcal{R}(\rho(1)) \\ \sqrt{\theta \bar{\theta}} \mathcal{R}(\rho(1)) & \bar{\theta} \mathcal{F}(\rho(1)) \end{bmatrix} \begin{bmatrix} \mathcal{G}^\dagger & 0 \\ 0 & \mathcal{G}^\dagger \end{bmatrix} \\ &= \begin{bmatrix} \theta \mathcal{G} \mathcal{F}(\rho(1)) \mathcal{G}^\dagger & \sqrt{\theta \bar{\theta}} \mathcal{G} \mathcal{R}(\rho(1)) \mathcal{G}^\dagger \\ \sqrt{\theta \bar{\theta}} \mathcal{G} \mathcal{R}(\rho(1)) \mathcal{G}^\dagger & \bar{\theta} \mathcal{G} \mathcal{F}(\rho(1)) \mathcal{G}^\dagger \end{bmatrix} \end{aligned}$$

$$\begin{aligned} \mathcal{G} \mathcal{F}(\rho(1)) \mathcal{G}^\dagger &= \mathcal{G} \mathcal{F}(f_\rho \rho(1) + f_{\mathbb{I}} \text{Tr}[\rho(1)] \frac{\mathbb{I}_d}{d}) \mathcal{G}^\dagger \\ &= f_\rho \mathcal{G} \rho(1) \mathcal{G}^\dagger + f_{\mathbb{I}} \mathcal{G} \text{Tr}[\rho(1)] \frac{\mathbb{I}_d}{d} \mathcal{G}^\dagger = f_\rho \rho(2) + f_{\mathbb{I}} \frac{\mathbb{I}_d}{d} = \underline{\mathcal{F}(\rho(2))} \quad (\text{A.37}) \end{aligned}$$

$$\begin{aligned} \mathcal{G} \mathcal{R}(\rho(1)) \mathcal{G}^\dagger &= \mathcal{G} \mathcal{R}(r_\rho \rho(1) + r_{\mathbb{I}} \text{Tr}[\rho(1)] \frac{\mathbb{I}_d}{d}) \mathcal{G}^\dagger \\ &= r_\rho \mathcal{G} \rho(1) \mathcal{G}^\dagger + r_{\mathbb{I}} \mathcal{G} \text{Tr}[\rho(1)] \frac{\mathbb{I}_d}{d} \mathcal{G}^\dagger = r_\rho \rho(2) + r_{\mathbb{I}} \frac{\mathbb{I}_d}{d} = \underline{\mathcal{R}(\rho(2))} \quad (\text{A.38}) \end{aligned}$$

$$\mathcal{G} \mathcal{F}(\rho(1)) \mathcal{G}^\dagger = \begin{bmatrix} \theta \mathcal{F}(\rho(2)) & \sqrt{\theta \bar{\theta}} \mathcal{R}(\rho(2)) \\ \sqrt{\theta \bar{\theta}} \mathcal{R}(\rho(2)) & \bar{\theta} \mathcal{F}(\rho(2)) \end{bmatrix} = \rho_{\omega,1}(2) \quad (\text{A.39})$$

Now we apply the noise as  $(D_{\sqrt{t}} \otimes \mathbb{I}_d)$  because the switch is noiseless. We can express the Kraus operators of the switch with two identical channels,  $(D_{\sqrt{t}} \otimes \mathbb{I}_d)$ , and the second control qubit  $\rho_{e_2}$  as:

$$\begin{aligned} \mathcal{W}_{ij}^{(2)} &= (K_i \otimes \mathbb{I}_d) (K_j \otimes \mathbb{I}_d) \otimes |0\rangle \langle 0| + (K_i \otimes \mathbb{I}_d) (K_j \otimes \mathbb{I}_d) \otimes |1\rangle \langle 1| \\ &= (K_i K_j \otimes \mathbb{I}_d) \otimes |0\rangle \langle 0| + (K_j K_i \otimes \mathbb{I}_d) \otimes |1\rangle \langle 1| \quad (\text{A.40}) \end{aligned}$$

$$\begin{aligned}
\because (A \otimes B)(C \otimes D) &= (a_{ij}B)_{ij} (C_{ij}D)_{ij} \\
&= \left( \sum_K (a_{iK}B) (c_{Kj}D) \right)_{ij} = \left( \sum_K (a_{iK}c_{Kj}) (BD) \right)_{ij} \\
&= AB \otimes CD = AC \otimes BD
\end{aligned}$$

$$\rho_{\omega,2}(2) = \mathcal{S}(D_{\sqrt{t}}, D_{\sqrt{t}})(\rho_{\omega,1}(2) \otimes \rho_{c_2}) = \sum_{i,j=0}^{d^2} \mathcal{W}_{ij}^{(2)}(\rho_{\omega,1}(2) \otimes \rho_{c_2}) \mathcal{W}_{ij}^{(2)\dagger} \quad (\text{A.41})$$

$$\begin{aligned}
&= \sum_{i,j=0}^{d^2} \left\{ (K_i K_j \otimes \mathbb{I}_d) \otimes |0\rangle \langle 0| + (K_j K_i \otimes \mathbb{I}_d) \otimes |1\rangle \langle 1| \right\} (\rho_{\omega,1}(2) \otimes \rho_{c_2}) \\
&\quad \left\{ (K_i K_j \otimes \mathbb{I}_d)^\dagger \otimes |0\rangle \langle 0| + (K_j K_i \otimes \mathbb{I}_d)^\dagger \otimes |1\rangle \langle 1| \right\} \\
&= \sum_{i,j=0}^{d^2} \left\{ (K_i K_j \otimes \mathbb{I}_d) \rho_{\omega,1}(2) (K_i K_j \otimes \mathbb{I}_d)^\dagger \otimes |0\rangle \langle 0| \rho_{c_2} |0\rangle \langle 0| \right. \\
&\quad + (K_i K_j \otimes \mathbb{I}_d) \rho_{\omega,1}(2) (K_j K_i \otimes \mathbb{I}_d)^\dagger \otimes |0\rangle \langle 0| \rho_{c_2} |1\rangle \langle 1| \\
&\quad + (K_j K_i \otimes \mathbb{I}_d) \rho_{\omega,1}(2) (K_i K_j \otimes \mathbb{I}_d)^\dagger \otimes |1\rangle \langle 1| \rho_{c_2} |0\rangle \langle 0| \\
&\quad \left. + (K_j K_i \otimes \mathbb{I}_d) \rho_{\omega,1}(2) (K_j K_i \otimes \mathbb{I}_d)^\dagger \otimes |1\rangle \langle 1| \rho_{c_2} |1\rangle \langle 1| \right\}
\end{aligned}$$

$$\begin{aligned}
&= \sum_{i,j=0}^{d^2} \left\{ \begin{aligned}
&\begin{bmatrix} K_i K_j & 0 \\ 0 & K_i K_j \end{bmatrix} \begin{bmatrix} \theta \mathcal{F}(\rho(2)) & \sqrt{\theta \bar{\theta}} \mathcal{F}(\rho(\epsilon)) \\ \sqrt{\theta \bar{\theta}} \mathcal{R}(\rho(2)) & \bar{\theta} \mathcal{F}(\rho(2)) \end{bmatrix} \begin{bmatrix} K_j^\dagger K_i^\dagger & 0 \\ 0 & K_j^\dagger K_i^\dagger \end{bmatrix} \otimes \theta |0\rangle \langle 0| \\
&+ \begin{bmatrix} K_i K_j & 0 \\ 0 & K_i K_j \end{bmatrix} \begin{bmatrix} \theta \mathcal{F}(\rho(2)) & \sqrt{\theta \bar{\theta}} \mathcal{R}(\rho(2)) \\ \sqrt{\theta \bar{\theta}} \mathcal{R}(\rho(2)) & \bar{\theta} \mathcal{F}(\rho(2)) \end{bmatrix} \begin{bmatrix} K_i^\dagger K_j^\dagger & 0 \\ 0 & K_i^\dagger K_j^\dagger \end{bmatrix} \otimes \sqrt{\theta \bar{\theta}} |0\rangle \langle 1| \\
&+ \begin{bmatrix} K_j K_i & 0 \\ 0 & K_j K_i \end{bmatrix} \begin{bmatrix} \theta \mathcal{F}(\rho(2)) & \sqrt{\theta \bar{\theta}} \mathcal{F}(\rho(\epsilon)) \\ \sqrt{\theta \bar{\theta}} \mathcal{R}(\rho(2)) & \bar{\theta} \mathcal{F}(\rho(2)) \end{bmatrix} \begin{bmatrix} K_j^\dagger K_i^\dagger & 0 \\ 0 & K_j^\dagger K_i^\dagger \end{bmatrix} \otimes \sqrt{\theta \bar{\theta}} |1\rangle \langle 0| \\
&+ \begin{bmatrix} K_j K_i & 0 \\ 0 & K_j K_i \end{bmatrix} \begin{bmatrix} \theta \mathcal{F}(\rho(2)) & \sqrt{\theta \bar{\theta}} \mathcal{F}(\rho(\epsilon)) \\ \sqrt{\theta \bar{\theta}} \mathcal{R}(\rho(2)) & \bar{\theta} \mathcal{F}(\rho(2)) \end{bmatrix} \begin{bmatrix} K_i^\dagger K_j^\dagger & 0 \\ 0 & K_i^\dagger K_j^\dagger \end{bmatrix} \otimes \bar{\theta} |1\rangle \langle 1| \end{aligned} \right\} \\
&= \sum_{i,j=0}^{d^2} \left\{ \begin{aligned}
&\begin{bmatrix} \theta K_i K_j \mathcal{F}(\rho(2)) K_j^\dagger K_i^\dagger & \sqrt{\theta \bar{\theta}} K_i K_j \mathcal{R}(\rho(2)) K_j^\dagger K_i^\dagger \\ \sqrt{\theta \bar{\theta}} K_i K_j \mathcal{R}(\rho(2)) K_j^\dagger K_i^\dagger & \bar{\theta} K_i K_j \mathcal{F}(\rho(2)) K_j^\dagger K_i^\dagger \end{bmatrix} \otimes \theta |0\rangle \langle 0| \\
&+ \begin{bmatrix} \theta K_i K_j \mathcal{F}(\rho(2)) K_i^\dagger K_j^\dagger & \sqrt{\theta \bar{\theta}} K_i K_j \mathcal{R}(\rho(2)) K_i^\dagger K_j^\dagger \\ \sqrt{\theta \bar{\theta}} K_i K_j \mathcal{R}(\rho(2)) K_i^\dagger K_j^\dagger & \bar{\theta} K_i K_j \mathcal{F}(\rho(2)) K_i^\dagger K_j^\dagger \end{bmatrix} \otimes \sqrt{\theta \bar{\theta}} |0\rangle \langle 1| \\
&+ \begin{bmatrix} \theta K_j K_i \mathcal{F}(\rho(2)) K_j^\dagger K_i^\dagger & \sqrt{\theta \bar{\theta}} K_j K_i \mathcal{R}(\rho(2)) K_j^\dagger K_i^\dagger \\ \sqrt{\theta \bar{\theta}} K_j K_i \mathcal{R}(\rho(2)) K_j^\dagger K_i^\dagger & \bar{\theta} K_j K_i \mathcal{F}(\rho(2)) K_j^\dagger K_i^\dagger \end{bmatrix} \otimes \sqrt{\theta \bar{\theta}} |1\rangle \langle 0| \\
&+ \begin{bmatrix} \theta K_j K_i \mathcal{F}(\rho(2)) K_i^\dagger K_j^\dagger & \sqrt{\theta \bar{\theta}} K_j K_i \mathcal{R}(\rho(2)) K_i^\dagger K_j^\dagger \\ \sqrt{\theta \bar{\theta}} K_j K_i \mathcal{R}(\rho(2)) K_i^\dagger K_j^\dagger & \bar{\theta} K_j K_i \mathcal{F}(\rho(2)) K_i^\dagger K_j^\dagger \end{bmatrix} \otimes \bar{\theta} |1\rangle \langle 1| \end{aligned} \right\} \quad (\text{A.42})
\end{aligned}$$

Eqn.A.42 can be written in block matrix form as:

$$\rho_{\omega,2}(2) = \begin{bmatrix} A_{00} & A_{01} \\ A_{10} & A_{11} \end{bmatrix} \quad (\text{A.43})$$

And for calculating each of the matrix elements in this block matrix, we can divide this summation into four parts as before: I.  $j = 0, i = 0$ , II.  $i \neq 0, j = 0$ , III.  $i = 0, j \neq 0$  and IV.  $i \neq 0, j \neq 0$ .

$$\begin{aligned}
A_{00} = & \left\{ \begin{aligned} & \left[ \begin{array}{cc} \theta \sum_{i,j=1}^{d^2} K_i K_j \mathcal{F}(\rho(2)) K_j^\dagger K_i^\dagger & \sqrt{\theta\bar{\theta}} \sum_{i,j=1}^{d^2} K_i K_j \mathcal{R}(\rho(2)) K_j^\dagger K_i^\dagger \\ \sqrt{\theta\bar{\theta}} \sum_{i,j=1}^{d^2} K_i K_j \mathcal{R}(\rho(2)) K_j^\dagger K_i^\dagger & \bar{\theta} \sum_{i,j=1}^{d^2} K_i K_j \mathcal{F}(\rho(2)) K_j^\dagger K_i^\dagger \end{array} \right] \\ & + \left[ \begin{array}{cc} \theta \sum_{j=1}^{d^2} K_0 K_j \mathcal{F}(\rho(2)) K_j^\dagger K_0^\dagger & \sqrt{\theta\bar{\theta}} \sum_{j=1}^{d^2} K_0 K_j \mathcal{R}(\rho(2)) K_j^\dagger K_0^\dagger \\ \sqrt{\theta\bar{\theta}} \sum_{j=1}^{d^2} K_0 K_j \mathcal{R}(\rho(2)) K_j^\dagger K_0^\dagger & \bar{\theta} \sum_{j=1}^{d^2} K_0 K_j \mathcal{F}(\rho(2)) K_j^\dagger K_0^\dagger \end{array} \right] \\ & + \left[ \begin{array}{cc} \theta \sum_{i=1}^{d^2} K_i K_0 \mathcal{F}(\rho(2)) K_0^\dagger K_i^\dagger & \sqrt{\theta\bar{\theta}} \sum_{i=1}^{d^2} K_i K_0 \mathcal{R}(\rho(2)) K_0^\dagger K_i^\dagger \\ \sqrt{\theta\bar{\theta}} \sum_{i=1}^{d^2} K_i K_0 \mathcal{R}(\rho(2)) K_0^\dagger K_i^\dagger & \bar{\theta} \sum_{i=1}^{d^2} K_i K_0 \mathcal{F}(\rho(2)) K_0^\dagger K_i^\dagger \end{array} \right] \\ & + \left[ \begin{array}{cc} \theta K_0 K_0 \mathcal{F}(\rho(2)) K_0^\dagger K_0^\dagger & \sqrt{\theta\bar{\theta}} K_0 K_0 \mathcal{R}(\rho(2)) K_0^\dagger K_0^\dagger \\ \sqrt{\theta\bar{\theta}} K_0 K_0 \mathcal{R}(\rho(2)) K_0^\dagger K_0^\dagger & \bar{\theta} K_0 K_0 \mathcal{F}(\rho(2)) K_0^\dagger K_0^\dagger \end{array} \right] \end{aligned} \right\} \otimes \theta |0\rangle \langle 0|
\end{aligned}$$

$$\begin{aligned}
A_{00} = & \left\{ (1 - \sqrt{t})^2 \left[ \begin{array}{cc} \theta \text{Tr}[\mathcal{F}(\rho(2))] \frac{\mathbb{I}_d}{d} & \sqrt{\theta\bar{\theta}} \text{Tr}[\mathcal{R}(\rho(2))] \frac{\mathbb{I}_d}{d} \\ \sqrt{\theta\bar{\theta}} \text{Tr}[\mathcal{R}(\rho(2))] \frac{\mathbb{I}_d}{d} & \bar{\theta} \text{Tr}[\mathcal{F}(\rho(2))] \frac{\mathbb{I}_d}{d} \end{array} \right] + t \left[ \begin{array}{cc} \theta \mathcal{F}(\rho(2)) \frac{\mathbb{I}_d}{d} & \sqrt{\theta\bar{\theta}} \mathcal{R}(\rho(2)) \frac{\mathbb{I}_d}{d} \\ \sqrt{\theta\bar{\theta}} \mathcal{R}(\rho(2)) \frac{\mathbb{I}_d}{d} & \bar{\theta} \mathcal{F}(\rho(2)) \frac{\mathbb{I}_d}{d} \end{array} \right] \right. \\ & \left. + 2\sqrt{t}(1 - \sqrt{t}) \left[ \begin{array}{cc} \theta \text{Tr}[\mathcal{F}(\rho(2))] \frac{\mathbb{I}_d}{d} & \sqrt{\theta\bar{\theta}} \text{Tr}[\mathcal{R}(\rho(2))] \frac{\mathbb{I}_d}{d} \\ \sqrt{\theta\bar{\theta}} \text{Tr}[\mathcal{R}(\rho(2))] \frac{\mathbb{I}_d}{d} & \bar{\theta} \text{Tr}[\mathcal{F}(\rho(2))] \frac{\mathbb{I}_d}{d} \end{array} \right] \right\} \otimes \theta |0\rangle \langle 0| \quad (\text{A.44})
\end{aligned}$$

$$\begin{aligned}
A_{01} = & \left\{ \begin{aligned} & \left[ \begin{array}{cc} \theta \sum_{i,j=1}^{d^2} K_i K_j \mathcal{F}(\rho(2)) K_i^\dagger K_j^\dagger & \sqrt{\theta\bar{\theta}} \sum_{i,j=1}^{d^2} K_i K_j \mathcal{R}(\rho(2)) K_i^\dagger K_j^\dagger \\ \sqrt{\theta\bar{\theta}} \sum_{i,j=1}^{d^2} K_i K_j \mathcal{R}(\rho(2)) K_i^\dagger K_j^\dagger & \bar{\theta} \sum_{i,j=1}^{d^2} K_i K_j \mathcal{F}(\rho(2)) K_i^\dagger K_j^\dagger \end{array} \right] \\ & + \left[ \begin{array}{cc} \theta \sum_{j=1}^{d^2} K_0 K_j \mathcal{F}(\rho(2)) K_0^\dagger K_j^\dagger & \sqrt{\theta\bar{\theta}} \sum_{j=1}^{d^2} K_0 K_j \mathcal{R}(\rho(2)) K_0^\dagger K_j^\dagger \\ \sqrt{\theta\bar{\theta}} \sum_{j=1}^{d^2} K_0 K_j \mathcal{R}(\rho(2)) K_0^\dagger K_j^\dagger & \bar{\theta} \sum_{j=1}^{d^2} K_0 K_j \mathcal{F}(\rho(2)) K_0^\dagger K_j^\dagger \end{array} \right] \\ & + \left[ \begin{array}{cc} \theta \sum_{i=1}^{d^2} K_i K_0 \mathcal{F}(\rho(2)) K_i^\dagger K_0^\dagger & \sqrt{\theta\bar{\theta}} \sum_{i=1}^{d^2} K_i K_0 \mathcal{R}(\rho(2)) K_i^\dagger K_0^\dagger \\ \sqrt{\theta\bar{\theta}} \sum_{i=1}^{d^2} K_i K_0 \mathcal{R}(\rho(2)) K_i^\dagger K_0^\dagger & \bar{\theta} \sum_{i=1}^{d^2} K_i K_0 \mathcal{F}(\rho(2)) K_i^\dagger K_0^\dagger \end{array} \right] \\ & + \left[ \begin{array}{cc} \theta K_0 K_0 \mathcal{F}(\rho(2)) K_0^\dagger K_0^\dagger & \sqrt{\theta\bar{\theta}} K_0 K_0 \mathcal{R}(\rho(2)) K_0^\dagger K_0^\dagger \\ \sqrt{\theta\bar{\theta}} K_0 K_0 \mathcal{R}(\rho(2)) K_0^\dagger K_0^\dagger & \bar{\theta} K_0 K_0 \mathcal{F}(\rho(2)) K_0^\dagger K_0^\dagger \end{array} \right] \end{aligned} \right\} \otimes \sqrt{\theta\bar{\theta}} |0\rangle \langle 1|
\end{aligned}$$

$$\begin{aligned}
A_{01} = & \left\{ (1 - \sqrt{t})^2 \left[ \begin{array}{cc} \theta \frac{\mathcal{F}(\rho(2))}{d^2} & \sqrt{\theta\bar{\theta}} \frac{\mathcal{R}(\rho(2))}{d} \\ \sqrt{\theta\bar{\theta}} \frac{\mathcal{R}(\rho(2))}{d^2} \mathbb{I}_d & \bar{\theta} \frac{\mathcal{F}(\rho(2))}{d^2} \end{array} \right] + t \left[ \begin{array}{cc} \theta \mathcal{F}(\rho(2)) & \sqrt{\theta\bar{\theta}} \mathcal{R}(\rho(2)) \\ \sqrt{\theta\bar{\theta}} \mathcal{R}(\rho(2)) & \bar{\theta} \mathcal{F}(\rho(2)) \end{array} \right] \right. \\
& \left. + 2\sqrt{t}(1 - \sqrt{t}) \left[ \begin{array}{cc} \theta \text{Tr}[\mathcal{F}(\rho(2))] \frac{\mathbb{I}_d}{d} & \sqrt{\theta\bar{\theta}} \text{Tr}[\mathcal{R}(\rho(2))] \frac{\mathbb{I}_d}{d} \\ \sqrt{\theta\bar{\theta}} \text{Tr}[\mathcal{R}(\rho(2))] \frac{\mathbb{I}_d}{d} & \bar{\theta} \text{Tr}[\mathcal{F}(\rho(2))] \frac{\mathbb{I}_d}{d} \end{array} \right] \right\} \otimes \sqrt{\theta\bar{\theta}} |0\rangle \langle 1| \quad (\text{A.45})
\end{aligned}$$

Other matrix elements  $A_{10}$  and  $A_{11}$  will also be similarly expanded as  $A_{01}$  in A.45 and  $A_{00}$  in A.44, respectively, (eqn. except for the coefficients of the switch. Hence, A.42 can be expanded as:

$$\begin{aligned}
(1 - \sqrt{t})^2 & \left\{ \left[ \begin{array}{cc} \theta \text{Tr}[\mathcal{F}(\rho(2))] \frac{\mathbb{I}_d}{d} & \sqrt{\theta\bar{\theta}} \text{Tr}[\mathcal{R}(\rho(2))] \frac{\mathbb{I}_d}{d} \\ \sqrt{\theta\bar{\theta}} \text{Tr}[\mathcal{R}(\rho(2))] \frac{\mathbb{I}_d}{d} & \bar{\theta} \text{Tr}[\mathcal{F}(\rho(2))] \frac{\mathbb{I}_d}{d} \end{array} \right] \otimes \theta |0\rangle \langle 0| \right. \\
& \left[ \begin{array}{cc} \theta \frac{\mathcal{F}(\rho(2))}{d^2} & \sqrt{\theta\bar{\theta}} \frac{\mathcal{R}(\rho(2))}{d} \\ \sqrt{\theta\bar{\theta}} \frac{\mathcal{R}(\rho(2))}{d^2} & \bar{\theta} \frac{\mathcal{F}(\rho(2))}{d^2} \end{array} \right] \otimes \sqrt{\theta\bar{\theta}} |0\rangle \langle 1| \\
& \left[ \begin{array}{cc} \theta \frac{\mathcal{F}(\rho(2))}{d^2} & \sqrt{\theta\bar{\theta}} \frac{\mathcal{R}(\rho(2))}{d} \\ \sqrt{\theta\bar{\theta}} \frac{\mathcal{R}(\rho(2))}{d^2} & \bar{\theta} \frac{\mathcal{F}(\rho(2))}{d^2} \end{array} \right] \otimes \sqrt{\theta\bar{\theta}} |1\rangle \langle 0| \\
& \left. \left[ \begin{array}{cc} \theta \text{Tr}[\mathcal{F}(\rho(2))] \frac{\mathbb{I}_d}{d} & \sqrt{\theta\bar{\theta}} \text{Tr}[\mathcal{R}(\rho(2))] \frac{\mathbb{I}_d}{d} \\ \sqrt{\theta\bar{\theta}} \text{Tr}[\mathcal{R}(\rho(2))] \frac{\mathbb{I}_d}{d} & \bar{\theta} \text{Tr}[\mathcal{F}(\rho(2))] \frac{\mathbb{I}_d}{d} \end{array} \right] \otimes \bar{\theta} |1\rangle \langle 1| \right\} \\
+ 2\sqrt{t}(1 - \sqrt{t}) & \left[ \begin{array}{cc} \theta \text{Tr}[\mathcal{F}(\rho(2))] \frac{\mathbb{I}_d}{d} & \sqrt{\theta\bar{\theta}} \text{Tr}[\mathcal{R}(\rho(2))] \frac{\mathbb{I}_d}{d} \\ \sqrt{\theta\bar{\theta}} \text{Tr}[\mathcal{R}(\rho(2))] \frac{\mathbb{I}_d}{d} & \bar{\theta} \text{Tr}[\mathcal{F}(\rho(2))] \frac{\mathbb{I}_d}{d} \end{array} \right] \otimes (\theta |0\rangle \langle 0| + \sqrt{\theta\bar{\theta}} (|0\rangle \langle 1| + |1\rangle \langle 0|) + \bar{\theta} |1\rangle \langle 1|) \\
+ t & \left[ \begin{array}{cc} \theta \mathcal{F}(\rho(2)) & \sqrt{\theta\bar{\theta}} \mathcal{R}(\rho(2)) \\ \sqrt{\theta\bar{\theta}} \mathcal{R}(\rho(2)) & \bar{\theta} \mathcal{F}(\rho(2)) \end{array} \right] \otimes (\theta |0\rangle \langle 0| + \sqrt{\theta\bar{\theta}} (|0\rangle \langle 1| + |1\rangle \langle 0|) + \bar{\theta} |1\rangle \langle 1|) \quad (\text{A.46})
\end{aligned}$$

$$\begin{aligned}
= & (1 - \sqrt{t})^2 \left\{ \left[ \begin{array}{cc} \theta \text{Tr}[\mathcal{F}(\rho(2))] \frac{\mathbb{I}_d}{d} & \sqrt{\theta\bar{\theta}} \text{Tr}[\mathcal{R}(\rho(2))] \frac{\mathbb{I}_d}{d} \\ \sqrt{\theta\bar{\theta}} \text{Tr}[\mathcal{R}(\rho(2))] \frac{\mathbb{I}_d}{d} & \bar{\theta} \text{Tr}[\mathcal{F}(\rho(2))] \frac{\mathbb{I}_d}{d} \end{array} \right] \otimes (\theta |0\rangle \langle 0| + \bar{\theta} |1\rangle \langle 1|) \right. \\
& \left. + \left[ \begin{array}{cc} \theta \frac{\mathcal{F}(\rho(2))}{d^2} & \sqrt{\theta\bar{\theta}} \frac{\mathcal{R}(\rho(2))}{d} \\ \sqrt{\theta\bar{\theta}} \frac{\mathcal{R}(\rho(2))}{d^2} & \bar{\theta} \frac{\mathcal{F}(\rho(2))}{d^2} \end{array} \right] \otimes \sqrt{\theta\bar{\theta}} (|0\rangle \langle 1| + |1\rangle \langle 0|) \right\} \\
& + \left\{ 2\sqrt{t}(1 - \sqrt{t}) \left[ \begin{array}{cc} \theta \text{Tr}[\mathcal{F}(\rho(2))] \frac{\mathbb{I}_d}{d} & \sqrt{\theta\bar{\theta}} \text{Tr}[\mathcal{R}(\rho(2))] \frac{\mathbb{I}_d}{d} \\ \sqrt{\theta\bar{\theta}} \text{Tr}[\mathcal{R}(\rho(2))] \frac{\mathbb{I}_d}{d} & \bar{\theta} \text{Tr}[\mathcal{F}(\rho(2))] \frac{\mathbb{I}_d}{d} \end{array} \right] + t \left[ \begin{array}{cc} \theta \mathcal{F}(\rho(2)) & \sqrt{\theta\bar{\theta}} \mathcal{R}(\rho(2)) \\ \sqrt{\theta\bar{\theta}} \mathcal{R}(\rho(2)) & \bar{\theta} \mathcal{F}(\rho(2)) \end{array} \right] \right\} \otimes \rho_{c_2}
\end{aligned}$$

Similar to  $k = 1$ , collecting terms in the above result, we have

$$\begin{aligned}
& \left\{ t \begin{bmatrix} \theta \mathcal{F}(\rho(2)) & \sqrt{\theta \bar{\theta}} \mathcal{R}(\rho(2)) \\ \sqrt{\theta \bar{\theta}} \mathcal{R}(\rho(2)) & \bar{\theta} \mathcal{F}(\rho(2)) \end{bmatrix} + (1-t) \begin{bmatrix} \theta \text{Tr}[\mathcal{F}(\rho(2))] \frac{\mathbb{I}_d}{d} & \sqrt{\theta \bar{\theta}} \text{Tr}[\mathcal{R}(\rho(2))] \frac{\mathbb{I}_d}{d} \\ \sqrt{\theta \bar{\theta}} \text{Tr}[\mathcal{R}(\rho(2))] \frac{\mathbb{I}_d}{d} & \bar{\theta} \text{Tr}[\mathcal{F}(\rho(2))] \frac{\mathbb{I}_d}{d} \end{bmatrix} \right\} \\
& \otimes (\theta |0\rangle \langle 0| + \bar{\theta} |1\rangle \langle 1|) \\
& + \left\{ \left( \left( \frac{1-t}{d} \right)^2 + t \right) \begin{bmatrix} \theta \mathcal{F}(\rho(2)) & \sqrt{\theta \bar{\theta}} \mathcal{R}(\rho(2)) \\ \sqrt{\theta \bar{\theta}} \mathcal{R}(\rho(2)) & \bar{\theta} \mathcal{F}(\rho(2)) \end{bmatrix} \right. \\
& \left. + 2\sqrt{t}(1-\sqrt{t}) \begin{bmatrix} \theta \text{Tr}[\mathcal{F}(\rho(2))] \frac{\mathbb{I}_d}{d} & \sqrt{\theta \bar{\theta}} \text{Tr}[\mathcal{R}(\rho(2))] \frac{\mathbb{I}_d}{d} \\ \sqrt{\theta \bar{\theta}} \text{Tr}[\mathcal{R}(\rho(2))] \frac{\mathbb{I}_d}{d} & \bar{\theta} \text{Tr}[\mathcal{F}(\rho(2))] \frac{\mathbb{I}_d}{d} \end{bmatrix} \right\} \otimes \sqrt{\theta \bar{\theta}} (|0\rangle \langle 1| + |1\rangle \langle 0|)
\end{aligned}$$

Now, following a similar substitution/notation eqn.(4.24) as  $k = 1$ ,

$$\begin{aligned}
= & \left\{ f_\rho \begin{bmatrix} \theta \mathcal{F}(\rho(2)) & \sqrt{\theta \bar{\theta}} \mathcal{R}(\rho(2)) \\ \sqrt{\theta \bar{\theta}} \mathcal{R}(\rho(2)) & \bar{\theta} \mathcal{F}(\rho(2)) \end{bmatrix} + f_{\mathbb{I}} \begin{bmatrix} \theta \text{Tr}[\mathcal{F}(\rho(2))] \frac{\mathbb{I}_d}{d} & \sqrt{\theta \bar{\theta}} \text{Tr}[\mathcal{R}(\rho(2))] \frac{\mathbb{I}_d}{d} \\ \sqrt{\theta \bar{\theta}} \text{Tr}[\mathcal{R}(\rho(2))] \frac{\mathbb{I}_d}{d} & \bar{\theta} \text{Tr}[\mathcal{F}(\rho(2))] \frac{\mathbb{I}_d}{d} \end{bmatrix} \right\} \\
& \otimes (\theta |0\rangle \langle 0| + \bar{\theta} |1\rangle \langle 1|) \\
& + \left\{ r_\rho \begin{bmatrix} \theta \mathcal{F}(\rho(2)) & \sqrt{\theta \bar{\theta}} \mathcal{R}(\rho(2)) \\ \sqrt{\theta \bar{\theta}} \mathcal{R}(\rho(2)) & \bar{\theta} \mathcal{F}(\rho(2)) \end{bmatrix} + r_{\mathbb{I}} \begin{bmatrix} \theta \text{Tr}[\mathcal{F}(\rho(2))] \frac{\mathbb{I}_d}{d} & \sqrt{\theta \bar{\theta}} \text{Tr}[\mathcal{R}(\rho(2))] \frac{\mathbb{I}_d}{d} \\ \sqrt{\theta \bar{\theta}} \text{Tr}[\mathcal{R}(\rho(2))] \frac{\mathbb{I}_d}{d} & \bar{\theta} \text{Tr}[\mathcal{F}(\rho(2))] \frac{\mathbb{I}_d}{d} \end{bmatrix} \right\} \\
& \otimes \sqrt{\theta \bar{\theta}} (|0\rangle \langle 1| + |1\rangle \langle 0|) \tag{A.47}
\end{aligned}$$

Comparing this equation with the notations in eqn.(4.26) and eqn.(4.27)

$$\begin{aligned}
= & \underbrace{\left\{ f_\rho \begin{bmatrix} \theta \mathcal{F}(\rho(2)) & \sqrt{\theta \bar{\theta}} \mathcal{R}(\rho(2)) \\ \sqrt{\theta \bar{\theta}} \mathcal{R}(\rho(2)) & \bar{\theta} \mathcal{F}(\rho(2)) \end{bmatrix} \right\}}_{f_\rho(\cdot)+} + \underbrace{\left\{ f_{\mathbb{I}} \begin{bmatrix} \theta \text{Tr}[\mathcal{F}(\rho(2))] & \sqrt{\theta \bar{\theta}} \text{Tr}[\mathcal{R}(\rho(2))] \\ \sqrt{\theta \bar{\theta}} \text{Tr}[\mathcal{R}(\rho(2))] & \bar{\theta} \text{Tr}[\mathcal{F}(\rho(2))] \end{bmatrix} \frac{\mathbb{I}_d}{d} \right\}}_{f_{\mathbb{I}} \text{Tr}_{d \times d}(\cdot) \frac{\mathbb{I}_d}{d}} \\
& \otimes (\theta |0\rangle \langle 0| + \bar{\theta} |1\rangle \langle 1|) \\
& + \underbrace{\left\{ r_\rho \begin{bmatrix} \theta \mathcal{F}(\rho(2)) & \sqrt{\theta \bar{\theta}} \mathcal{R}(\rho(2)) \\ \sqrt{\theta \bar{\theta}} \mathcal{R}(\rho(2)) & \bar{\theta} \mathcal{F}(\rho(2)) \end{bmatrix} \right\}}_{r_\rho(\cdot)+} + \underbrace{\left\{ r_{\mathbb{I}} \frac{\mathbb{I}_d}{d} \otimes \begin{bmatrix} \theta \text{Tr}[\mathcal{F}(\rho(2))] & \sqrt{\theta \bar{\theta}} \text{Tr}[\mathcal{R}(\rho(2))] \\ \sqrt{\theta \bar{\theta}} \text{Tr}[\mathcal{R}(\rho(2))] & \bar{\theta} \text{Tr}[\mathcal{F}(\rho(2))] \end{bmatrix} \right\}}_{r_{\mathbb{I}} \text{Tr}_{d \times d}(\cdot) \frac{\mathbb{I}_d}{d}} \\
& \otimes \sqrt{\theta \bar{\theta}} (|0\rangle \langle 1| + |1\rangle \langle 0|)
\end{aligned}$$

Thus, eqn.(4.35) is a  $4d$  dimensional block matrix which is again structurally similar to eqn.(4.26) and we can expand the previous notation of  $\mathcal{F}$  and  $\mathcal{R}$  to write the above result as:

$$\begin{aligned}
& = \{f_\rho(\rho_{\omega,1}(2)) + f_{\mathbb{I}} \text{Tr}_{d \times d}[\rho_{\omega,1}(2)] \frac{\mathbb{I}_d}{d}\} \otimes (\theta |0\rangle \langle 0| + \bar{\theta} |1\rangle \langle 1|) \\
& \quad + \{r_\rho(\rho_{\omega,1}(2)) + r_{\mathbb{I}} \text{Tr}_{d \times d}[\rho_{\omega,1}(2)] \frac{\mathbb{I}_d}{d}\} \otimes \sqrt{\theta \bar{\theta}} (|0\rangle \langle 1| + |1\rangle \langle 0|) \\
& = \mathcal{F}(\rho_{\omega,1}(2)) \otimes (\theta |0\rangle \langle 0| + \bar{\theta} |1\rangle \langle 1|) + \mathcal{R}(\rho_{\omega,1}(2)) \otimes \sqrt{\theta \bar{\theta}} (|0\rangle \langle 1| + |1\rangle \langle 0|) \\
\rho_{\omega,2}(2) & = \begin{bmatrix} \theta \mathcal{F}(\rho_{\omega,1}(2)) & \sqrt{\theta \bar{\theta}} \mathcal{R}(\rho_{\omega,1}(2)) \\ \sqrt{\theta \bar{\theta}} \mathcal{R}(\rho_{\omega,1}(2)) & \bar{\theta} \mathcal{F}(\rho_{\omega,1}(2)) \end{bmatrix}
\end{aligned}$$

Here, we use the shorthand notation introduced in eqn.(4.30). The superscript denotes the number of switches correlated to the input state, and  $\omega$  in the subscript signifies the second framework. The subscript also contains the number of iterations of Grover's Algorithm the input state has traversed through,

## A.4 Find the state after k Grover iterations where the system is correlated with k switches = $\rho_{\omega,k}(k)$

We denote the state of the system after measurement after k iterations as  $M_k$ :

$$M_k[\rho_{\omega,k}(k)] = (\mathbb{I}_d \otimes \langle + |^{\otimes k}) \rho_{\omega,k}(k) (\mathbb{I}_d \otimes | + \rangle^{\otimes k}) \quad (\text{A.48})$$

We have  $\mathbb{I}_d$  as part of the measurement operation because we want to keep the input state intact and only trace out the quantum switches correlated with the input state.

$$\begin{aligned} &= \left( (\mathbb{I}_d \otimes \langle + |^{\otimes k-1}) \otimes \langle + | \right) \rho_{\omega,k}(k) \left( (\mathbb{I}_d \otimes | + \rangle^{\otimes k-1}) \otimes | + \rangle \right) \\ &= \left( (\mathbb{I}_d \otimes \langle + |^{\otimes k-1}) \otimes \left[ \frac{1}{\sqrt{2}} \quad \frac{1}{\sqrt{2}} \right] \right) \rho_{\omega,k}(k) \left( (\mathbb{I}_d \otimes | + \rangle^{\otimes k-1}) \otimes \left[ \frac{1}{\sqrt{2}} \right. \right. \\ &\quad \left. \left. \frac{1}{\sqrt{2}} \right] \right) \\ &= \left[ \frac{\mathbb{I}_d \otimes \langle + |^{\otimes k-1}}{\sqrt{2}} \quad \frac{\mathbb{I}_d \otimes \langle + |^{\otimes k-1}}{\sqrt{2}} \right] \begin{bmatrix} \theta \mathcal{F}(\rho_{\omega,k-1}(k)) & \sqrt{\theta \bar{\theta}} \mathcal{R}(\rho_{\omega,k-1}(k)) \\ \sqrt{\theta \bar{\theta}} \mathcal{R}(\rho_{\omega,k-1}(k)) & \bar{\theta} \mathcal{F}(\rho_{\omega,k-1}(k)) \end{bmatrix} \begin{bmatrix} \frac{\mathbb{I}_d \otimes \langle + |^{\otimes k-1}}{\sqrt{2}} \\ \frac{\mathbb{I}_d \otimes \langle + |^{\otimes k-1}}{\sqrt{2}} \end{bmatrix} \\ &= \left( \frac{1}{\sqrt{2}} \right)^2 \left[ \mathbb{I}_d \otimes \langle + |^{\otimes k-1} \quad \mathbb{I}_d \otimes \langle + |^{\otimes k-1} \right] \begin{bmatrix} \theta \mathcal{F}(\rho_{\omega,k-1}(k)) & \sqrt{\theta \bar{\theta}} \mathcal{R}(\rho_{\omega,k-1}(k)) \\ \sqrt{\theta \bar{\theta}} \mathcal{R}(\rho_{\omega,k-1}(k)) & \bar{\theta} \mathcal{F}(\rho_{\omega,k-1}(k)) \end{bmatrix} \begin{bmatrix} \mathbb{I}_d \otimes | + \rangle^{\otimes k-1} \\ \mathbb{I}_d \otimes | + \rangle^{\otimes k-1} \end{bmatrix} \\ &= \begin{bmatrix} (\mathbb{I}_d \otimes \langle + |^{\otimes k-1}) (\theta \mathcal{F}(\rho_{\omega,k-1}(k))) + (\mathbb{I}_d \otimes \langle + |^{\otimes k-1}) (\sqrt{\theta \bar{\theta}} \mathcal{R}(\rho_{\omega,k-1}(k))) \\ (\mathbb{I}_d \otimes \langle + |^{\otimes k-1}) (\sqrt{\theta \bar{\theta}} \mathcal{R}(\rho_{\omega,k-1}(k))) + (\mathbb{I}_d \otimes \langle + |^{\otimes k-1}) (\bar{\theta} \mathcal{F}(\rho_{\omega,k-1}(k))) \end{bmatrix}^T \begin{bmatrix} \mathbb{I}_d \otimes | + \rangle^{\otimes k-1} \\ \mathbb{I}_d \otimes | + \rangle^{\otimes k-1} \end{bmatrix} \\ &= (\mathbb{I}_d \otimes \langle + |^{\otimes k-1}) (\theta \mathcal{F}(\rho_{\omega,k-1}(k))) (\mathbb{I}_d \otimes | + \rangle^{\otimes k-1}) + (\mathbb{I}_d \otimes \langle + |^{\otimes k-1}) (\sqrt{\theta \bar{\theta}} \mathcal{R}(\rho_{\omega,k-1}(k))) (\mathbb{I}_d \otimes | + \rangle^{\otimes k-1}) \\ &\quad + (\mathbb{I}_d \otimes \langle + |^{\otimes k-1}) (\sqrt{\theta \bar{\theta}} \mathcal{R}(\rho_{\omega,k-1}(k))) (\mathbb{I}_d \otimes | + \rangle^{\otimes k-1}) + (\mathbb{I}_d \otimes \langle + |^{\otimes k-1}) (\bar{\theta} \mathcal{F}(\rho_{\omega,k-1}(k))) (\mathbb{I}_d \otimes | + \rangle^{\otimes k-1}) \\ &= (\mathbb{I}_d \otimes \langle + |^{\otimes k-1}) (\mathcal{F}(\rho_{\omega,k-1}(k))) (\mathbb{I}_d \otimes | + \rangle^{\otimes k-1}) + 2\sqrt{\theta \bar{\theta}} (\mathbb{I}_d \otimes \langle + |^{\otimes k-1}) (\mathcal{R}(\rho_{\omega,k-1}(k))) (\mathbb{I}_d \otimes | + \rangle^{\otimes k-1}) \end{aligned}$$

Using eqn.(4.38) and eqn.(4.39) in the result above:

$$\begin{aligned} &\frac{1}{2} (\mathbb{I}_d \otimes \langle + |^{\otimes k-1}) \left( f_\rho(\rho_{\omega,k-1}(k)) + f_{\mathbb{I}} \frac{\mathbb{I}_d}{d} \otimes \text{Tr}_{d \times d}[\rho_{\omega,k-1}(k)] \right) (\mathbb{I}_d \otimes | + \rangle^{\otimes k-1}) \\ &+ 2\sqrt{\theta \bar{\theta}} (\mathbb{I}_d \otimes \langle + |^{\otimes k-1}) \left( r_\rho(\rho_{\omega,k-1}(k)) + r_{\mathbb{I}} \frac{\mathbb{I}_d}{d} \otimes \text{Tr}_{d \times d}[\rho_{\omega,k-1}(k)] \right) (\mathbb{I}_d \otimes | + \rangle^{\otimes k-1}). \quad (\text{A.49}) \end{aligned}$$

Rearranging the terms, we get:

$$\begin{aligned} &\frac{1}{2} \left\{ (f_\rho + 2\sqrt{\theta \bar{\theta}} r_\rho) (\mathbb{I}_d \otimes \langle + |^{\otimes k-1}) (\rho_{\omega,k-1}(k)) (\mathbb{I}_d \otimes | + \rangle^{\otimes k-1}) \right. \\ &\left. + (f_{\mathbb{I}} + 2\sqrt{\theta \bar{\theta}} r_{\mathbb{I}}) (\mathbb{I}_d \otimes \langle + |^{\otimes k-1}) \left( \frac{\mathbb{I}_d}{d} \otimes \text{Tr}_{d \times d}[\rho_{\omega,k-1}(k)] \right) (\mathbb{I}_d \otimes | + \rangle^{\otimes k-1}) \right\} \quad (\text{A.50}) \end{aligned}$$

Substituting eqn. A.48

$$\begin{aligned}
&= \frac{1}{2} \left\{ (f_\rho + 2\sqrt{\theta\bar{\theta}}r_\rho)M_{k-1}(\rho_{\omega,k-1}(k)) \right. \\
&\quad \left. + (f_{\mathbb{I}} + 2\sqrt{\theta\bar{\theta}}r_{\mathbb{I}})(\mathbb{I}_d \otimes \langle + |^{\otimes k-1}) \left( \frac{\mathbb{I}_d}{d} \otimes \text{Tr}_{d \times d}[\rho_{\omega,k-1}(k)] (\mathbb{I}_d \otimes |+\rangle^{\otimes k-1}) \right) \right\} \quad (\text{A.51})
\end{aligned}$$

Thus, we get a recursive recipe to get the density operator after k iterations:

$$M_k(\rho_{\omega,k}(k)) = \frac{1}{2} \left\{ (f_\rho + 2\sqrt{\theta\bar{\theta}}r_\rho)M_{k-1}(\rho_{\omega,k-1}(k)) + (f_{\mathbb{I}} + 2\sqrt{\theta\bar{\theta}}r_{\mathbb{I}})(\mathbb{I}_d \otimes \langle + |^{\otimes k-1} \text{Tr}_{d \times d}[\rho_{\omega,k-1}(k)] |+\rangle^{\otimes k-1}) \right\} \quad (\text{A.52})$$

After that, we can analyze the density operator obtained for success probability after k Grover iterations.

## Related Publications

- Suryansh Srivastava, Arun K. Pati, Samyadeb Bhattacharya, and Indranil Chakrabarty.  
“Using Quantum Switches to Mitigate Noise in Grover’s Search Algorithm.”  
arXiv:2401.05866 [quant-ph] (2024) <https://doi.org/10.48550/arXiv.2401.05866>.  
(Under Review)

## Bibliography

- [1] P. Benioff, *Journal of Statistical Physics* **22**, 563 (1980).
- [2] R. P. Feynman, *International Journal of Theoretical Physics* **21**, 467 (1982).
- [3] K. Bharti, A. Cervera-Lierta, T. H. Kyaw, T. Haug, S. Alperin-Lea, A. Anand, M. Degroote, H. Heimonen, J. S. Kottmann, T. Menke, W.-K. Mok, S. Sim, L.-C. Kwek, and A. Aspuru-Guzik, *Rev. Mod. Phys.* **94**, 015004 (2022), publisher: American Physical Society.
- [4] J. Preskill, *Quantum* **2**, 79 (2018), arXiv:1801.00862 [cond-mat, physics:quant-ph].
- [5] M. M. Taddei, J. Carine, D. Martínez, T. Garcia, N. Guerrero, A. A. Abbott, M. Araujo, C. Branciard, E. S. Gomez, S. P. Walborn, L. Aolita, and G. Lima, *PRX Quantum* **2**, 010320 (2021).
- [6] P. A. Guerin, A. Feix, M. Araujo, and C. Brukner, *Phys. Rev. Lett.* **117**, 100502 (2016), publisher: American Physical Society.
- [7] S. L. Braunstein and A. K. Pati, *Quantum Info. Comput.* **2**, 399 (2002).
- [8] S. Chakraborty, S. Banerjee, S. Adhikari, and A. Kumar, *Entanglement in the Grover's Search Algorithm* (2013), arXiv:1305.4454 [quant-ph].
- [9] S. Chakraborty and S. Adhikari, *Non-classical Correlations in the Quantum Search Algorithm* (2013), arXiv:1302.6005 [quant-ph].
- [10] H. P. Breuer and F. Petruccione, *The theory of open quantum systems* (Oxford University Press, Great Clarendon Street, 2002).
- [11] I. Cohn, A. L. F. de Oliveira, E. Buksman, and J. G. L. de Lacalle, *Int. J. Quant. Inf.* **14**, 1650009 (2016), arXiv: 1508.03302.
- [12] P. Vrana, D. Reeb, D. Reitzner, and M. M. Wolf, *New J. Phys.* **16**, 073033 (2014), publisher: IOP Publishing.

- [13] O. Regev and L. Schiff, in *Automata, Languages and Programming*, Lecture Notes in Computer Science, edited by L. Aceto, I. Damgård, L. A. Goldberg, M. M. Halldórsson, A. Ingólfssdóttir, and I. Walukiewicz (Springer, Berlin, Heidelberg, 2008) pp. 773–781.
- [14] K. Temme, *Phys. Rev. A* **90**, 022310 (2014), publisher: American Physical Society.
- [15] J. Chen, D. Kaszlikowski, L. C. Kwek, and C. H. Oh, *Physics Letters A* **306**, 296 (2003).
- [16] A. Saha, R. Majumdar, D. Saha, A. Chakrabarti, and S. Sur-Kolay, *Phys. Rev. A* **105**, 062453 (2022), publisher: American Physical Society.
- [17] J. Avron, O. Casper, and I. Rozen, *Phys. Rev. A* **104**, 052404 (2021), publisher: American Physical Society.
- [18] F. B. Maciejewski, Z. Zimborás, and M. Oszmaniec, *Quantum* **4**, 257 (2020), publisher: Verein zur Förderung des Open Access Publizierens in den Quantenwissenschaften.
- [19] L. Hardy, [www.arxiv.org/abs/gr-qc/0509120](http://www.arxiv.org/abs/gr-qc/0509120) (2005).
- [20] L. Hardy, *J. Phys. A* **40**, 3081 (2007).
- [21] G. Chiribella, G. M. D’Ariano, P. Perinotti, and B. Valiron, *Physical Review A* **88**, 022318 (2013), arXiv: 0912.0195.
- [22] O. Oreshkov, F. Costa, and C. Brukner, *Nat Commun* **3**, 1092 (2012), number: 1 Publisher: Nature Publishing Group.
- [23] G. Chiribella, *Phys. Rev. A* **86**, 040301 (2012), publisher: American Physical Society.
- [24] X. Zhao, Y. Yang, and G. Chiribella, *Phys. Rev. Lett.* **124**, 190503 (2020), publisher: American Physical Society.
- [25] D. Ebler, S. Salek, and G. Chiribella, *Phys. Rev. Lett.* **120**, 120502 (2018), publisher: American Physical Society.
- [26] S. Salek, D. Ebler, and G. Chiribella, *Quantum communication in a superposition of causal orders* (2018), arXiv:1809.06655 [quant-ph].
- [27] G. Chiribella, M. Banik, S. S. Bhattacharya, T. Guha, M. Alimuddin, A. Roy, S. Saha, S. Agrawal, and G. Kar, *New J. Phys.* **23**, 033039 (2021), publisher: IOP Publishing.
- [28] S. Koudia, A. S. Cacciapuoti, K. Simonov, and M. Caleffi, *IEEE Commun. Surv. Tutorials* **24**, 1926 (2022), arXiv:2108.07108 [quant-ph].
- [29] M. Caleffi and A. S. Cacciapuoti, *IEEE J. Select. Areas Commun.* **38**, 575 (2020).

- [30] M. Araujo, F. Costa, and C. Brukner, *Phys. Rev. Lett.* **113**, 250402 (2014), publisher: American Physical Society.
- [31] K. Simonov, M. Caleffi, J. Illiano, and A. S. Cacciapuoti, *Universal Quantum Computation via Superposed Orders of Single-Qubit Gates* (2023), arXiv:2311.13654 [quant-ph].
- [32] T. Guha, M. Alimuddin, and P. Parashar, *Phys. Rev. A* **102**, 032215 (2020), publisher: American Physical Society.
- [33] S. Yanamandra, P. V. Srinidhi, S. Bhattacharya, I. Chakrabarty, and S. Goswami, *Breaking absolute separability with quantum switch* (2023), arXiv:2310.04819 [quant-ph].
- [34] L. M. Procopio, A. Moqanaki, M. Araujo, F. Costa, I. Alonso Calafell, E. G. Dowd, D. R. Hamel, L. A. Rozema, C. Brukner, and P. Walther, *Nat Commun* **6**, 7913 (2015), number: 1 Publisher: Nature Publishing Group.
- [35] G. Rubino, L. A. Rozema, A. Feix, M. Araujo, J. M. Zeuner, L. M. Procopio, C. Brukner, and P. Walther, *Science Advances* **3**, e1602589 (2017), publisher: American Association for the Advancement of Science.
- [36] K. Goswami, C. Giarmatzi, M. Kewming, F. Costa, C. Branciard, J. Romero, and A. White, *Phys. Rev. Lett.* **121**, 090503 (2018), publisher: American Physical Society.
- [37] S. Sazim, M. Sedlak, K. Singh, and A. K. Pati, *Phys. Rev. A* **103**, 062610 (2021), arXiv:2004.14339.
- [38] M. Frey, *Quantum Information Processing* **18**, 96 (2019).
- [39] D. Das and S. Bandyopadhyay, *Proc. R. Soc. A.* **478**, 20220231 (2022), arXiv:2111.08266 [quant-ph].
- [40] J. J. Sakurai, *Modern Quantum Mechanics (Revised Edition)*, 1st ed. (Addison Wesley, 1993).
- [41] D. J. Griffiths and D. F. Schroeter, *Introduction to Quantum Mechanics*, 3rd ed. (Cambridge University Press, 2018).
- [42] N. D. Mermin, *Physics Today* **38**, 38 (1985).
- [43] J. S. Bell, *Physics Physique Fizika* **1**, 195 (1964), publisher: American Physical Society.
- [44] S. J. Axler, *Linear algebra done right*, 3rd ed., Undergraduate texts in mathematics (Springer, Cham Heidelberg, 2015).
- [45] K. Hoffman and R. Kunze, *Linear algebra* (Prentice Hall India Learning Private Limited 2nd edition (1 January 2015), 2015) oCLC: 1286140844.

- [46] P. a. M. Dirac, *Mathematical Proceedings of the Cambridge Philosophical Society* **35**, 416 (1939), publisher: Cambridge University Press.
- [47] J. von Neumann and R. T. Beyer, *Mathematical Foundations of Quantum Mechanics: New Edition*, ned - new edition ed., edited by N. A. Wheeler (Princeton University Press, 2018).
- [48] G. W. Mackey, *Mathematical Foundations of Quantum Mechanics*, Dover Books on Physics (Dover Publications, 2004).
- [49] P. W. Shor, *J. ACM* **50**, 87 (2003).
- [50] D. Deutsch and R. Jozsa, *Rapid Solution of Problems by Quantum Computation*, Technical Report (University of Bristol, GBR, 1992).
- [51] P. W. Shor, *SIAM J. Comput.* **26**, 1484 (1997).
- [52] L. K. Grover, *STOC 96* , 212 (1996).
- [53] J. Preskill, Lecture notes for physics 229: Quantum information and computation (1998), available online: <http://www.theory.caltech.edu/people/preskill/ph229/>.
- [54] M. A. Nielsen and I. L. Chuang, *Quantum computation and quantum information*, 10th ed. (Cambridge university press, Cambridge, 2010).
- [55] M. M. Wilde, *Quantum information theory*, 2nd ed. (Cambridge university press, Cambridge, 2017).
- [56] S. Das and M. M. Wilde, *IEEE Trans. Inform. Theory* **65**, 7566 (2019), arXiv:1703.03706 [quant-ph].
- [57] J. E. Martinez, A. d. iOlius, and P. M. Crespo, *Phys. Rev. A* **108**, 032602 (2023), arXiv:2301.10132 [quant-ph].
- [58] M. Frey, D. Collins, and K. Gerlach, *J. Phys. A: Math. Theor.* **44**, 205306 (2011), arXiv: 1008.1557.
- [59] C. Zalka, *Phys. Rev. A* **60**, 2746 (1999), publisher: American Physical Society.
- [60] C. H. Bennett, E. Bernstein, G. Brassard, and U. Vazirani, *SIAM J. Comput.* **26**, 1510 (1997), publisher: Society for Industrial and Applied Mathematics.
- [61] A. Ambainis, A. Bačkurs, N. Nahimovs, and A. Rivosh, in *Mathematical and Engineering Methods in Computer Science*, Lecture Notes in Computer Science, edited by A. Kučera, T. A. Henzinger, J. Nešetřil, T. Vojnar, and D. Antoš (Springer, Berlin, Heidelberg, 2013) pp. 180–189.

- [62] H. Azuma, *Phys. Rev. A* **65**, 042311 (2002), publisher: American Physical Society.
- [63] P. J. Salas, *Eur. Phys. J. D* **46**, 365 (2008), arXiv:0801.1261 [quant-ph].
- [64] P. W. Shor, *Fault-tolerant quantum computation* (1997), arXiv:quant-ph/9605011.
- [65] M. Boyer, G. Brassard, P. Hoyer, and A. Tapp, *Fortschr. Phys.* **46**, 493 (1998), arXiv:quant-ph/9605034.
- [66] F. Chapeau-Blondeau, *Phys. Rev. A* **103**, 032615 (2021), arXiv:2104.06284 [quant-ph].
- [67] F. Chapeau-Blondeau, *Physics Letters A* **447**, 128300 (2022), arXiv:2211.01684 [quant-ph].
- [68] S. S. Bhattacharya, A. G. Maity, T. Guha, G. Chiribella, and M. Banik, *PRX Quantum* **2**, 020350 (2021), publisher: American Physical Society.
- [69] Y. Aharonov, J. Anandan, S. Popescu, and L. Vaidman, *Phys. Rev. Lett.* **64**, 2965 (1990).
- [70] R. S. Gupta, N. Sundaresan, T. Alexander, C. J. Wood, S. T. Merkel, M. B. Healy, M. Hillenbrand, T. Jochym-O'Connor, J. R. Wootton, T. J. Yoder, A. W. Cross, M. Takita, and B. J. Brown, *Nature* **625**, 259 (2024), arXiv:2305.13581 [quant-ph].
- [71] C. Durr and P. Hoyer, (1999), arXiv:quant-ph/9607014.
- [72] R. R. Tucci, (2014), arXiv:1404.0668 [quant-ph].
- [73] L. K. Grover, (1996), arXiv:quant-ph/9607024.
- [74] M. Fürer, in *LATIN 2008: Theoretical Informatics*, Lecture Notes in Computer Science, edited by E. S. Laber, C. Bornstein, L. T. Nogueira, and L. Faria (Springer, Berlin, Heidelberg, 2008) pp. 784–792.
- [75] A. Ambainis, *Quantum search algorithms* (2005), arXiv:quant-ph/0504012.
- [76] N. J. Cerf, L. K. Grover, and C. P. Williams, *AAECC* **10**, 311 (2000).
- [77] G. Brassard, P. Hoyer, and A. Tapp, in *LATIN'98: Theoretical Informatics*, Lecture Notes in Computer Science, edited by C. L. Lucchesi and A. V. Moura (Springer, Berlin, Heidelberg, 1998) pp. 163–169.
- [78] D. J. Bernstein, J. Buchmann, and E. Dahmen, eds., *Post-Quantum Cryptography* (Springer Berlin Heidelberg, Berlin, Heidelberg, 2009).
- [79] S. Jaques, M. Naehrig, M. Roetteler, and F. Virdia, (2019).
- [80] A. Mandal, R. S. Sarkar, S. Chakraborty, and B. Adhikari, *Phys. Rev. A* **106**, 042405 (2022), publisher: American Physical Society.

- [81] F. Chapeau-Blondeau, Fluctuation and Noise Letters [10.1142/S0219477523500360](#) (2023), publisher: World Scientific Publishing Company.
- [82] Z. Cao, [Phys. Rev. A \*\*108\*\*, 012428 \(2023\)](#), arXiv:2307.13477 [quant-ph].